# The Institute of Paper Chemistry

Appleton, Wisconsin

## Doctor's Dissertation

The Role of Surface Chemistry
in the Bonding of a Cellulose Substrate
Treated in a Corona Discharge

Philip F. Brown

January, 1971

# THE ROLE OF SURFACE CHEMISTRY IN THE BONDING OF A CELLULOSE SUBSTRATE TREATED IN A CORONA DISCHARGE

A thesis submitted by

Philip F. Brown

B.S. 1965, University of Maine

M.S. 1967, Lawrence University

in partial fulfillment of the requirements
of The Institute of Paper Chemistry
for the degree of Doctor of Philosophy
from Lawrence University,
Appleton, Wisconsin



January, 1971

TABLE OF CONTENTS

## SUMMARY

The strength of water-induced bonds between sheets of cellophane, treated in a corona discharge, has been related to changes in solid surface free energy produced by the treatment. The theories of interfacial energy were applied to contact-angle data in order to separately evaluate the polar and nonpolar components of the solid surface free energies. Very significant increases were found in the polarity of the surfaces with corona treatment. The magnitudes of the calculated components of surface free energy were also found to depend upon relative humidity and upon the character of the substrate against which the films had been previously dried.

Estimates of the degree to which the treated material was swollen by water were obtained by application of solubility-parameter theory to the calculated values of solid surface free energy. It was indicated that the cellulose surface was made more hydrophilic by the treatment, and it was concluded that this effect played a significant role in the mechanism of increased bonding.

The Chapman smoothness tester was employed to obtain measures of surface roughness and conformability at three levels of humidity. These results were in qualitative agreement with the calculations based on solubility parameters.

Multiple internal reflection spectroscopy was used to determine the nature of chemical changes induced in the substrate by the corona treatment. Changes in the spectra were attributed to an increase in carboxyl content with treatment. Attempts to measure changes in carboxyl content as a percentage of the total bulk material failed, and it was concluded that the chemical changes were confined within very thin surface layers.

Laminates were formed between treated sheets by a wet-pressing technique, and the bond strengths were evaluated by measuring the force required for rupture from tensile extension perpendicular to the plane of the bond. The strength values increased most rapidly during the early stages of corona treatment, and appeared to follow a linear relationship with the logarithm of treatment time. This was interpreted as further evidence that the primary effect of the treatment was confined to a modification of the surface.

Electron micrographs indicated that the bonds between samples which had received extensive corona treatment were often locally stronger than the adjacent bulk material. When these laminates were ruptured by peeling, failure often occurred outside the original interface.

## INTRODUCTION

The importance of surface preparation has long been recognized by those concerned with adhesion phenomena. Various procedures have been used to treat the surfaces of interest in order to obtain a joint of superior strength or durability.

The conditions which most commonly give rise to the necessity for surface pretreatment are the presence of mechanically weak surface layers along with contaminants such as oils or corrosion products, usually oxides. These materials can inhibit good adhesion in two ways. If the physical state and chemical nature of the surface region are not appropriate to obtain intimate molecular contact with the adhesive, then good adhesion is prevented. Secondly, if the surface layer is mechanically weak, or if its strength is lowered by reaction with the adhesive system, then the effective strength of the bond will be low even if good contact is obtained between the surface and the adhesive.

Basically there are three possible approaches to this general problem. Perhaps most commonly, the pretreatment methods have employed solvent cleaning or mechanical abrasion to remove the troublesome material from the surface. A second approach is to chemically modify the surface to achieve the desired interaction with the adhesive or to strengthen it physically, perhaps by a cross-linking reaction. A third alternative is to deposit an additional layer having the desired properties. Obviously, the latter procedure is not appropriate if it is the strength of the original surface layer which is the limiting factor.

Along with the increasing availability and widespread use of the various synthetic polymers has come a need to develop methods of bonding these polymers to themselves and to other materials. This demand has resulted in a new technology of surface pretreatment. Typically, these methods involve means for chemical modification of very thin surface layers without changing the bulk properties of the polymer.

One of the more important of these methods is that of corona-discharge treatment. Although this process has received rather widespread industrial use, its mechanisms are not entirely understood. Fundamental studies of its application to the treatment of cellulose have been rather limited, particularly with respect to considerations of surface chemistry.

## LITERATURE REVIEW

It is pertinent to consider some of the characteristics of a corona discharge and to review briefly its application to the treatment of cellulose and other polymers. The reader is referred to the literature for descriptions of pretreatment techniques involving other processes: oxidizing flames (1,2), microwaves (3), reactive gases (4,5), ultraviolet radiation (6), and high-energy radiation (7).

A brief review of the theories of adhesion is provided to acquaint the reader with some of the fundamentals of adhesion phenomena. More extensive coverage of these subjects may be found in the literature (8-14).

Finally, a summary is given of the experimental methods which have been used to estimate wettability and solid surface free energy. Primary emphasis is given to methods which make use of liquid-solid contact angles, and to the application of these methods to cellulosic materials.

## FUNDAMENTALS OF CORONA DISCHARGE

In contrast to the familiar Ohm's Law behavior of most solid conductors, the voltage-current curve for two electrodes immersed in a gas is generally not a linear relationship, but is commonly a multivalued function of the voltage drop across the electrodes (15). The shape of this curve is dependent upon electrode configuration and spacing, as well as gas-phase composition and pressure.

One common pattern of behavior for parallel-plate electrodes (in air at atmospheric pressure) is illustrated in Fig. 1. Segment a-b of this curve defines the so-called "dark-discharge" region. In this region the

current is caused by collision-produced ionization, with the initial electrons and ions being supplied by ionization due to cosmic rays and radiation from radioactive sources. When the voltage across the gap reaches a certain value called the "sparking potential," Vs, the process becomes unstable, and breakdown occurs. The current then concentrates into a small path, and arcing takes place (15).

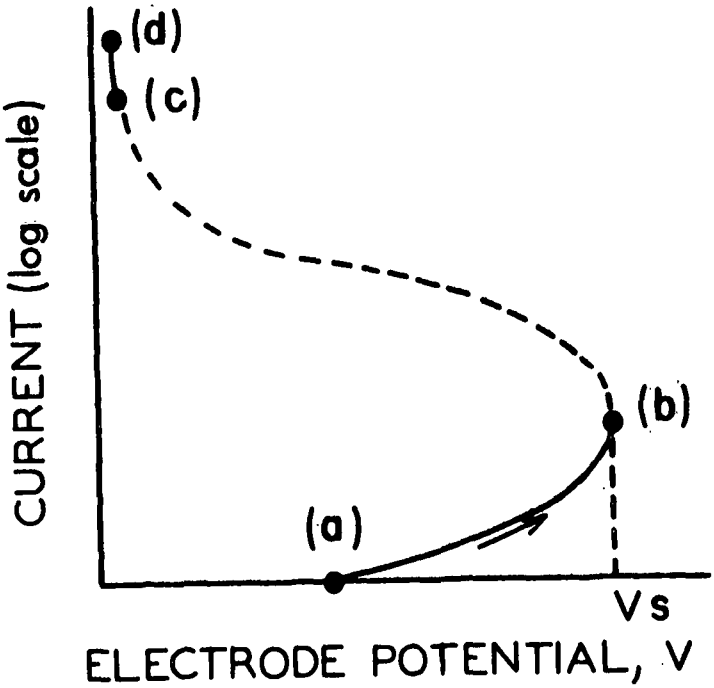


Figure 1. Schematic Current — Voltage Curve for Parallel-Plate Electrodes in Air at P = 1 atm. (15)

If a corona discharge is to be obtained, it is necessary to impede the passage of ions to the opposite electrodes (16). This gives rise to a concentration of space charges which can effectively neutralize the electric field and prevent complete breakdown. This may be accomplished by replacing one of the

plates with a rod-shaped electrode which has a small radius of curvature compared with the gap length (15). (The rod is positioned perpendicular to the plane of the opposing plate.) This arrangement results in an effective decrease in the effective field strength in the vicinity of the rod, as a result of the accumulation of space charge, and gives rise to the behavior shown schematically in Fig. 2. In this case, the dark discharge region (a-b) is succeeded by a discharge in which the current increases rather uniformly with impressed voltage (Segment b-c). This is the so-called "corona discharge" and is usually accompanied by a hissing sound, along with the emission of light which is characteristic of the particular gas and for air has a violet color (15). The voltage required for the onset of corona is referred to as the "corona voltage," Vc, and is generally in the range of 10,000-15,000 volts (16). If the voltage is further increased, breakdown eventually occurs and arcing results as before (Segment d-e).

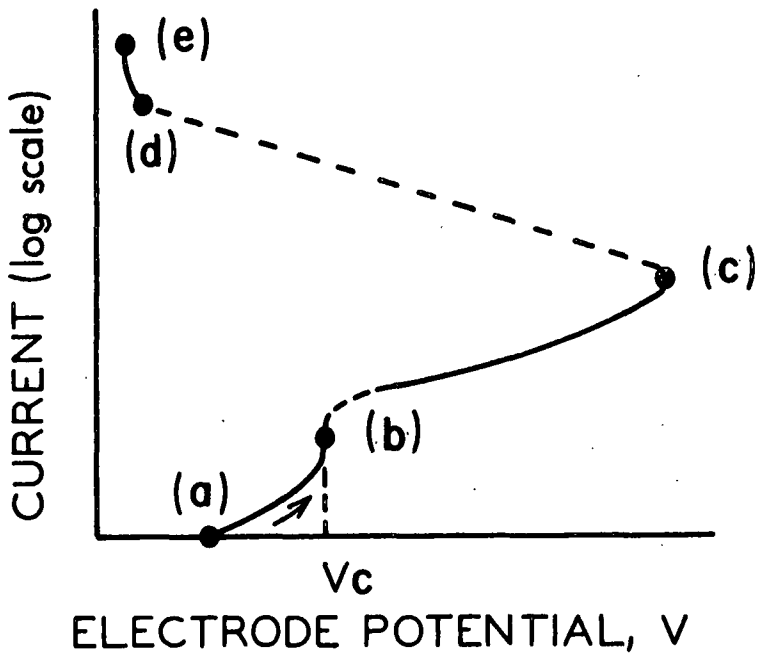


Figure 2. Schematic Current-Voltage Curve for Electrode Configuration Capable of Producing a Corona Discharge (15)

An alternate arrangement for producing a corona discharge consists of parallel-plate electrodes which are covered with a dielectric material of sufficient (dielectric) strength to prevent breakdown before the onset of corona. This arrangement is effective because the capacity of each electrode to receive oppositely charged species is greatly inhibited.

The mechanism of the corona discharge which has been described above accounts for the importance of frequency effects. Once the electric field has been suppressed by the accumulation of space charge, very little further ionization occurs. If the field is reversed, however, the space charge is temporarily dissipated and another burst of ionization can then take place. Therefore, the rate of chemical reactions induced by the process is generally found to be proportional to the frequency of the discharge (16).

As a result of the collisions between energetic electrons (10-15 electron volts) and gas molecules, various charged ions and highly reactive free radicals are produced (16). These can further interact with other gas molecules or with an adjacent solid material to produce chemical changes. In air or oxygen, the primary gaseous product of these reactions is ozone ($O_3$), which is itself a very reactive oxidant that can promote further reaction. The nature of the charged species produced by coronas in several different atmospheres has been investigated by Shahin (17,18), using techniques of mass spectrometry. Table I summarizes the list of species found by Shahin when the corona atmosphere was air containing trace amounts of water vapor and carbon dioxide. It is apparent that a variety of chemical changes could be induced in a substrate upon interaction with these species.

TABLE I

CHARGE CARRIERS IN CORONA DISCHARGES
IN AIR CONTAINING WATER VAPOR, AND $CO_2$

[From Shahin (17,18)]

| Negative Species | Positive Species |
|---|---|
| $O^-$ | $No^+$ |
| $O_3^-$ | $NO_2^+$ |
| $CO_3^-$ | $NO_2^+$ |
| $NO_2^-$ | $N_3H^+$ |
| $NO_3^-$ | $(H_2O)_nH^+$, n=1, 2, 3, 4 |
| $OH^-$ | $(NO^+)(H_2O)_n$, n=1, 2 |
| $O_3^-(H_2O)$ | $O_2^+(H_2O)$ |
| $CO_3^-(H_2O)$ | |

Because of the great reactivity of the species generated in the corona, the initial reaction between these and a solid substrate is generally confined within a very thin surface region. For example, when polypropylene was treated in a corona discharge, the resulting chemical changes were confined within surface layers of under 500 A. thickness, except when high ozone concentrations were used (19). This is a very important characteristic of the process in applications of surface activation, since it permits modification of the surface without alteration of the bulk material.

## CORONA TREATMENT OF POLYMERS

The surface treatment of a variety of substrates with corona discharge has been reported in the literature.

A series of doctoral theses at Washington University investigated extensively the treatment of polyethylene films (20-22). They observed an increase in ketone, acid, ether, and hydroxyl groups in the films after treatment. It was also reported that unsaturation and cross-linking resulted from the corona treatment (23). Anderson (24) and Rossman (25) have also reported evidence of carbonyl formation and occurrence of unsaturation in corona-treated polyethylene. Similar effects have also been obtained with polypropylene (19).

The effects of several treatment variables on the rates of bond-strength development have also been investigated. The rate was found to depend upon the exposure time, the potential and frequency of the power, the gap distance, the electrode design, the atmospheric conditions, and the molecular structure of the film (23). The effect of temperature on the rate of the reaction was also investigated, and the activation energy was found to be of the order of 40-70 Kcal./mol. (20). This is in the range of energies expected for the formation of a primary valence bond.

The application of these principles to the development of equipment and technology for the industrial treatment of polyethylene films and other substrates has been extensively reported in the literature (2,26-31).

Information regarding the use of corona discharge to improve cellulose-to-cellulose bonds has been reported by Dr. David Goring and his associates (5,32) at the Pulp and Paper Research Institute of Canada. Working with strips of bleached sulfite handsheets, deacetylated cellulose acetate, and birch veneer, these workers studied the effect of the corona on the strength of water-induced bonds between treated samples of the same materials. When the strengths of these bonds were evaluated by rupture in

shear, the bonds between corona-treated samples were found to be as much as twenty-five times stronger than those between the control samples (32). The treatment was found to have little effect on the tensile strength of the strips themselves, and this was interpreted as further evidence that the treatment is confined to a thin surface region. An increase in the carboxyl content of samples exposed to prolonged treatment was detected by infrared absorption techniques. Microscopic observation of the treated materials indicated that the surfaces were markedly roughened by the corona. An examination of the surfaces after bond rupture indicated that, after high treatment times, the bond strengths exceeded the cohesive strength of the bulk material, and failure occurred outside the interface (32). This interpretation was further supported by the observation that the bond strengths increased rapidly during the initial stages of treatment, but reached a maximum at a treatment time of about five minutes. Thereafter, the bond strengths were somewhat lowered by further treatment (32).

Initially, it was reported (32) that discharge treatment in an atmosphere of nitrogen was not effective in improving the strength of water-induced bonds between treated cellulose substrates. It was later observed, however, that when special precautions were taken to remove trace amounts of oxygen from the nitrogen atmosphere, the nitrogen corona was very effective in improving heat-induced bonds between cellulose and synthetic polymers if the bonding was performed immediately after treatment of the two substrates (33). No chemical changes due to the treatment could be detected in these samples. Neither did microscopic observations reveal any changes in the character of the surface. It was observed that the effect was greatly reduced if these materials were allowed to stand in air for a period of time before bonding (33). This decay of effective treatment with

aging time was not observed with any of the samples treated in an oxygen-containing corona (32). It is not clear, however, whether care was taken in the initial study to control the age of cellulose samples treated in a nitrogen atmosphere. It is, therefore, not known whether the above observations would apply to water-induced bonds between cellulose samples treated in a nitrogen corona. Neither does the importance of high-purity nitrogen appear to have been clearly established.

It is possible that a different mechanism predominates when the activation is carried out in a nitrogen atmosphere rather than in an oxygen-containing gas. It was postulated (33) that a free-radical mechanism may be operative in the absence of oxygen, but that these species are rapidly quenched when oxygen is present.

In his initial experiments, Dr. Goring did not observe increased bonding between samples which had been treated with ozone or atomic oxygen without exposure to an electrical discharge (32). Later experiments (5) showed that ozone could, in fact, be effective if the samples were suitably agitated during exposure to the gases or if prolonged exposure times were used. It was also observed in the course of these experiments that the bonding could be enhanced if treated cellulose strips were soaked in mild alkali before bonding, whereas alkali soaking of untreated samples did not increase the strength of the bonds (5). This effect was attributed to enhanced swelling of the treated layer by the alkali.

In their study of heat-induced bonding between cellulose and synthetic polymers, Goring and his students observed that enhanced bonding was obtained if either of the substrates (cellulose or polymer) was treated in the

corona (33). Further increases in bond strength were obtained if both substrates were treated before bonding. They were unable to reconcile these observations with the concepts of surface wettability which had been successfully applied to the adhesion of polymers to cellulose by Swanson and Becher (34), and by Glossman (35).

Very little attention appears to have been given to a quantitative consideration of surface chemistry in relation to corona-treated cellulose and its bonding properties. Some surface-chemical information is available, however, on the treatment of synthetic polymers. Rauhut (36) determined the critical surface tension of wetting (37) of polyethylene surfaces which had been exposed to several pretreatment conditions, including electric discharge. The critical surface tension of the solid was substantially increased by the treatments. Similar results were obtained by Allen (1) using flame treatment of polyethylene. Anderson (24) exposed a variety of synthetic polymers to an electrical discharge, and observed that with treatment the surfaces became more wettable by polar liquids.

## GENERAL THEORIES OF ADHESION

Basic to the phenomena of adhesion are the forces of attraction which exist between all molecules. These intermolecular forces have been classified into five different types (38): (1) the so-called dispersion forces between all types of molecules; (2) orientation forces between rigid dipoles; (3) induction forces between polarizable molecules and rigid dipoles; (4) coulombic forces between ions; (5) metallic forces. It is the first three of these groups which are of predominant importance

in most adhesion situations involving nonmetallic materials, and the remainder of the list will not be further considered here.

The dispersion forces are the result of mutual interaction of the electronic oscillations surrounding each molecule. This effect was first quantitatively described by London, and derives its name from its relation to the dispersion of light of varying frequencies upon interaction with molecular species (38). Notable features of this type of force are that it is universal among all molecules, is approximately additive, and is not temperature dependent.

The orientation forces are caused by the interaction of permanent dipoles. A satisfactory expression for the magnitude of these forces between thermally agitated molecules was first provided by Keesom. It should be noted Keesom's expression is not directly applicable to solid phases (38). An important special case of this effect is the phenomenon commonly known as hydrogen bonding. An important characteristic of the orientation force is that it is temperature dependent.

The induction effect is a result of the ability of a permanent dipole to induce a temporary dipole in another molecule, and was first described by Debye. The magnitude of the induction forces is generally found to be small in comparison to the dispersion and orientation forces (38).

Without further reviewing the quantitative expressions for these three types of forces, it is sufficient to note that their relative magnitudes will be affected by such molecular properties as polarity, polarizability, and ionization potential. It is also important to note that the magnitude

of each force is inversely proportional to the seventh power of the intermolecular distance. Molecules must therefore be brought into close proximity before these forces become significant.

Several theories have been proposed in the literature to explain the phenomena of adhesion, as observed at a macroscopic level. Basically, these theories reflect a consideration of the conditions required for bonding at the molecular level by virtue of the types of forces described above. The theories of adhesion may be divided into the following categories (39): (1) the mechanical model; (2) the adsorption theory; (3) the diffusion theory; (4) the electrical theory; (5) the quantum-mechanical theory. To some degree all of these theories are probably relevant to any particular adhesion process. However, the group of factors which are of predominant importance will vary from one system to another — depending upon the physical and chemical properties of the substances involved.

According to the mechanical model (39), the adhesive bond is pictured as an intertwining network of surface irregularites at the interface between the two materials. This model is probably applicable to systems of liquid adhesives and porous adherends such as paper and wood. It has also been reported (40) that mechanical interlocking can be important to the adhesion of two metals. Generally it is felt, however, that other factors will have overriding significance in most systems (39).

For adhesion processes involving solid-liquid interfaces, the adsorption theory has been found to be useful. According to this theory (8), the adhesion process is described by the thermodynamics of adsorption of the liquid film onto the solid surface. It requires that the work of adhesion of the liquid to the solid be greater than the work of cohesion of the

liquid in order for spreading to occur. The application of this principle requires a knowledge of the surface energies of the substances involved, and is only useful when one phase is a liquid. In many important applications, this condition is met during the early stages of bond formation, but the situation may be quite different if the adhesive subsequently becomes rigid as is often the case. Under such circumstances, the work of plastic deformation greatly exceeds that due to changes in free surface energy (41). It has therefore been recognized (39) that this theory is often useful in providing some necessary but often insufficient criteria for good adhesion.

According to the diffusion theory of adhesion, there is a mutual interdiffusion which takes place when two thermoplastic materials are brought into intimate contact. The Russian workers in this field, notably Voyutskii and his colleagues (42-44) and Vasenin (45), have reported extensively on this model. They have found good correlations between the adhesion strengths of several polymer systems and factors such as molecular weight, temperature, and time of contact, which would affect the diffusional properties of the molecular chain segments. Further support has been given to this theory by Bueche (46), who studied the interdiffusion between polystyrene and polybutyl acrylate.

According to the electrical adhesion theory of Deryagin and Krotova (43,47-49), the interfacial region is regarded as an electrical condenser. The work of adhesion is then associated with the energy involved in the separation of charges. Evidence for the validity of this theory has been provided by Skinner and his associates (50,51), who observed that the separation of laminates between dielectric materials by peeling was often

accompanied by an electrical discharge, with potentials of the order of 100 to 10,000 volts.

The quantum-mechanical theory of adhesion involves rigorous application of the fundamental expressions for the different types of intermolecular forces. The application of this theory to a description of adhesion phenomena has been restricted to the most elementary systems thus far (39,52).

## WETTABILITY AND MEASURES OF SOLID SURFACE FREE ENERGY

The contact angle formed by a sessile drop of liquid resting on a solid surface has long been used as an inverse measure of the wettability of the solid. Young (53), in 1805, presented the following relationship from a consideration of mechanical equilibrium at the three-phase junction: $\gamma_{sv} - \gamma_{s\ell} = \gamma_{\ell v} \cos \theta$. In this equation, $\gamma_{sv}$ is the specific surface free energy (ergs/cm.$^2$) of the solid in equilibrium with vapor, $\gamma_{s\ell}$ is the specific free energy of the solid-liquid interface, $\gamma_{\ell v}$ is the specific free energy of the free liquid surface in equilibrium with its vapor, and $\theta$ is the solid-liquid contact angle as measured through the liquid between the solid surface and a tangent to the liquid surface at the three-phase boundary. A thermodynamic justification of Young's equation has been presented by Johnson (54). Deformation of the solid surface in the vicinity of the three-phase boundary has been theoretically considered by Lester (55).

Bangham and Razouk (56,57) emphasized in 1937 that the term $\gamma_{sv}$ is not generally equal to $\gamma_s$, the surface free energy of the solid in a vacuum. The difference between these two quantities is often labelled $\pi_e$, the equilibrium film pressure of the adsorbed vapor, and represents the amount by which the solid surface free energy is decreased by adsorption of vapor.

The value of $\pi_e$ at equilibrium conditions can be calculated from an integration of the liquid-solid adsorption isotherm. This term has been frequently neglected, and a critical review of such an assumption has been recently presented by Fowkes (58).

The familiar relationship defining the reversible work of adhesion at a solid-liquid interface was first described by Dupre (58A), and may be written as, $W_A = \gamma_s + \gamma_{\ell v} - \gamma_{s\ell}$, with all symbols having the same meaning as previously defined. This has been combined with the Young equation, with $\gamma_s = \gamma_{sv} - \pi_e$, to give, $W_A = \pi_e + \gamma_{\ell v}(1 + \cos \theta)$. The practical utility of this equation in adhesion problems can be seen from the experiments of Barbarisi (59), who observed a positive, linear relationship between the strength of polyethylene-epoxy bonds and the quantity $(1 + \cos \theta)$, where $\theta$ is the contact angle formed by the liquid adhesive on the solid surface.

A positive spreading coefficient has commonly been used as a thermodynamic requirement for a liquid to spread spontaneously on a solid. It is defined as the difference $(W_A - W_c)$, where $W_c$ is the work of cohesion of the liquid and is equal to $2\gamma_{\ell v}$.

The effects of surface roughness on the contact angle were considered by Wenzel (60), and later by Cassie and Baxter (61,62). It was shown that the effects were most important for contact angles in the vicinity of zero or 180 degrees. Roughness can also be responsible for a hysteresis between contact angles measured when the liquid front is caused to advance along the solid surface, and those observed when the liquid is caused to recede (63). Partially adsorbed films can also give rise to contact angle hysteresis, as was noted by Yarnold and Mason (64,65). An extensive treatment of the subject of contact angle hysteresis has been reported by Dettre and Johnson (66-69).

Quantitative application of contact angle measurements to the determination of solid surface free energy has been limited by the difficulty in evaluating the interfacial-energy term $\gamma_{s\ell}$, in the Young equation.

In many practical situations, a very useful concept has been Zisman's (37) "critical surface tension of wetting," $\gamma_c$. This quantity is determined by measuring contact angles between a given solid and several liquids. It was observed that when the liquids were chosen from a homologous series, a plot of cosine $\theta$ vs. $\gamma_\ell$ was often a linear relationship. Under these conditions, $\gamma_c$ was defined by the intercept of this line at cosine $(\theta) = 1$. The theoretical implications of this procedure have been discussed by several authors (70-75).

This method was used successfully to account for the adhesion of paper substrates to polyethylene by Swanson and Becher (34) and to various waxes by Glossman (35). The wettability of films of cellulose and cellulose derivatives has also been investigated according to this method by the laboratories of Ray (24,76-78) and by Luner and Sandell (79,80). The values of $\gamma_c$ obtained for regenerated cellulose films have been in the range of 35 to 49 ergs/cm.$^2$, while the values obtained of hemicellulose films were somewhat lower (33 to 36 ergs/cm.$^2$).

Girifalco and Good (71,81-83) and Fowkes (58,74,84-86) have advocated the use of geometric-mean relationships to describe the system of combined molecular forces acting across an interface. These theories have been extended to cover particular situations by several authors, including Owens and Wendt (75), Dann (73), Chan (72), and Wu (87). The application of these considerations to the relationships between contact angles and solid surface energy will be dealt with in a later section.

Other methods, not involving contact angles, for the estimation of solid surface energy have been described in the literature, and these have been suitably reviewed by Adamson (88).

## OBJECTIVES OF THE THESIS

The strength of water-induced bonds between cellulosic materials can be greatly increased if the substrate is treated, before bonding, in a corona discharge. The role of surface chemistry in this increased adhesion has not been established.

The primary objective of this thesis was to determine the effect of this treatment on the solid surface free energy and its polar and nonpolar components, and to relate these measurements to the observed increases in bond strength, according to the principles of surface chemistry.

## EXPERIMENTAL APPROACH

This section provides a brief summary of the experimental approach used to meet the objectives of the thesis. The reader is referred to the Experimental section for further detail.

Cellophane was chosen as a substrate in order to minimize effects due to chemical heterogeneity and surface roughness. Water-soluble extractives were removed from this material by a procedure involving alternate soaking and rinsing with distilled water. Procedures were developed for drying these films without wrinkling.

Equipment was designed to permit reproducible treatment of a six-inch wide, continuous film in a corona discharge between two electrodes covered with a dielectric material, and separated by an air gap. The treatment zone was enclosed, and a manifold system was provided for the safe removal and subsequent scrubbing of toxic gases formed by the discharge. The degree of treatment was varied by changing the speed at which the film passed through the corona chamber.

Procedures were developed for soaking the treated samples and forming bonds between them by wet-pressing and subsequent drying at room temperature. Care was taken throughout these procedures to guard the purity of the water and to ensure that all glassware was clean.

The strength of these bonds was evaluated by straining the laminates to rupture in the direction perpendicular to the plane of the sheets. The test involved the use of an epoxy adhesive to adhere opposite sides of a laminate to the plane surfaces of carefully machined steel cylinders which could be connected to the crosshead of a tensile-testing machine with their axes coincident with the line of force.

Contact angles were measured by means of a contact-angle goniometer, using purified contacting liquids. Steps were taken to control the humidity of the atmosphere in the vicinity of the liquid drops. The liquid surface tensions were determined by the duNouy ring method.

Oxidative effects of the corona treatment were evaluated by the techniques of methylene-blue adsorption and multiple internal reflection of infrared radiation. Physical effects were observed by means of electron-transmission microscopy on replicas of the treated surfaces.

## THEORETICAL CONSIDERATIONS

It has already been noted that a quantitative application of the Young equation to contact-angle data will require an evaluation of the specific free energy at the solid-liquid interface.

## THEORY OF INTERFACIAL FREE ENERGIES

The concepts of interfacial free energy have been considered in some detail by Good and his associates (71,81-83). They have found it useful to define a quantity, $\phi_{12}$, as the ratio of the free energy of adhesion between two phases, 1 and 2, to the geometric mean of the free energies of cohesion of the separate phases:

$$\phi_{12} \equiv - \Delta F_{12}{}^{a} / \sqrt{\Delta F_1{}^{c} \cdot \Delta F_2{}^{c}} \quad . \tag{1}$$

In terms of surface free energies, these quantities are expressed as follows:

$$- \Delta F_{12}{}^{a} \equiv \gamma_1 + \gamma_2 - \gamma_{12} \quad , \tag{2}$$

$$- \Delta F_1{}^{c} = 2\gamma_1 \quad , \quad - \Delta F_2{}^{c} = 2\gamma_2 \quad . \tag{3}$$

Combination of the above equations provides an expression for the interfacial free energy, $\gamma_{12}$, in terms of surface free energies.

$$\gamma_{12} = \gamma_1 + \gamma_2 - 2\phi_{12}\sqrt{\gamma_1\gamma_2} \quad . \tag{4}$$

Expressions for the free energies of adhesion and cohesion in terms of molecular properties were derived by integration of a Lennard-Jones potential energy function from equilibrium intermolecular distance to infinite separation (83). The resulting expressions for $\phi$ are of the form,

$$\phi_{12} = (A_{12}/\sqrt{A_{11} \cdot A_{22}}) \cdot (r_1 r_2 / r_{12}^2) = \phi_A \cdot \phi_r \ , \qquad (5)$$

where the A's are the attractive constants in the potential energy function, and the r's represent equilibrium intermolecular distances.

The term $\phi_r$ is generally very close to unity, provided that the molecular sizes of the two substances are not drastically different (83). The other component of $\phi$,

$$\phi_A \equiv A_{12}/\sqrt{A_{11} \cdot A_{22}} \ , \qquad (6)$$

is evaluated from the parameters that determine intermolecular potential functions. For the general case where all three of the common types of secondary valence forces are operative,

$$A = A(\text{dispersion}) + A(\text{induction}) + A(\text{orientation}). \qquad (7)$$

The separate contributions are expressed as

$$\text{dispersion:} \quad A_{12}^{d} = (3/4)\alpha_1\alpha_2 \cdot 2I_1I_2/(I_1 + I_2) \qquad (8)$$

$$\text{induction:} \quad A_{12}^{i} = \alpha_1\mu_2^2 + \alpha_2\mu_1^2 \qquad (9)$$

$$\text{orientation:} \quad A_{12}^{o} = (2/3)\mu_1^2\mu_2^2/kT \ , \qquad (10)$$

where the $\alpha$'s are polarizabilities, the $\mu$'s are dipole moments, and the I's are ionization energies, k is the Boltzmann constant, and T is the absolute temperature.

The induction terms are, in general, relatively small (83), and can often be neglected. Under these conditions, the components of $A_{12}$ can be expressed as geometric means of the components of $A_{11}$ and $A_{22}$:

$$A_{12}^{d} \approx \sqrt{A_{11}^{d} \cdot A_{22}^{d}} \ , \qquad (11)^{*}$$

$$A_{12}^{o} = \sqrt{A_{11}^{o} \cdot A_{22}^{o}} \ . \qquad (12)$$

It should be noted that it is due to the particular way in which dispersion- and orientation-forces interact that this simplication can be made. The form of Equation (9) does not permit the description of induction-force interactions in this way (i.e., as a geometric-mean relationship).

Assuming the approximation of Equation (11) to be valid, Equation (6) may be combined with Equations (7), (11), and (12), to give

$$\Phi_A = \sqrt{(A_{11}^{d}/A_{11}) \cdot (A_{22}^{d}/A_{22})} + \sqrt{(A_{11}^{o}/A_{11}) \cdot (A_{22}^{o}/A_{22})} \ . \qquad (13)$$

It is useful to define a quantity, $\underline{p}$, which may be termed the "fractional polarity" for each surface:

$$p_1 = A_{11}^{o}/A_{11} \ , \qquad (14)$$

$$p_2 = A_{22}^{o}/A_{22} \ . \qquad (15)$$

The complements, $\underline{d}$, of these quantities represent the relative significance of dispersion forces at each surface:

$$d_i = A_{ii}^{d}/A_{ii} \ , \qquad (16)$$

$$d_i + p_i = 1, \ i = 1, 2 \ . \qquad (17)$$

*The strict equality of Equation (11) is dependent upon the equality of the arithmetic- and geometric-means of the terms $\underline{I}_1$ and $\underline{I}_2$. This will be a good approximation unless the ionization energies differ greatly.

Equation (13) then becomes:

$$\phi_A = \sqrt{d_1\ d_2} + \sqrt{p_1\ p_2} \quad . \tag{18}$$

A relationship similar in form to Equation (18) was recently suggested by Wu (87) without proof. The fractional quantities corresponding to p and d were defined in terms of polar and nonpolar components of surface free energy:

$$d_i = \gamma_i^d/\gamma_i \quad , \tag{19}$$

$$p_i = \gamma_i^p/\gamma_i \quad . \tag{20}$$

If these quantities are substituted into Equation (18), Equation (4) then becomes (with $\phi_r = 1$):

$$\gamma_{12} = \gamma_1 + \gamma_2 - 2\sqrt{\gamma_1^d\gamma_2^d} - 2\sqrt{\gamma_1^p\gamma_2^p} \quad . \tag{21}$$

This relationship is the same equation which was recently proposed by Owens and Wendt (75).

If one of the substances is nonpolar, and capable of interaction by dispersion forces only, then Equation (21) reduces to that proposed by Fowkes (74):

$$\gamma_{12} = \gamma_1 + \gamma_2 - 2\sqrt{\gamma_1^d\gamma_2} \quad , \text{ for } \gamma_2^p = 0. \tag{22}$$

## APPLICATION TO CONTACT-ANGLE DATA

The Young equation may be written in the following form:

$$\gamma_{lv} \cos\theta = \gamma_{sv} - \gamma_{ls} \tag{23}$$

where $\gamma_{lv}$ is the specific free energy of the liquid-vapor interface, $\gamma_{ls}$ is the corresponding quantity for the liquid-solid interface, $\gamma_{sv}$ is specific free energy of the solid-vapor interface, and $\theta$ is the contact angle as previously defined.

It is recognized that the term, $\gamma_{sv}$, is different from the specific surface free energy of the clean solid surface, by virtue of vapor adsorption. The subscript, v, will be omitted in the following treatment, but it is kept in mind that the solid surface under consideration is in equilibrium with vapor, and its characteristics will therefore be dependent on the composition of the vapor phase.

It is also recognized that the effects of surface roughness on the contact angles may need to be considered. These may be taken into account by application of Wenzel's (60) equation, which is obtained by multiplying the right-hand side of Equation (23) by a quantity, R, which represents the relative roughness of the surface and which has a value of unity for a perfectly smooth surface. (R represents the ratio of actual surface area to projected area, and is always greater than unity for a real surface.)

With the above conditions, Equations (23) and (4) are combined:

$$\cos \theta = -1 + 2 \phi_{s\ell} \sqrt{\gamma_s / \gamma_\ell} \ . \tag{24}$$

Equation (25) illustrates the relationship between Zisman's (37) "critical surface tension of wetting," $\gamma_c$, and the solid surface free energy, $\gamma_s$. This equation is obtained by allowing cosine $\theta$ to approach unity as $\gamma_\ell$ approaches $\gamma_c$ in Equation (24), assuming that $\phi_{s\ell}$ is a constant. It may be seen from Equation (18) that the constancy of $\phi_{s\ell}$ is dependent upon the use of a series of liquids which have mutually similar values of fractional polarity,

$$\gamma_c = \phi_{s\ell}^2 \gamma_s \ . \tag{25}$$

It can also be seen from Equations (18) and (25) that $\gamma_c$ will only be equal to $\gamma_s$ when the fractional polarities of the liquids are equivalent to those of the solid.

A more useful form of Equation (24), for the present application, can be obtained by combining Equation (21) with the Young equation:

$$\cos\theta = -1 + 2\sqrt{\gamma_s^d \cdot \gamma_\ell^{d'}/\gamma_\ell} + 2\sqrt{\gamma_s^p \cdot \gamma_\ell^{p'}/\gamma_\ell} \qquad (26)$$

This equation permits the calculation of both $\gamma_{\underline{s}}^{\underline{d}}$ and $\gamma_{\underline{s}}^{\underline{p}}$ from contact angles with two liquids for which $\gamma_{\underline{\ell}}$, $\gamma_{\underline{\ell}}^{\underline{d}}$, and $\gamma_{\underline{\ell}}^{\underline{p}}$ are known. This technique was first described by Owens and Wendt (75), and was used by them to calculate the components of surface energy for several solid polymers. The parameters $\gamma_{\underline{\ell}}^{\underline{d}}$ and $\gamma_{\underline{\ell}}^{\underline{p}}$ for a particular liquid can be calculated from a measurement of interfacial tension against a second liquid for which the components are already known, using Equation (21).

# EXPERIMENTAL EQUIPMENT, MATERIALS, AND PROCEDURES

## WATER PURIFICATION AND CLEANSING OF GLASSWARE

The bulk of the water used in this study was obtained from a large-scale supply of water which had been first deionized and then distilled. Water from this source is referred to as "distilled water." This product was further purified for use in the final stages of all soaking and rinsing procedures by two additional stages of distillation. Following the procedure of Bauer and Lewin (89), the first stage consisted of distillation from a solution of 0.02% potassium permanganate and 0.05% sodium hydroxide. This was followed by distillation from dilute sulfuric acid in the second stage. All components of the still were constructed of pyrex. Water prepared in this manner is referred to as "triply-distilled water."

All glassware was cleaned with a saturated solution of sodium dichromate in concentrated sulfuric acid. This was followed by thorough rinsing with distilled water and finally with triply-distilled water. The glassware was then dried in an oven.

## DESCRIPTION OF SUBSTRATE

The cellophane substrate used throughout this study was obtained from E. I. du Pont de Nemours & Co. The manufacturer's designation was 215-PD. This product had a nominal thickness of 0.001 inch and was obtained in the form of 6-inch wide rolls, wound on 3-inch fiber cores. Information received from the supplier stated that this grade of cellophane had been manufactured from cellulose xanthate and contained no plasticizers.

In spite of this information, very significant amounts of water-soluble material were found to be present in this substrate. Repeated soaking in cold water resulted in weight losses of about 18% on an original ovendry basis. No further weight losses were observed when the substrate was subsequently soaked in carbon tetrachloride or ethanol.

A Perkin-Elmer Model 700 grating spectrophotometer was used to record the infrared absorption spectra of films before and after treatment. Absorption peaks at 920 and 850 $cm.^{-1}$ in the spectra of the untreated films were not found in the spectra of the water-soaked samples. Absorption peaks were found at the same frequencies in spectra of glycerol. These observations were taken as evidence that glycerol was present in the cellophane as a plasticizer and that it could be removed by cold-water extraction.

## SOAKING PROCEDURES

A standard procedure was developed for soaking the cellophane sheets in water to remove soluble materials and for subsequently drying the films without wrinkles.

Sheets of cellophane approximately two feet in length by six inches in width were cut from the roll as supplied. One corner of each sheet was cut so that the respective sides could be later identified. Each sheet was then soaked for two hours in one liter of distilled water held in a clean pyrex tray. A set of stainless-steel spring clips, designed for use in paper chromatography, were used throughout this procedure to obviate the necessity of direct hand contact with the samples.

Each sheet was then removed from the bath and hung in a vertical position, where it was thoroughly rinsed with triply-distilled water from a

wash bottle. Each sheet was then soaked for an additional half hour in one liter of fresh triply-distilled water. From a consideration of film volume in relation to bath volume it is estimated that the amount of glycerol in the samples after this sequence should be of the order of a hundred parts per million.

The sheets were laid out flat on a wet Lucite surface, which had been cleaned first with Alconox solution followed by rinsing with distilled water and finally with triply-distilled water. A teflon-covered roller, manufactured for the purpose of photographic processing and loaded to a total weight of twenty pounds, was used to flatten the sheets against the Lucite surface. The edges of the sheets were then constrained with cellophane tape, and the samples were allowed to air dry at 23°C. and 50% R.H. The tape was finally removed from the dried sheets, which were then peeled away from the Lucite surface. The "air-sides" were so identified.

The physical character of the cellophane surfaces is illustrated in Fig. 3 and 4. These figures are transmission electron-micrographs of surface replicas. Figure 3 shows the surface of the cellophane as received. No differences were noted between the two sides of this material. Figure 4 illustrates, at the same magnification, the effect of soaking the sample in water with subsequent drying against Lucite. The surface which was in contact with air during drying is viewed here. The large lumps visible in Fig. 3 are not present on the surface of the soaked sample. On a smaller scale, however, there is an irregular pattern of small surface cracks present on the surface of the soaked material, which was not found on the surfaces before soaking. (Although this pattern was clearly visible in glossy prints of these micrographs, it is not readily apparent in the halftone print of Fig. 4.)

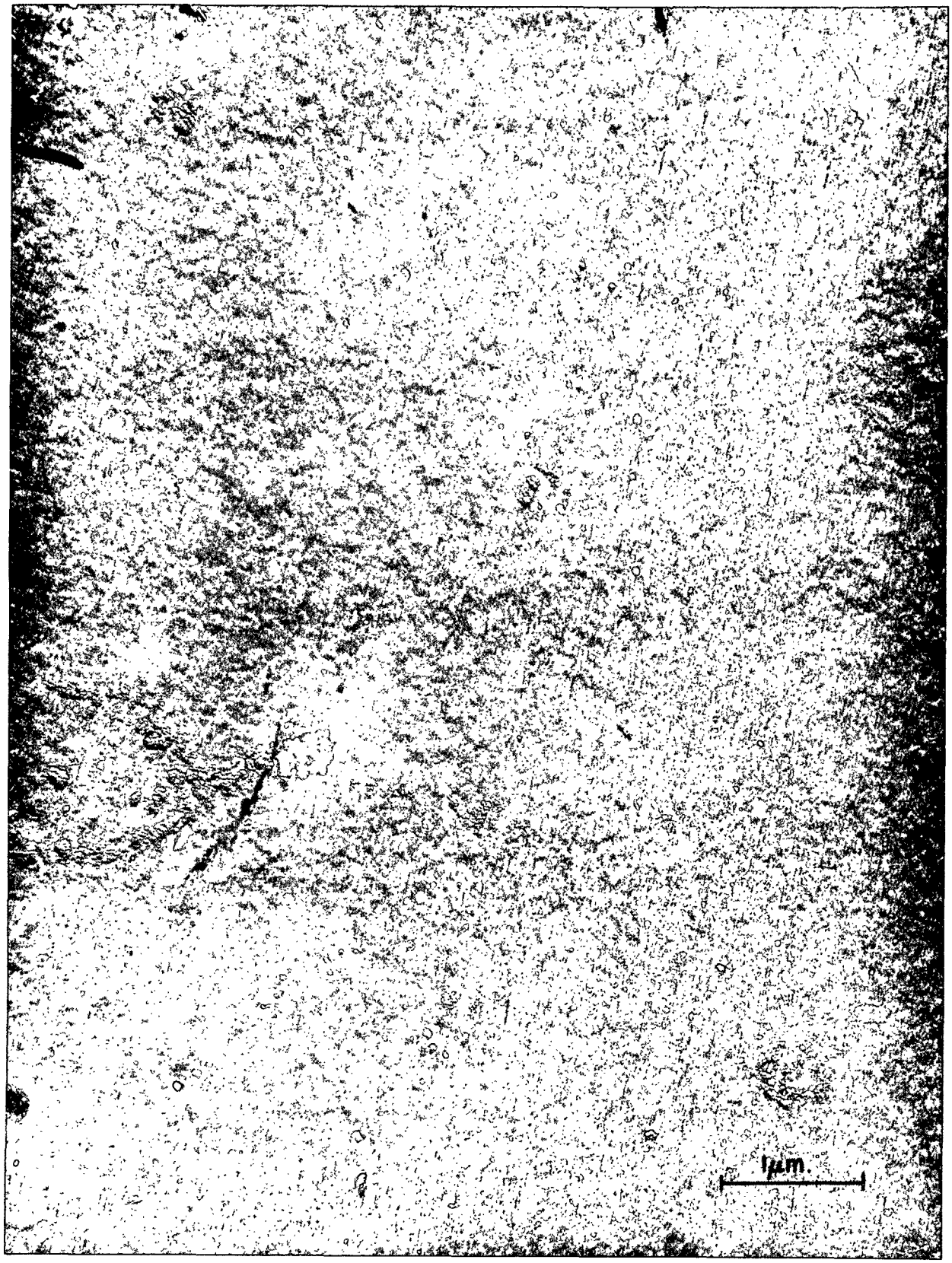


Figure 3. Replica of Cellophane as Received

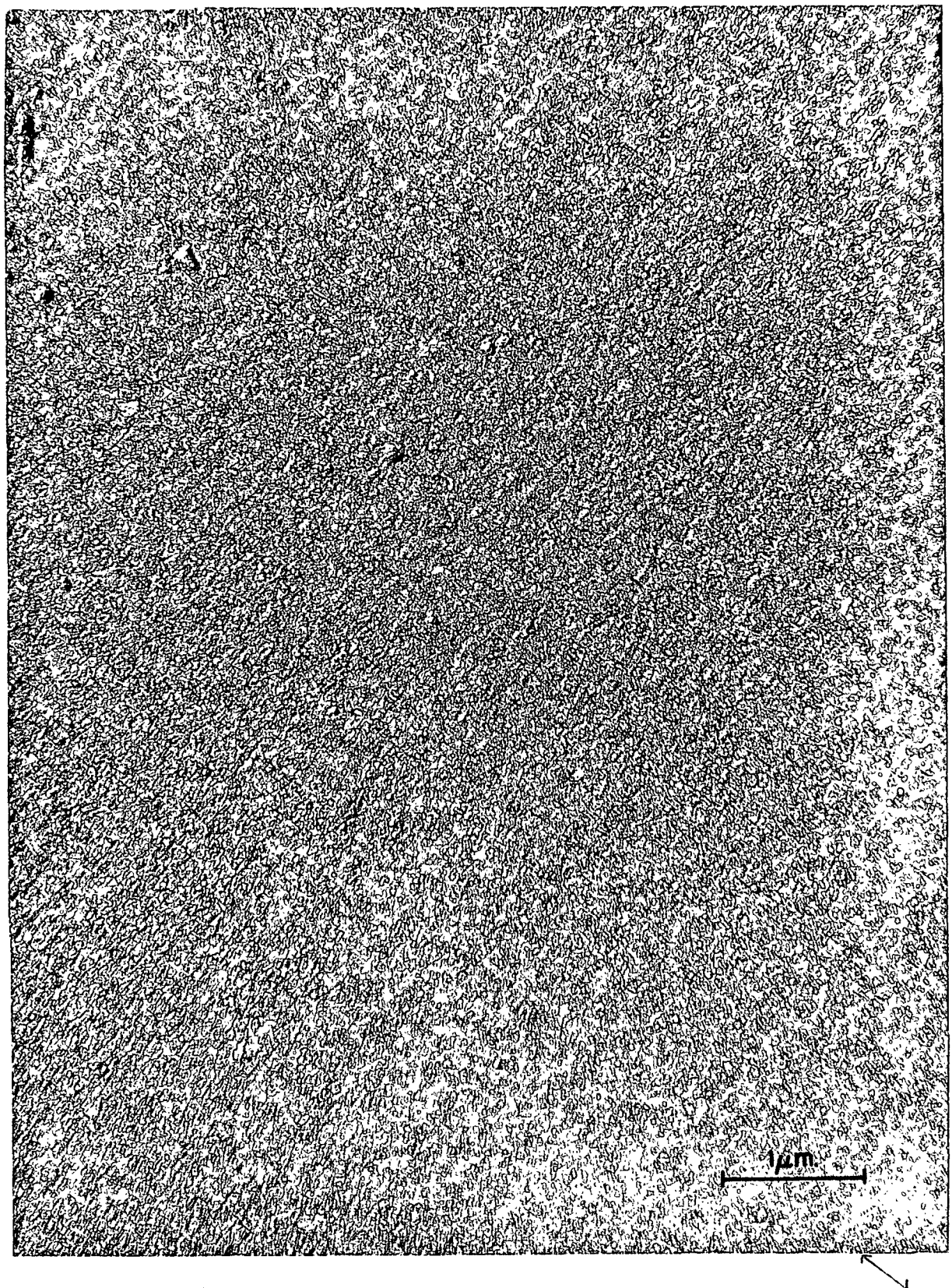


Figure 4. Replica of Cellophane Soaked in Water, Air-Dried Against Lucite: (Air Side)

## SURFACE ROUGHENING PROCEDURES

In the preparation of samples for bond-strength evaluation, an additional step was included in the above procedure. It was necessary to roughen one surface of these sheets in order to obtain suitably strong adhesion between the cellophane surface and the epoxy adhesive used in the strength tests.

The roughening was done after drying, but before removal of the sheets from the Lucite surface. The exposed sample surface was dusted with American Optical Company's emery powder No. 303. (This product is a graded abrasive with an average particle size of 15 μm.) The surface was then abraded with a soft felt pad backed by a 1/2-inch thick, 3 inch by 5 inch brass plate. The felt-brass fixture was moved manually in a rotary fashion with no vertical hand pressure.

Normally, one surface of each sheet received 400 strokes in the above manner. The surfaces appeared uniformly opalescent following this treatment. The remaining emery dust was then removed by gentle sweeping with a camel-hair brush.

## CORONA DISCHARGE EQUIPMENT

Equipment to permit treatment of a continuous, 6-inch web of material in a corona discharge was designed and constructed. A schematic diagram of the general configuration is given in Fig. 5. A detailed description of the design and calibration procedures may be found in Appendix I.

A continuous-treatment scheme was chosen over batch treatment in order to minimize variation in surface treatment due to edge effects and

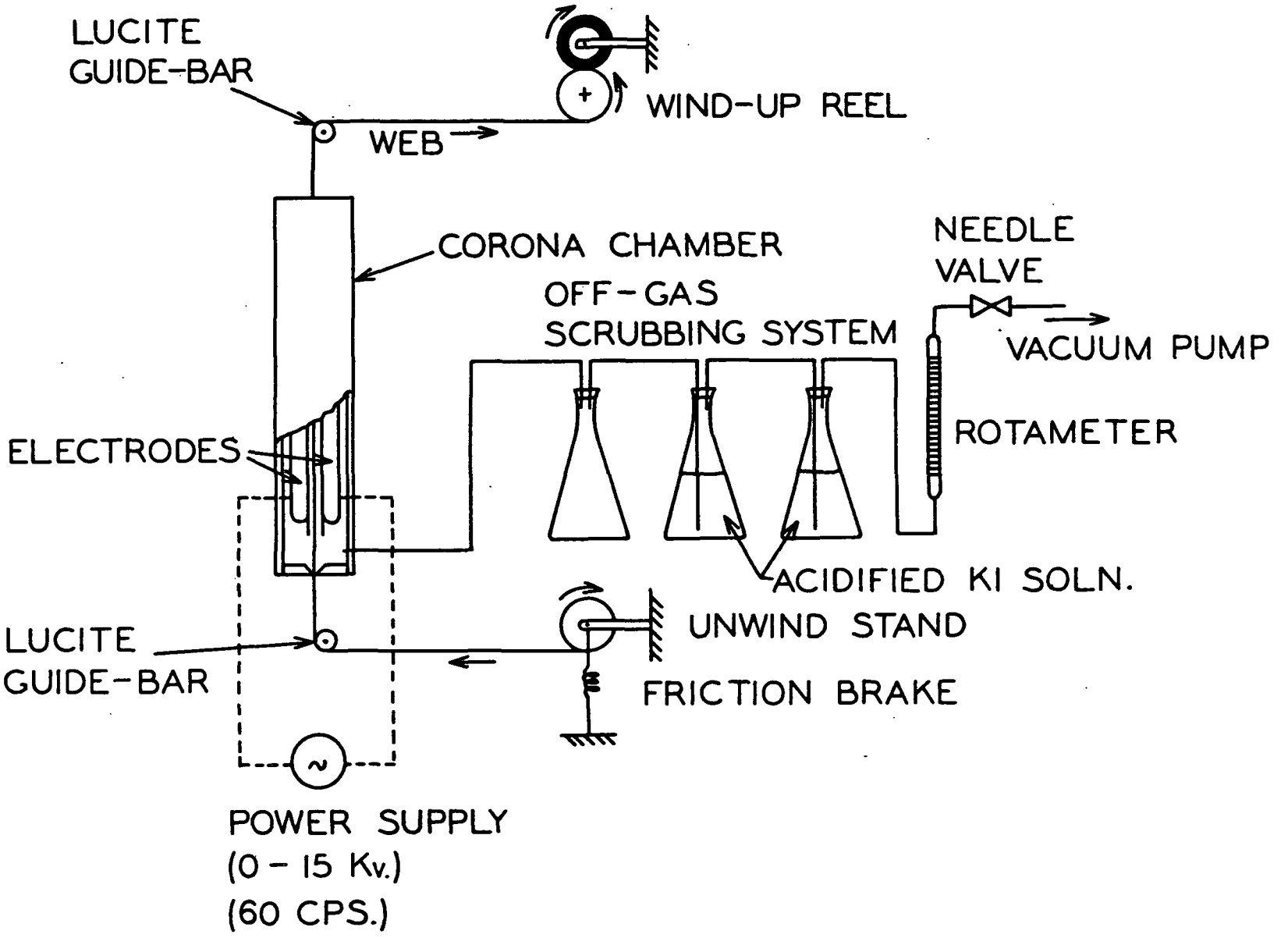


Figure 5. Schematic Diagram of Corona-Treating Equipment

local variations in the intensity of the discharge. This scheme also permitted reproducible treatment of large quantities of material at one time.

The electrodes were constructed of 1-inch thick aluminum and measured 12 inches in the machine direction by 6 inches in the cross-machine direction. All edges and corners were carefully rounded and the entire surface of each electrode was polished to minimize the chance for local arcing to occur. The inner surface of each electrode was in contact with a sheet of 0.030-inch thick, natural mica, which served as a dielectric barrier. The mica sheets overlapped the extremities of the electrodes by one inch on all sides. The mica sheets were separated by a 1/4-inch air-gap, through the center of which the sample web was passed. The electrodes were positioned vertically in order to minimize nonuniformity of treatment due to web sag.

The web was advanced by a variable-speed drive mechanism, with tension being controlled by a friction brake on the unwind stand. The web speed was continuously variable in the range of 2.0 to 26.0 inches/minute, using drive sprockets having a 1/1 ratio. An additional set of sprockets was available in the ratio of 2.4/1, which could be used to extend the range of available web speeds. The effective treatment time was arbitrarily taken as the ratio of the length of the discharge zone (12 inches) to the linear speed of the web.

The power supply was constructed from a 15,000-volt neon-lamp transformer. The electrode potential was measured by means of a calibrated, low-range AC voltmeter in conjunction with a step down transformer. A variable transformer was placed in the primary circuit of the power

transformer so that the electrode potential could be varied from 0 to 15,000 volts. Provision was also made for measuring the current in the primary circuit. The frequency was constant at 60 cycles/second.

The electrode area was carefully insulated and enclosed with Micarta. A manifold system was installed near the bottom of the treatment chamber to permit the continuous removal of product gases. The purpose of this system was to control the composition of the gas phase as well as to protect the operator from toxic product gases. The product-gas stream was scrubbed by bubbling through acidic potassium iodide solution. The amount of reducible species in the product gases could be estimated by titrating aliquots of the scrubbing solution with sodium thiosulfate. At an electrode potential of 13 kilovolts, the rate of generation of oxidizing species was found to be about 0.07 meq./min.

## CORONA TREATING PROCEDURES

Following the presoaking sequence and conditioning at 23°C. and 50% R.H., the cellophane samples were removed from the Lucite surface by peeling and corona treated. Leaders were attached to the sheets so that they could be fed through the apparatus under suitable tension and with a minimum of wrinkling. Normally the electrode potential was held constant at 13,000 volts, the primary current was 1.15 amps., and the web speed was varied to obtain treatment times in the range of 0.2 to 0.5 min. Following treatment, the films were stored at 73°F. and 50% R.H. until further use. (Normally the samples were removed from the free section of the web, after passage through the corona chamber, but before wind-up.)

## BONDING PROCEDURES

Following the procedures of Janes (90), water-induced bonds were formed between treated samples after repeating the soaking sequence previously described. Following removal of the sheets from the second bath, they were placed on the Lucite surface, and each sheet was folded in half upon itself with the roughened sides out. The fold was always in the cross-machine direction with the machine direction of each half of the laminate parallel to that of its counterpart. The laminates were then rolled flat as before, and were allowed to air-dry with the edges constrained by cellophane tape.

## EVALUATION OF BOND STRENGTHS

The bond strengths were evaluated by straining these laminates to rupture in the direction perpendicular to the plane of the bond, using the Z-direction tensile test described by Wink and Van Eperen (91).

The procedure may be summarized as follows: Disks with a diameter of 1.125 inches were cut from the laminates with a circular die. Shell Chemical's Epon 907, mixed from equal volumes of epoxy resin and activator, was used to adhere each side of a disk to the plane surface of a carefully-machined steel cylinder. A filming jig facilitated the application of a uniform, 0.0035-inch thick, adhesive film to the cylinder surfaces after cleaning with methanol. An interval of 15 minutes was arbitrarily set as the maximum elapsed time between mixing of the adhesive and its use.

A V-groove alignment jig was used to provide axial alignment of the specimen disk and the cylinders during assembly and to provide dead-weight compressive loading of the assemblies during the curing of the adhesive. The curing conditions were 24 hours at 23°C. and 50% R.H., with a compressive load of 5.7 p.s.i.

After curing of the adhesive, the test assemblies were mounted between the stressing jaws of a Baldwin-Southwark testing machine. (The Baldwin unit, rather than an Instron tester, was used here to accommodate the large loads required for rupture of these samples.) The connection was made via cylindrical couplings attached to stirrups by means of cup-and-ball supports, as described by Wink and Van Eperen (91). This arrangement provided self-alignment of the cylindrical axis with the line of force. A loading rate of 0.05 inch/minute was employed in this study.

The ruptured surfaces were examined for evidence of adhesive-specimen failure or adhesive-metal failure. Only rarely was either of these modes significant, provided that the sample surfaces had been roughened with emery powder, and that care had been taken to use the adhesive within the prescribed time after mixing. In the small number of cases where either of these modes of failure was clearly predominant, the test was rejected and the procedures were repeated.

The hardened adhesive was removed from the test cylinders by soaking for one hour in methanol.

## MEASUREMENT OF CONTACT ANGLES

### CONTACTING LIQUIDS

The calculation of components of solid surface free energy from contact-angle data, according to the theory previously outlined, required the measurement of finite contact angles between each surface and at least two different liquids. It was further required that the liquids differ significantly with respect to the polar component of their surface tension.

Three suitable liquids were found to give reasonably stable, finite contact angles on all of the cellophane samples: water, methylene iodide, and 1,1,2,2-tetrabromoethane. Water represented a liquid having a high polar component to its surface tension and could be paired with either of the organic liquids, which have very weak polar forces. Pairing of the data in these two ways permitted replication of the calculations and a check on the validity of the method.

The water was triply distilled as previously described. The two organic liquids were obtained as reagent-grade compounds from a commercial supplier and were purified by vacuum distillation. The details of these procedures may be found in Appendix II.

The liquid surface tensions were measured at 23.4°C. using a Cenco-duNouy interfacial tensiometer, Model 10403. For water, the appropriate corrections to these data for meniscus shape were made using the published data of Harkins and Jordan (92). When attempts were made, however, to apply these corrections to the data of the two organic liquids, it was found that the appropriate correction factors were outside the range of the published data. The theoretical treatment of Freud and Freud (93) was used to reduce the data of Harkins and Jordan to dimensionless variables, which could then be extrapolated to cover the desired range. The details of this procedure are summarized in Appendix III.

The corrected values of surface tension and infrared absorption spectra for the purified liquids were in good agreement with published values. Analysis of the organic liquids was also accomplished with a gas chromatograph, equipped with a thermal conductivity detector and a Porapak Q

column for liquid separation. A single peak was obtained, and no evidence of water or other volatile contaminant was found.

## APPARATUS AND PROCEDURES

Contact-angle measurements were made at 23.4°C. and either 50% R.H. or in a dry nitrogen atmosphere. The samples were cut into small strips and mounted on clean microscope slides with cellophane tape, under tension to minimize wrinkling. The specimens were previously conditioned for at least 12 hours in the same atmosphere at which the measurements were to be made. A carefully cleaned micropipet was used to dispense 3 μ-liter drops, and all readings were made within 5 to 10 sec. after placement of the drop on the solid surface.

For the contact angles at 50% R.H., a direct-reading contact-angle goniometer, manufactured by Rame-Hart (Model A-100), was employed. This instrument was equipped with a variable-intensity light source and heat filter to minimize evaporation of the drops. The optical system contained two crosshairs which could be independently rotated within the internal focal plane. A protractor indicated, in degrees, the magnitude of the angle between the crosshairs. The procedure was to adjust one of the crosshairs to coincidence with the solid-liquid interface, and the other was rotated so as to form a tangent to the free liquid surface at the three-phase junction. The angle was measured through the liquid phase. The samples rested on a platform which was adjustable in three dimensions for proper positioning of the drops with respect to the optical system.

Readings in the dry atmosphere were made with a second goniometer which was equipped with a transparent chamber to permit control of the

atmosphere in the vicinity of the drop. This instrument was constructed of a petrographic microscope with the barrel mounted in a horizontal-position, as sketched in Fig. 6.

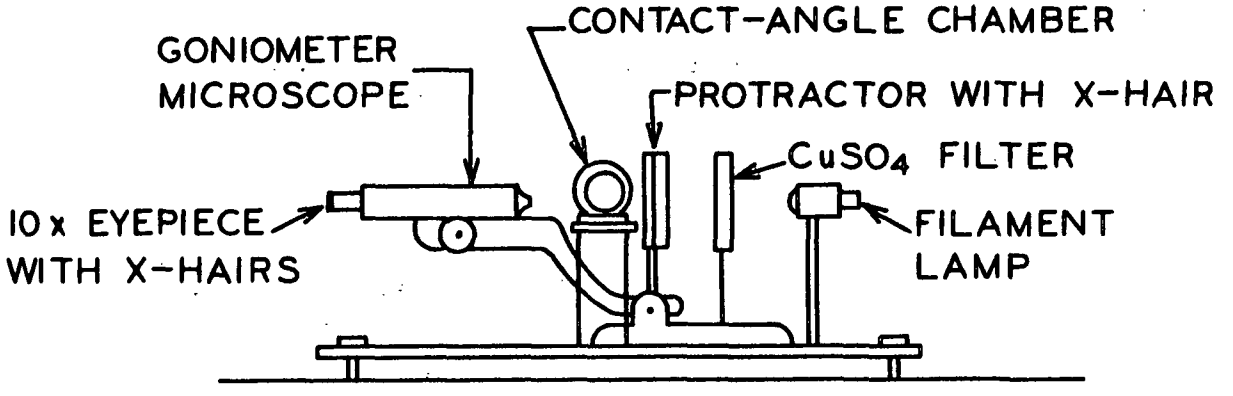


Figure 6. Contact-Angle Goniometer

Unlike the Rame-Hart goniometer, the crosshair of the protractor in this instrument was not coincident with the focal plane. The eyepiece was free to rotate and was equipped with a second set of crosshairs which could be adjusted to form a tangent to the drop image. The optical system was then refocused on the plane containing the protractor crosshair, which could then be aligned with the crosshair in the eyepiece to determine the contact angle.

The contact-angle chamber was constructed from a Lucite tube by milling away portions of the cylindrical surface and installing two parallel viewing windows perpendicular to the line of sight. A horizontal platform inside the chamber was provided to support the samples, and the entire assembly was mounted on a stage which was adjustable in three dimensions. A polyethylene glove-bag was

fitted to one side of the chamber to provide a conditioned storage area for the samples. A rubber stopper was fitted into the other side of the chamber and contained a humidity-sensing probe, which was connected to an Aminco-Dunmore electric hygrometer. The liquid drops were dispensed from a micropipet which was inserted in a slot in the top of the chamber. The design of the contact-angle chamber is given in more detail in Appendix IV.

The relative humidity within the chamber was kept below 2% by passing dry nitrogen into the glove bag and allowing it to exit through the slot, around the periphery of the pipet tip. An open dish of magnesium perchlorate was kept inside the glove bag to serve as a desiccant. The particular humidity-sensing probe which was used had a range of 1.6 to 6% R.H. All data at the low humidity were recorded at hygrometer readings of less than 1% of full scale, which should correspond to relative humidities of less than 2%.

## EVALUATION OF PHYSICAL SURFACE CHARACTERISTICS

### CHAPMAN SMOOTHNESS

Measures of surface roughness and conformability, and the effect of humidity on these properties, were obtained with a modified version of the Chapman smoothness tester. The instrument was essentially the same as that described by Sears, et al. (94), except that the electronic circuit had been modified to provide direct read-out of the printing-smoothness value, F, after proper calibration. The calibration procedures were as outlined in that publication, using an opal-glass block as a standard and a film of clear mineral oil to establish the complete-contact condition. These procedures are described in more detail in Appendix V.

The cellophane samples, with or without corona treatment, were first conditioned at 23°C. and a relative humidity of 15, 50, or 70%. During testing, the samples were backed by the same opal-glass block which had been used in the calibration of the instrument. A 1/8-inch thick, rubber blanket was inserted between the glass block and the lower prism of the instrument to ensure even load distribution and to protect the prism surface from damage at high load levels. Nominal loads were varied in the range of 0 to 400 p.s.i.

### ELECTRON MICROSCOPY

Transmission electron-microscopy was used to evaluate some of the physical effects of interest here. Surfaces of the cellophane were first shadowed with palladium at an angle of 30°. Carbon was then vaporized onto the palladium surface to increase the mechanical strength and complete the replica. These specimens were then covered with a support of polystyrene, soaked overnight in water, and the cellophane removed by peeling. The replicas were then cleaned with a 72% aqueous solution of sulfuric acid, placed over a 100-mesh nickel grid, and the polystyrene backing dissolved in benzene.

## EVALUATION OF CHEMICAL EFFECTS

### MULTIPLE INTERNAL REFLECTION SPECTROSCOPY

Chemical changes produced in the cellophane surface by the corona treatment were evaluated by the techniques of multiple internal reflection (MIR) of infrared radiation. A Perkin-Elmer Model 621 spectrometer, equipped with an MIR attachment, was used for this purpose. The spectra

were recorded differentially, with an identical cell containing an untreated sample in the reference beam. Both sample chambers were purged with dry nitrogen during the measurements. The reflection crystals were KRS-5 with 45° light-facets, and 45° was also the angle of light-incidence upon the sample.

METHYLENE BLUE ADSORPTION

The extent of oxidation produced by the corona treatment was determined from measurements of the adsorption of methylene blue by the cellophane samples, according to TAPPI Standard T 237 su-63. Each sample was rotated for 12 hours at 25°C. in contact with 50 ml. of a buffered solution which was $2 \times 10^{-4}$ M in methylene blue, $6.25 \times 10^{-4}$ M in barbital, and $4.0 \times 10^{-4}$ M in sodium hydroxide. Adsorption was determined by colorimetrically measuring the decrease in the concentration of methylene blue in the supernatant solution with a Beckman Model DU spectrophotometer at a wavelength of 620 nm.

## EXPERIMENTAL DATA AND DISCUSSION OF RESULTS

### BOND STRENGTHS

The observed bond strengths at several levels of corona treatment are given in Table II. The raw data may be found in Appendix VI. All of these data represent samples which were presoaked in water, corona treated at 13 kv., and bonded with the "Lucite-sides" in contact (the sides which had been dried against the Lucite surface after the soaking sequence). Samples bonded with the "air-sides" in contact gave substantially the same results.

TABLE II

OBSERVED BOND STRENGTHS

| Treatment Time, min. | Number of Replicates | Mean Breaking Load, lb. | Apparent Breaking[a] Stress, p.s.i. |
|---|---|---|---|
| 0 | 5 | 576 ± 48[b] | 748 ± 62[b] |
| 0.2 | 10 | 1280 ± 32 | 1662 ± 42 |
| 0.5 | 20 | 1520 ± 49 | 1974 ± 64 |
| 1.0 | 20 | 1680 ± 55 | 2181 ± 71 |
| 3.0 | 20 | 1960 ± 62 | 2545 ± 80 |
| 5.0 | 25 | 2051 ± 96 | 2663 ± 125 |

[a] Apparent breaking stress based on area of 0.7702 in.$^2$

[b] 95% Confidence limits = $\underline{t}$ · (standard error of mean) ($\underline{95}$).

The values of apparent breaking stress were calculated on the basis of the area of the test cylinders, which were 0.9903 inch in diameter. This quantity is shown as a function of treatment time in Fig. 7, and as a function of log-time in Fig. 8.

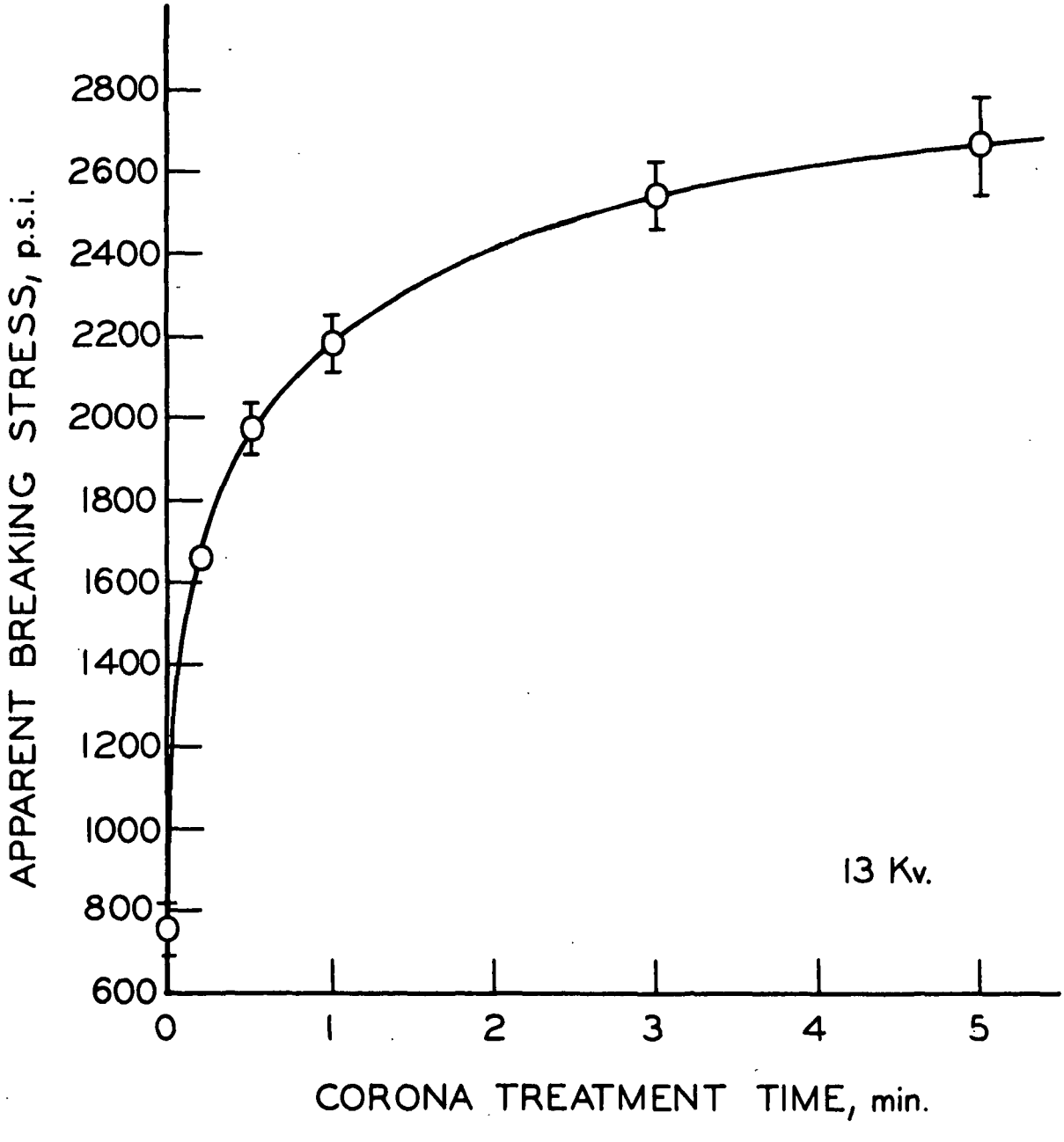


Figure 7. Apparent Breaking Stress Versus Corona Treatment Time

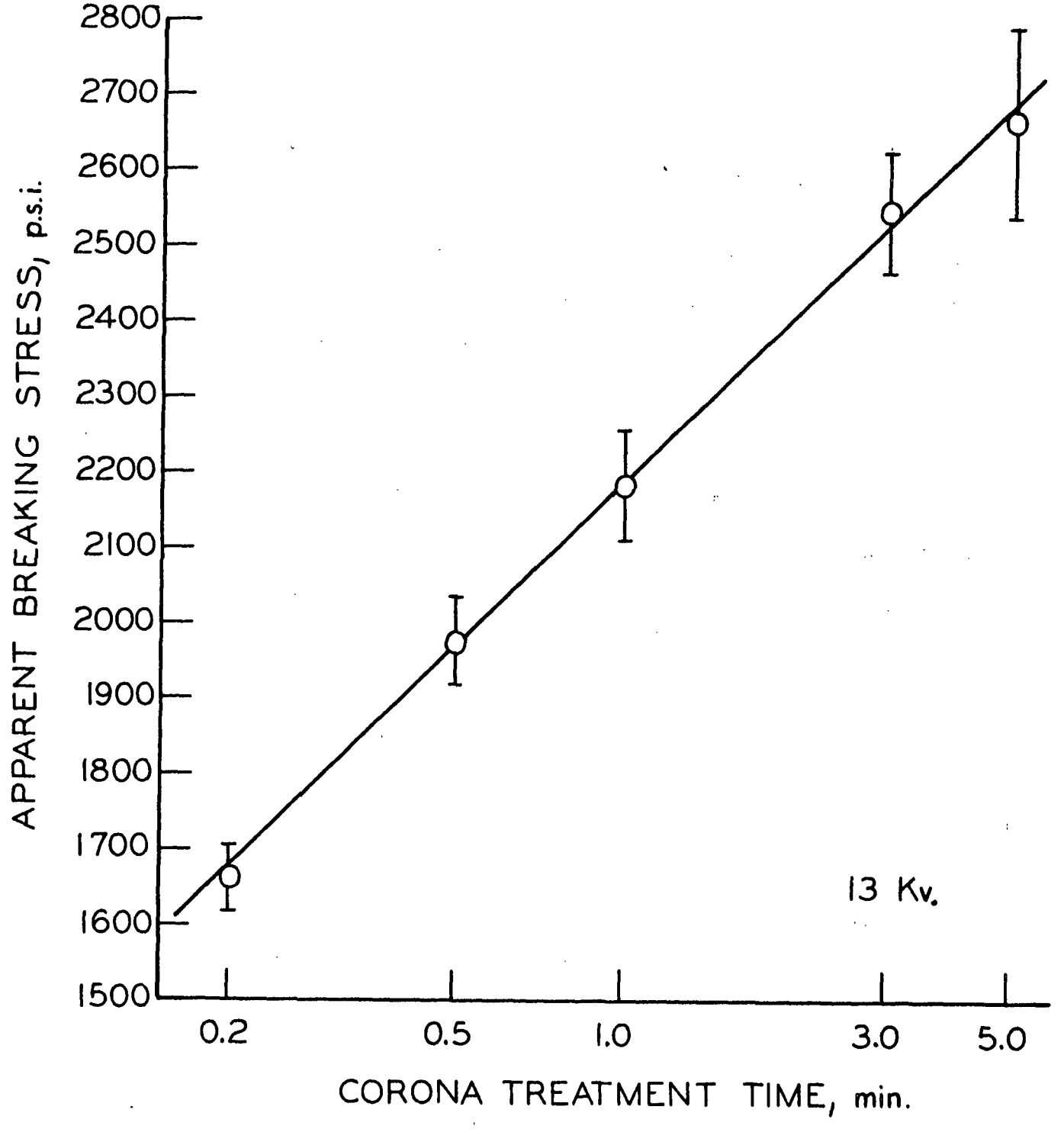


Figure 8. Apparent Breaking Stress Versus Logarithm of Corona-Treatment Time

No particular significance is placed on the apparent linear relationship between strength development and the log of time, except that this is a clear illustration that significant increases in strength can be obtained with relatively short treatment times. This observation is in agreement with the idea that the important feature of this treatment is that it is a surface effect, and that increased bonding can be obtained without modification of the substrate at any appreciable depth below the surface.

Smaller increments in strength are obtained as the time of treatment is increased. It was also noted that failure begins to occur at points beneath the interface as the strength of the interfacial bond is increased. It is not clear whether this is due to an increase in the strength of the interfacial bond above that of the original bulk material, or if the strength of the surface region itself is decreased by the treatment. (The cohesive strength of a similar material, without corona treatment, was measured by Jane's (90) to be about 4600 p.s.i., which is considerably greater than any of the apparent adhesive strengths measured in this study.)

The mode of failure will be given further consideration in a later discussion of electron micrographs made of surfaces after rupture.

## CONTACT ANGLES

The properties of the contacting liquids are summarized in Table III.* The components of surface tension for water are the values given by Fowkes (74).

*The values of surface tension in Table III have the units of dynes/cm. In the case of pure liquids, these values are numerically equivalent to the specific surface free energy in ergs/cm.$^2$

The components for the other two liquids were calculated from Equation (21), using literature values (97) of liquid- and interfacial tension.

TABLE III

PROPERTIES OF CONTACTING LIQUIDS

| | |
|---|---|
| Water | |
| Density at 20°C. (96) | 0.9982 g./cc. |
| Measured surface tension, 23.4°C. | 72.74 dynes/cm. |
| Literature value, 20°C. (97) | 72.80 dynes/cm. |
| Components of surface tension (74) | |
| Dispersion, $\gamma_{\underline{\ell}}^{d}$ | 21.80 dynes/cm. |
| Polar, $\gamma_{\underline{\ell}}^{p}$ | 51.00 dynes/cm. |
| Fractional polarity, $\underline{p} = \gamma_{\underline{\ell}}^{p}/\gamma_{\underline{\ell}}$ | 0.70 |
| Methylene Iodide ($CH_2I_2$) | |
| Density at 20°C. (96) | 3.3254 g./cc. |
| Measured surface tension, 23.4°C. | 50.89 dynes/cm. |
| Literature value, 20°C. (97) | 50.76 dynes/cm. |
| Interfacial tension against water (97) | 48.50 dynes/cm. |
| Components of surface tension[a] | |
| Dispersion, $\gamma_{\underline{\ell}}^{d}$ | 50.38 dynes/cm. |
| Polar, $\gamma_{\underline{\ell}}^{p}$ | 0.38 dynes/cm. |
| Fractional polarity, $\underline{p} = \gamma_{\underline{\ell}}^{p}/\gamma_{\underline{\ell}}$ | 0.01 |
| 1,1,2,2-Tetrabromoethane (TBE) | |
| Density at 20°C. (96) | 2.9672 g./cc. |
| Measured surface tension, 23.4°C. | 49.61 dynes/cm. |
| Literature value, 20°C. (97) | 49.67 dynes/cm. |
| Interfacial tension against water (97) | 38.82 dynes/cm. |
| Components of surface tension[a] | |
| Dispersion, $\gamma_{\underline{\ell}}^{d}$ | 47.90 dynes/cm. |
| Polar, $\gamma_{\underline{\ell}}^{p}$ | 1.77 dynes/cm. |
| Fractional polarity, $\underline{p} = \gamma_{\underline{\ell}}^{p}/\gamma_{\underline{\ell}}$ | 0.04 |

[a] Calculated from Equation (21), using literature values of liquid- and interfacial tension.

It should be noted that polar forces account for 70% of the surface tension of water. In contrast, polar forces contribute very little to the surface tension of the other two liquids — 1% for methylene iodide and 4% for tetrabromoethane.

The results of contact-angle measurements on the "air-side" of presoaked cellophane, at several degrees of corona treatment, are given in Table IV. Each entry represents an average of at least fifteen individual readings, which are tabulated in Appendix VII.

TABLE IV

CONTACT ANGLES ON PRESOAKED, CORONA-TREATED CELLOPHANE "AIR-SIDE"

| Relative Humidity, % | Treatment Time, min. | Advancing Contact Angles, degrees | | |
|---|---|---|---|---|
| | | Water ($\gamma_\ell$ = 72.74)[b] | $CH_2I_2$ ($\gamma_\ell$ = 50.89)[b] | TBE[a] ($\gamma_\ell$ = 49.61)[b] |
| 50 | Untreated | 37.2 ± 1.1[c] | 40.1 ± 0.6[c] | 28.2 ± 0.7[c] |
| | 0.5 | 31.7 ± 0.8 | 40.0 ± 0.6 | 26.4 ± 0.7 |
| | 1.0 | 29.3 ± 0.6 | 40.1 ± 0.7 | 26.1 ± 0.6 |
| | 3.0 | 26.3 ± 0.5 | 41.1 ± 0.7 | 27.0 ± 0.6 |
| | 5.0 | 24.7 ± 1.4 | 41.8 ± 0.6 | 28.1 ± 0.7 |
| Dry $N_2$ | Untreated | 44.6 ± 0.7 | 36.4 ± 0.6 | 25.4 ± 0.9 |
| | 0.5 | 38.0 ± 0.7 | 36.0 ± 0.7 | 23.8 ± 0.8 |
| | 1.0 | 35.2 ± 0.7 | 36.1 ± 0.7 | 23.5 ± 0.7 |
| | 3.0 | 31.6 ± 0.7 | 37.0 ± 0.7 | 24.3 ± 0.9 |
| | 5.0 | 29.6 ± 0.7 | 37.6 ± 0.7 | 25.3 ± 0.9 |

[a] TBE = 1,1,2,2-Tetrabromoethane.

[b] Liquid surface tensions in dynes/cm.

[c] 95% Confidence limits = $\underline{t}$ · (standard error of mean) ($\underline{95}$).

Qualitatively, it is observed that the contact angles formed by water are consistently reduced by the corona treatment. The contact angles formed by the two nonpolar liquids are affected to a much smaller extent. The same trends were noted by Anderson (24), working with corona-treated polyethylene.

An increase in the relative humidity results in lower contact angles with water and higher angles with the nonpolar liquids, at all levels of corona treatment. These observations are in agreement with those of Borgin (98), and are an indication of the importance of the term, $\pi_e$, in the Young equation.

Contact angles measured on the "Lucite-side" of corresponding samples are reported in Table V. The relative effects of corona treatment and humidity are similar to those observed on the "air-sides" of corresponding samples. The contact angles on the "Lucide-side" are, however, consistently higher than those measured on the "air-sides." These results are in apparent conflict with those reported by Ray and his associates (24,78), who noted that films of amylose, amylopectin, and polyvinyl alcohol which had been cast by evaporation of polymer solutions on Lucite surfaces, were more hydrophilic on the "Lucite-sides" than on the "air-sides." This effect was attributed to the ability of the Lucite surface to induce an outward orientation of polar groups in the surface of the adjacent material.

Other factors which could account for these observations are roughness effects, contamination from the Lucite surface, and local cohesive failure of either material during separation.

TABLE V

CONTACT ANGLES ON PRESOAKED, CORONA-TREATED CELLOPHANE "LUCITE-SIDE"

| Relative Humidity, % | Treatment Time, min. | Initial Advancing Contact Angle, degrees: Water ($\gamma_\ell$ = 72.74)[b] | $CH_2I_2$ ($\gamma_\ell$ = 50.89)[b] | TBE[a] ($\gamma_\ell$ = 49.61)[b] |
|---|---|---|---|---|
| 50 | Untreated | 61.0 ± 1.3[c] | 41.6 ± 1.2[c] | 35.8 ± 0.5[c] |
| | 0.5 | 51.1 ± 0.6 | 40.2 ± 0.7 | 31.5 ± 0.7 |
| | 1.0 | 47.9 ± 0.7 | 40.0 ± 0.7 | 30.3 ± 0.8 |
| | 3.0 | 44.1 ± 0.7 | 40.4 ± 0.7 | 30.0 ± 0.7 |
| | 5.0 | 41.6 ± 1.5 | 40.8 ± 0.4 | 30.0 ± 0.7 |
| Dry $N_2$ | Untreated | 73.2 ± 0.8 | 37.4 ± 0.7 | 32.2 ± 1.0 |
| | 0.5 | 61.3 ± 0.8 | 36.2 ± 0.7 | 28.3 ± 0.9 |
| | 1.0 | 57.4 ± 0.6 | 36.0 ± 0.7 | 27.3 ± 0.8 |
| | 3.0 | 52.9 ± 0.8 | 36.4 ± 0.7 | 27.0 ± 0.9 |
| | 5.0 | 49.9 ± 0.7 | 36.7 ± 0.7 | 27.0 ± 0.9 |

[a] TBE = 1,1,2,2-Tetrabromoethane.

[b] Liquid surface tensions in dynes/cm.

[c] 95% Confidence limits = $t$ · (standard error of mean) (95).

Wenzel's (60) equation indicates that contact angles less than 90° should decrease with increasing roughness of the surface, and that the effect should be greatest for small angles. These data can be qualitatively reconciled with the first condition if the "Lucite-side" is comparatively smoother than the "air-side." Evidence for this will be discussed in a later section of this report. It is difficult, however, to account on the basis of roughness for the greater change in the water contact angles as compared to the change in the smaller angles formed by the two organic liquids. It may be that a combination of molecular orientation and roughness effects is important here.

When cellophane samples which had been soaked and dried against Lucite were soaked a second time and subsequently dried with the opposite side against a Lucite surface, the wetting characteristics of the two sides were reversed. The side which had been originally dried against Lucite then became the "air-side," and this surface yielded contact angles with water which were substantially the same as those previously observed on the "air-side" following the initial soaking procedure. It therefore appears that whatever is the effect of the substrate, it can be reversed by soaking in water. These observations do not seem compatible with the theory that the difference between the two sides is the result of contamination by low-energy material removed from the Lucite.

## COMPONENTS OF SOLID SURFACE FREE ENERGY

The contact-angle data were used to evaluate the polar and nonpolar components of solid surface free energy by application of Equation (26), as outlined in Appendix VIII. The liquid properties used in these calculations are those given in Table III.

Two values were obtained for each parameter by pairing the contact-angle results in two different ways: (1) water-methylene iodide, and (2) water-tetrabromoethane. The calculations were then carried out separately for each liquid pair. As previously discussed, these two values should be in close agreement, provided that the effective size of the methylene iodide molecule is not drastically different from that of the tetrabromoethane molecule. The calculations of Good and Elbing (83) indicate that this condition is met by these two liquids.

In all cases the two values agreed within 2 ergs/cm.$^2$, and those obtained from water-methylene iodide data were consistently greater than the corresponding values obtained with the other liquid pair. This is presumably due to a small difference in the effective size of the two organic molecules. These results have been averaged and are reported in Tables VI and VII. They are given as functions of treatment time in Fig. 9 and 10. The separate results for each liquid pair may be found in Appendix IX.

These results indicate that the surface free energy of the film is substantially increased by the corona treatment, and that this change is primarily due to an increase in the polar component, $\gamma_s^p$. The changes in polarity are most rapid during the early stages of treatment. As with the strength values, the polarity appears to be an approximate linear function of log-time (Fig. 11).

The dispersion-force component, $\gamma_s^d$, is apparently affected by the corona treatment to a much smaller extent. In general, there appears to be a rather gradual decrease in this component with time of treatment.

When the contact-angle data of Anderson (24) were used by this author to calculate the components of solid surface free energy for corona-treated polyethylene, similar results were obtained. Similar results have also been obtained by Persinger and Rivas (99), working with corona-treated Saran.

It is again noted that different results are obtained for the two sides of the samples. The "Lucite-side" appears to be less polar at all levels of treatment. Although the effects of the Lucite substrate have not been fully accounted for, it is significant, qualitatively, that the relative effect of the corona treatment is the same on both sides of the cellophane.

TABLE VI

COMPONENTS OF SOLID SURFACE FREE ENERGY FOR PRESOAKED, CORONA-TREATED CELLOPHANE "AIR-SIDE"

| Relative Humidity, % | Treatment Time, min. | Components of Solid Surface Free Energy, ergs/cm.$^2$ [a] | | | Fractional Polarity, $\underline{p}$ |
|---|---|---|---|---|---|
| | | Dispersion, $\gamma_{\underline{s}}^{\underline{d}}$ | Polar, $\gamma_{\underline{s}}^{\underline{p}}$ | Total, $\gamma_{\underline{s}}$ | |
| 50 | Untreated | 33.4 | 28.9 | 62.3 | 0.474 |
| | 0.5 | 33.2 | 32.0 | 65.4 | 0.491 |
| | 1.0 | 33.1 | 33.4 | 66.6 | 0.503 |
| | 3.0 | 32.5 | 35.3 | 67.8 | 0.520 |
| | 5.0 | 32.0 | 36.4 | 68.4 | 0.533 |
| Dry $N_2$ | Untreated | 35.6 | 23.2 | 58.9 | 0.396 |
| | 0.5 | 35.2 | 27.4 | 62.6 | 0.437 |
| | 1.0 | 35.0 | 29.1 | 64.1 | 0.454 |
| | 3.0 | 34.4 | 31.4 | 65.8 | 0.478 |
| | 5.0 | 33.8 | 32.8 | 66.6 | 0.492 |

[a] Calculated from Equation (26).

TABLE VII

COMPONENTS OF SOLID SURFACE FREE ENERGY FOR PRESOAKED, CORONA-TREATED CELLOPHANE "LUCITE-SIDE"

| Relative Humidity, % | Treatment Time, min. | Components of Solid Surface Free Energy, ergs/cm.$^2$ [a] | | | Fractional Polarity, $\underline{p}$ |
|---|---|---|---|---|---|
| | | Dispersion, $\gamma_{\underline{s}}^{\underline{d}}$ | Polar, $\gamma_{\underline{s}}^{\underline{p}}$ | Total, $\gamma_{\underline{s}}$ | |
| 50 | Untreated | 34.2 | 14.0 | 48.2 | 0.290 |
| | 0.5 | 34.2 | 20.0 | 54.2 | 0.369 |
| | 1.0 | 34.2 | 22.0 | 56.2 | 0.392 |
| | 3.0 | 33.7 | 24.6 | 58.4 | 0.422 |
| | 5.0 | 33.3 | 26.4 | 59.6 | 0.442 |
| Dry $N_2$ | Untreated | 38.0 | 6.4 | 44.5 | 0.146 |
| | 0.5 | 37.3 | 12.6 | 50.0 | 0.253 |
| | 1.0 | 37.0 | 15.0 | 52.0 | 0.289 |
| | 3.0 | 36.4 | 18.0 | 54.2 | 0.329 |
| | 5.0 | 35.8 | 19.9 | 55.8 | 0.358 |

[a] Calculated from Equation (26).

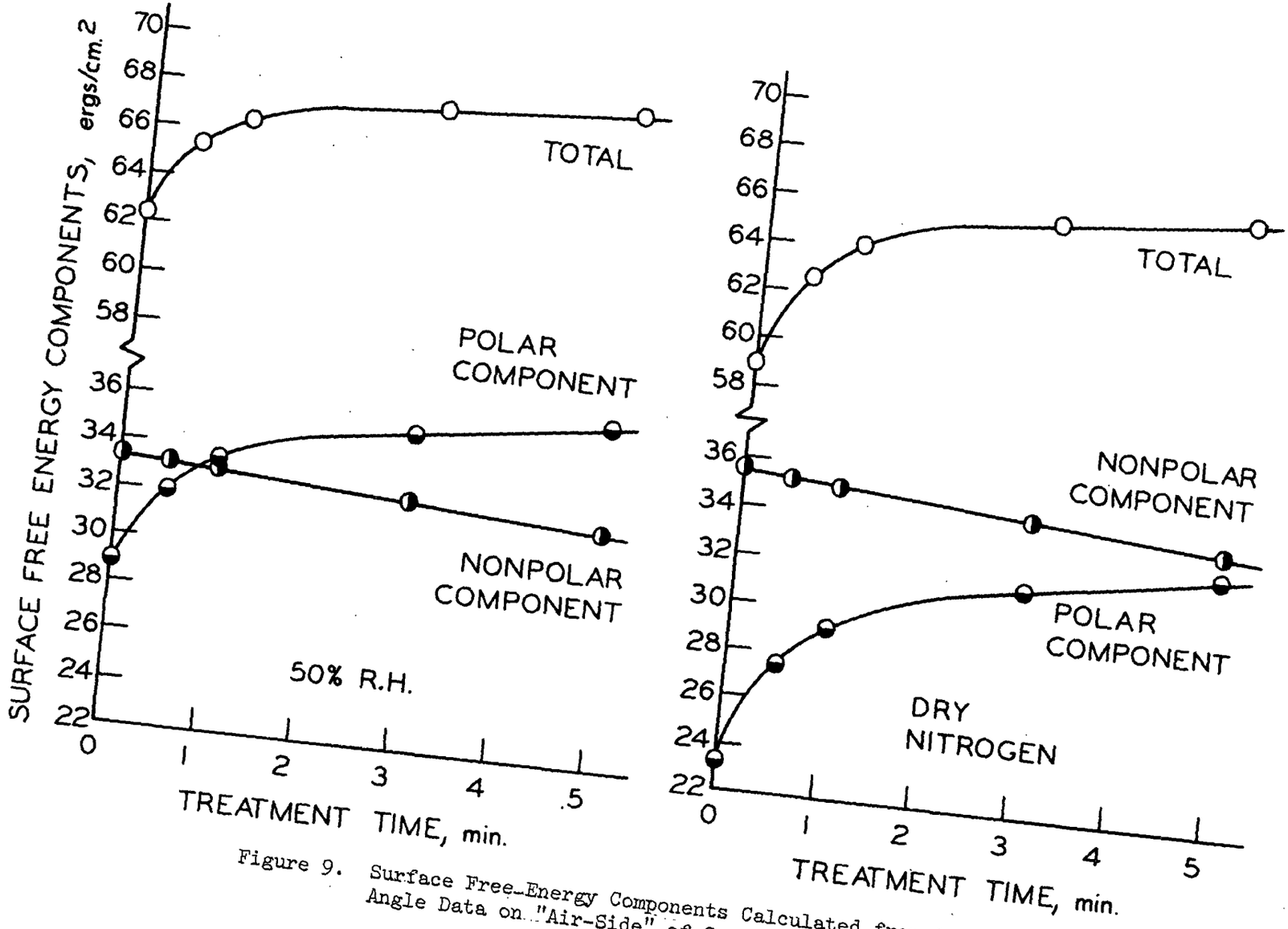


Figure 9. Surface Free-Energy Components Calculated from Contact Angle Data on "Air-Side" of Corona-Treated Samples

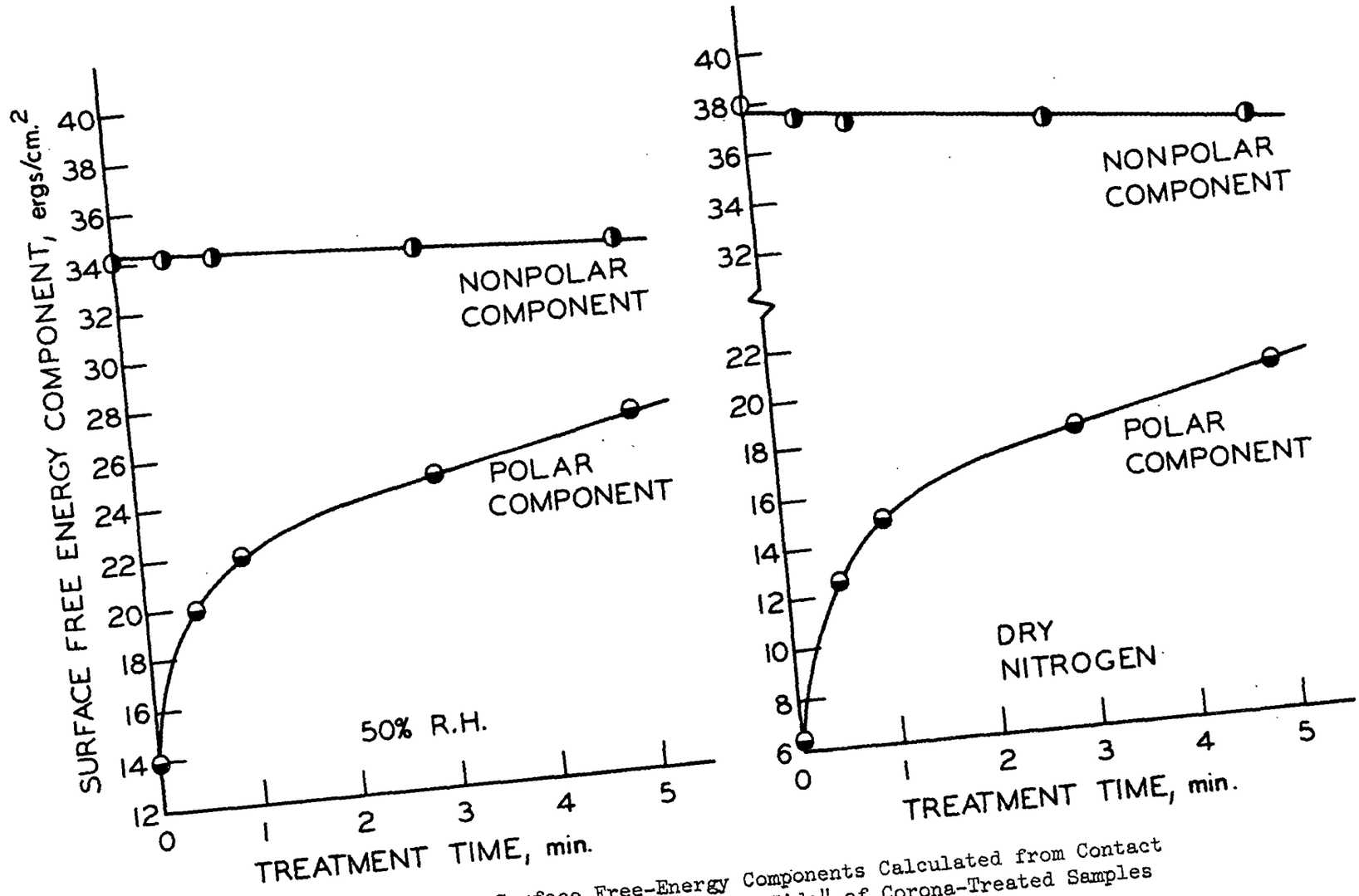


Figure 10. Surface Free-Energy Components Calculated from Contact Angle Data on "Lucite-Side" of Corona-Treated Samples

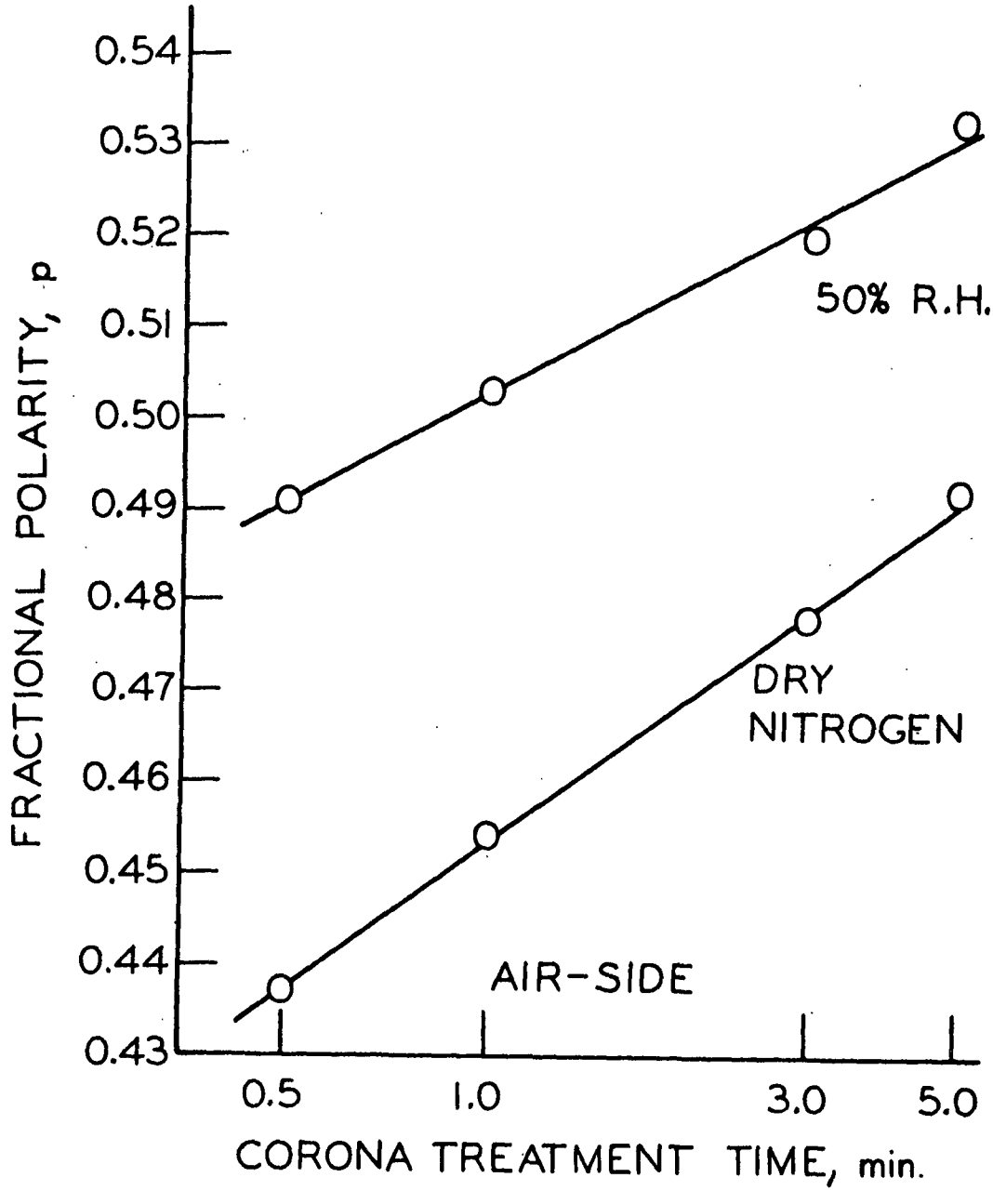


Figure 11. Fractional Polarities of Corona-Treated Surfaces

The effect of relative humidity is illustrated in Fig. 11. It can be seen that the surface is relatively more polar at the higher humidity. This is presumably due to increased adsorption of water.

## ESTIMATES OF SWELLABILITY

The increase in the polarity of the surface could, in itself, provide for stronger bonding to occur by virtue of an increased interaction of polar forces across the interface. Because water is an integral part of the bonding process which is under investigation here, it is necessary to consider how this change in polarity will affect the interaction of the surface with water.

The theories of solubility, as applied to the interaction between polar compounds, have been used to estimate changes in the ability of the treated surfaces to be swollen by water. Although the application of the theories to polymer systems has often been empirical, the basis for the theory appears to be sound, and lies in the fact that the forces which give rise to surface free energy are the same forces which govern solubility and swelling.

An empirical relationship between the solubility parameter and surface tension of nonpolar liquids has been described by Hildebrand and Scott (38). Lee (100) presented a modification of the Hildebrand-Scott equation to account for the solubility of nonpolar amorphous polymers:

$$\gamma_c^{0.43} \approx 0.24\ \delta\phi V_m^{0.143} \quad . \tag{27}$$

In Equation (27), $\gamma_c$ is the critical surface tension of the polymer in ergs/cm.$^2$, $\delta$ is the solubility parameter in (cal./cc.)$^{1/2}$, $\phi$ is the Girifalco-Good interaction parameter for the polymer-solvent system, and $V_m$ is the molar volume of a polymer repeating unit in cc./mole.

Equation (27) has been used to estimate the solubility parameters of the corona-treated materials from the calculated values of solid surface free energy in place of $\gamma_c$. The value of $\phi$ was assumed to be unity, and $V_m$ was approximated by assuming a density of 1.52 g./cc. and a repeating-unit molecular weight of 162. The results obtained for the "air-side" at the low humidity are given in Table VIII.

TABLE VIII

SOLUBILITY PARAMETERS OF CORONA-TREATED CELLOPHANE CALCULATED FROM EQUATION (27)

| Treatment Time, min. | $\gamma_s$, ergs/cm.$^2$ | $\delta$ (cal./cc.)$^{1/2}$ |
|---|---|---|
| Untreated | 58.9 | 12.4 |
| 0.5 | 62.6 | 12.7 |
| 1.0 | 64.1 | 12.8 |
| 3.0 | 65.8 | 12.9 |
| 5.0 | 66.6 | 13.0 |

The degree of swelling of nonpolar polymers has been found (101) to be inversely related to the quantity $(\delta - \delta_o)^2$, where $\delta_o$ is the solubility parameter of the solvent, and which for water has a value of 23.2 (cal./cc.)$^{1/2}$ (101). Gardon (101) has emphasized, however, that for polar systems, consideration must also be given to a balance between the fractional polarities of the two substances. It was proposed that for polar systems, the solubility parameter be divided into a polar and a nonpolar component:

$$\text{polar component} - \omega = \sqrt{p} \cdot \delta \ , \tag{28}$$

$$\text{nonpolar component} - \Omega = \sqrt{d} \cdot \delta \ , \tag{29}$$

$$\delta^2 = \omega^2 + \Omega^2 \ . \tag{30}$$

In these equations, p is the fractional polarity, and d its complement, as previously defined.

It was argued (101) that in such a system, the degree of swelling will be governed by a sum of the terms $(\omega - \omega_o)^2 + (\Omega - \Omega_o)^2$, where the subscript o refers to the solvent. The degree of swelling, Q, should then be defined by an equation of the form:

$$- \ln Q = A[(\omega - \omega_o)^2 + (\Omega - \Omega_o)^2] + B \ , \qquad (31)$$

where A and B are constants.

The quantity in brackets in Equation (31) has been evaluated for the interaction of the corona-treated materials with water. The results are in Table IX, and are plotted as a function of treatment time in Fig. 12. (Data from the "air-side" at the low humidity were used in these calculations.)

A more direct estimate of the degree of swelling may be obtained by differentiating Equation (31) with respect to the quantity in brackets:

$$- dQ/Q = A \cdot d[(\omega - \omega_o)^2 + (\Omega - \Omega_o)^2] \ . \qquad (32)$$

The theoretical treatment of Thode and Guide (102) indicates that the constant A in Equations (31) and (32) is equal to the quantity, $V_o/(RT)$, where $V_o$ is the molar volume of the solvent, R is the gas constant, and T the absolute temperature. Taking a value of 600 cal./mol. for RT, and a molar volume of 18 cc./mole for water, the resulting value of A is 0.03 cc./cal. This value of A was used in Equation (32) to obtain a rough approximation to the percentage changes in swelling as a result of changes in the value of the quantity in brackets. These results are plotted in Fig. 12.

TABLE IX

ESTIMATION OF THE ABILITY OF CORONA-TREATED SAMPLES TO BE SWOLLEN BY WATER

(For water: $\underline{p} = 0.701$, $\delta_{\underline{o}} = 23.2$, $\omega_{\underline{o}} = 19.4$, $\Omega_{\underline{o}} = 12.7$)

| Treatment Time, min. | Fractional Polarity, $\underline{p}$ | $(\text{cal./cc.})^{1/2}$ | | | $\frac{\text{cal.cc.}}{(\omega - \omega_{\underline{o}})^2 + (\Omega - \Omega_{\underline{o}})^2}$ |
|---|---|---|---|---|---|
| | | $\delta$ | $\omega = \sqrt{\underline{p}} \cdot \delta$ | $\Omega = \sqrt{1 - \underline{p}} \cdot \delta$ | |
| Untreated | 0.396 | 12.4 | 7.77 | 9.60 | 145.3 |
| 0.5 | 0.437 | 12.7 | 8.38 | 9.51 | 132.0 |
| 1.0 | 0.454 | 12.8 | 8.63 | 9.47 | 126.8 |
| 3.0 | 0.478 | 12.9 | 8.93 | 9.34 | 121.9 |
| 5.0 | 0.492 | 13.0 | 9.13 | 9.28 | 117.5 |

Because of the approximations involved in these calculations, and because of the semicrystalline nature of this material, little significance should be placed on the actual magnitude of the numbers obtained. They should provide, however, a relative measure of the degree of swelling in water.

These calculations indicate that the surface region of corona-treated samples is more easily swollen by water than is the untreated material. This could provide for better molecular contact to obtain between the corona-treated surfaces and may be a significant part of the mechanism of increased bonding.

## PHYSICAL EFFECTS

### SURFACE ROUGHNESS AND CONFORMABILITY

The measured values of Chapman smoothness for cellophane samples, at two levels of corona treatment and three humidities, are listed in Table X and are shown graphically in Fig. 13. These results did not depend upon whether the

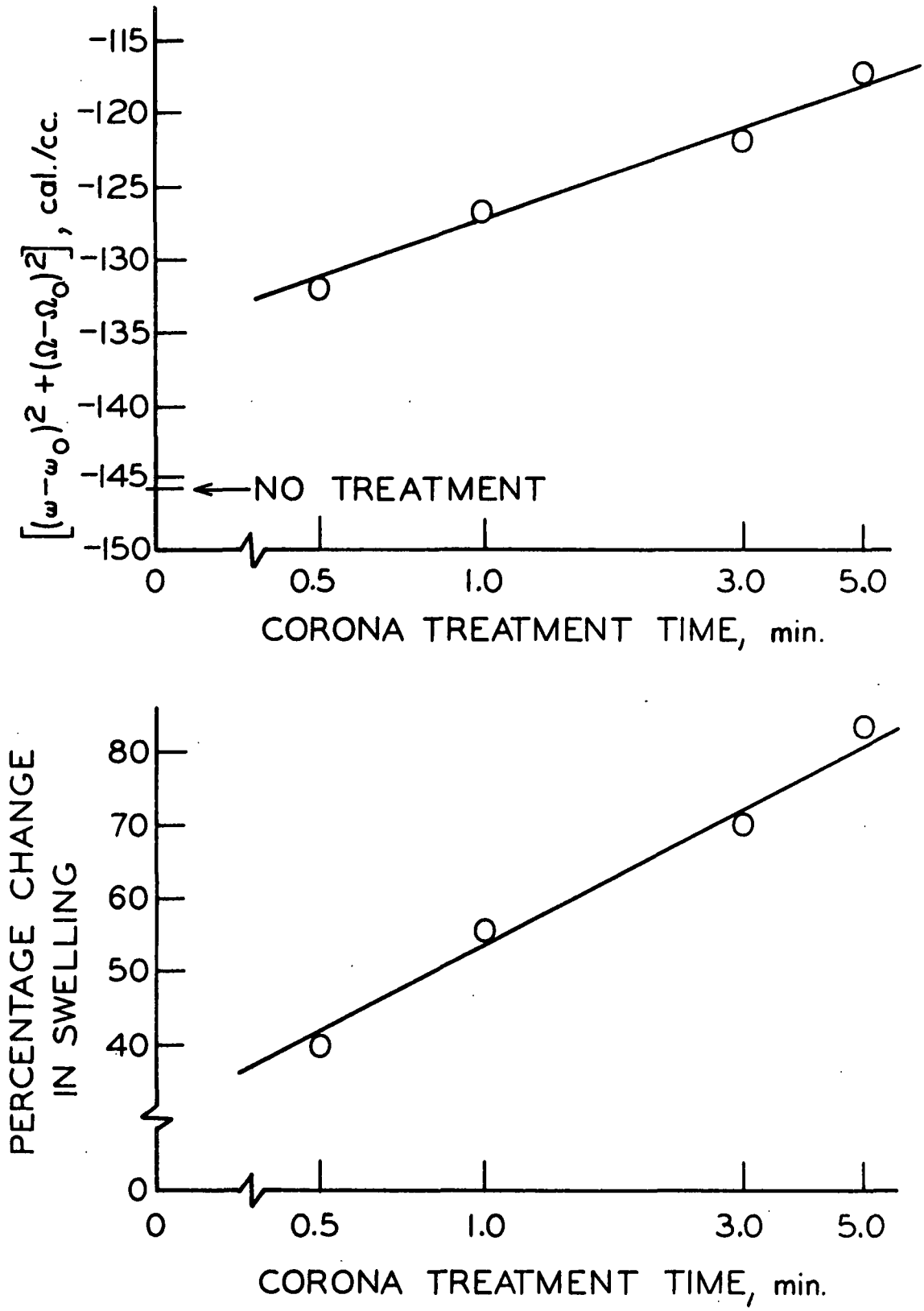


Figure 12. Estimated Degree of Swelling of Corona-Treated Surfaces by Water

"air-side" or the "Lucite-side" of a sheet was adjacent to the upper prism of the instrument. Each entry in Table X is an average of readings from at least three different samples.

TABLE X

ROUGHNESS AND CONFORMABILITY OF CORONA-TREATED SURFACES

| Nominal Pressure, p.s.i. | Smoothness Index, % | | | | | |
|---|---|---|---|---|---|---|
| | Untreated | | | 5-Min. Corona | | |
| | 15% R.H. | 50% R.H. | 70% R.H. | 15% R.H. | 50% R.H. | 70% R.H. |
| 0.0 | 2.2 | 1.9 | 2.2 | 2.2 | 2.0 | 2.2 |
| 17.7 | 3.0 | 2.9 | 4.5 | 3.0 | 2.8 | 3.8 |
| 35.4 | 9.7 | 15.0 | 25.5 | 5.0 | 6.2 | 20.8 |
| 53.1 | 24.7 | 37.1 | 48.0 | 12.5 | 19.0 | 49.5 |
| 70.8 | 37.7 | 52.4 | 59.0 | 26.2 | 34.4 | 59.0 |
| 88.5 | 45.5 | 60.4 | 66.0 | 37.5 | 46.0 | 66.5 |
| 133.0 | 58.7 | 72.0 | 75.3 | 55.0 | 61.2 | 76.0 |
| 177.0 | 69.0 | 78.8 | 82.3 | 64.5 | 69.8 | 82.8 |
| 354.0 | 84.3 | 93.0 | 92.8 | 82.5 | 86.2 | 93.0 |

Because of the transparent nature of these samples, it is difficult to give proper quantitative consideration to the effect of the opal-glass backing upon the instrument readings. The smoothness values will undoubtedly reflect changes in optical contact between the lower sample surface and the opal-glass backing, as well as between the top sample surface and the upper prism of the instrument. Each reading may, therefore, be regarded as an average value of the smoothness of the two sides of the sample, and is referred to here as a "smoothness index" to remind the reader of the particular conditions of measurement.

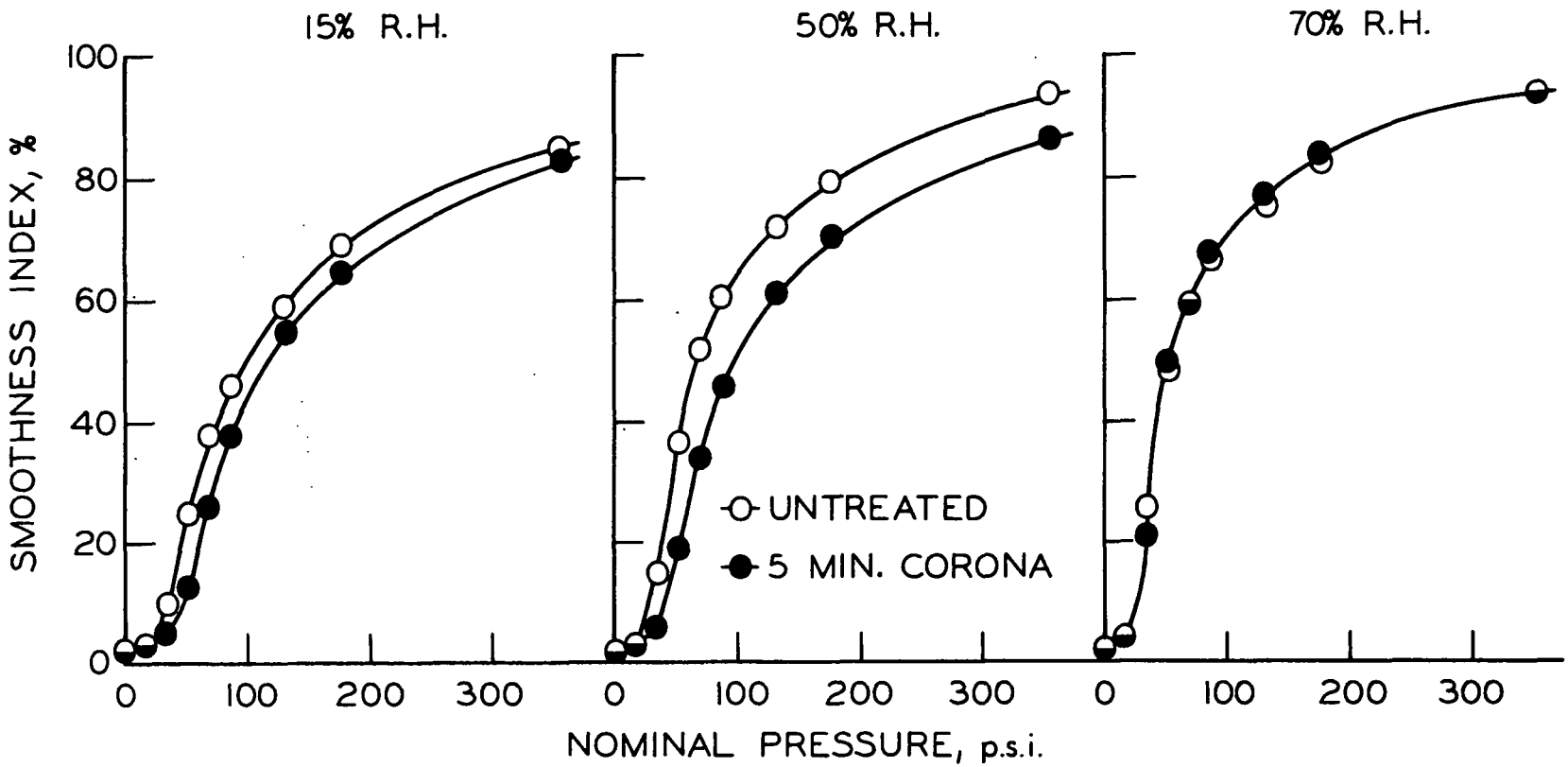


Figure 13. Smoothness Index for Cellophane Samples

Qualitatively, it appears that the cellophane is roughened somewhat during corona treatment. This is evidenced by the observation that, at the low level of relative humidity, the treated samples gave lower smoothness values at all pressures tested. As the humidity was increased, however, these differences became smaller so that at 70% R.H., the smoothness values were essentially the same for the treated and untreated samples at all levels of compression.

These results indicate that the corona-treated surface is made more pliable by exposure to water vapor and may reflect an increase in the swelling of the treated sample, as predicted from the solubility-parameter calculations.

ELECTRON MICROGRAPHS OF SURFACE REPLICAS

Figures 14 and 15 provide a comparison of the "Lucite-side" with the "air-side" of a presoaked sample without corona treatment. The surface which was dried in contact with the Lucite substrate (Fig. 15) is noticeably smoother than that dried in contact with air. This may account for some of the differences obtained between the contact angles measured on the two sides.

Figures 16 and 17 provide views of the two sides of a presoaked sample following 5 minutes of corona treatment. The small surface cracks which were present in the corresponding untreated surfaces seem to be greatly reduced in number. There are, however, a number of lumps and other irregularities which were not observed on the surface of the untreated material.

Figure 18 shows an untreated surface which had been soaked in water and bonded to a similar surface by wet-pressing. The bond was then ruptured by

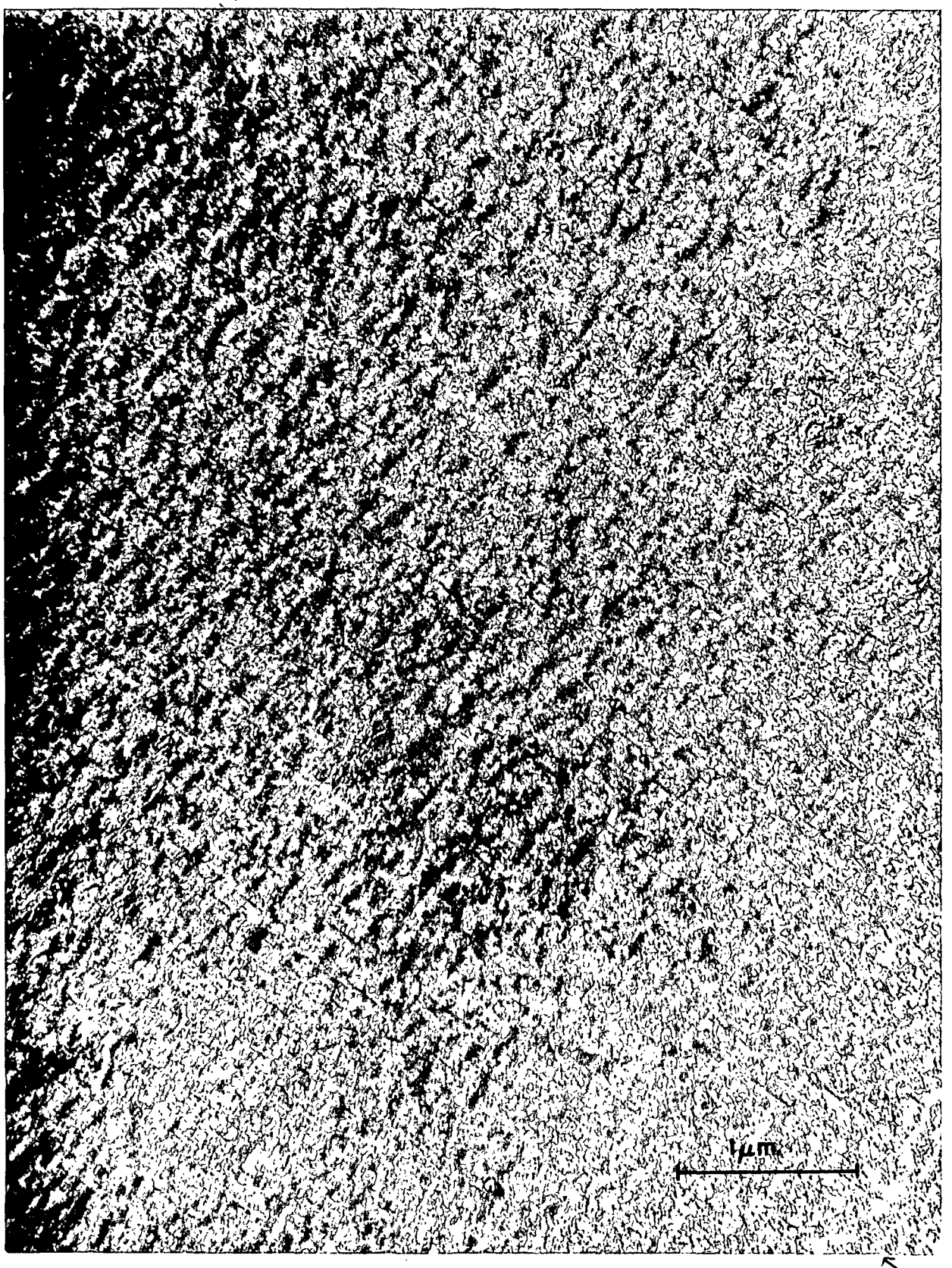


Figure 14. Replica of Cellophane Soaked in Water, Air-Dried Against Lucite: (Air Side)

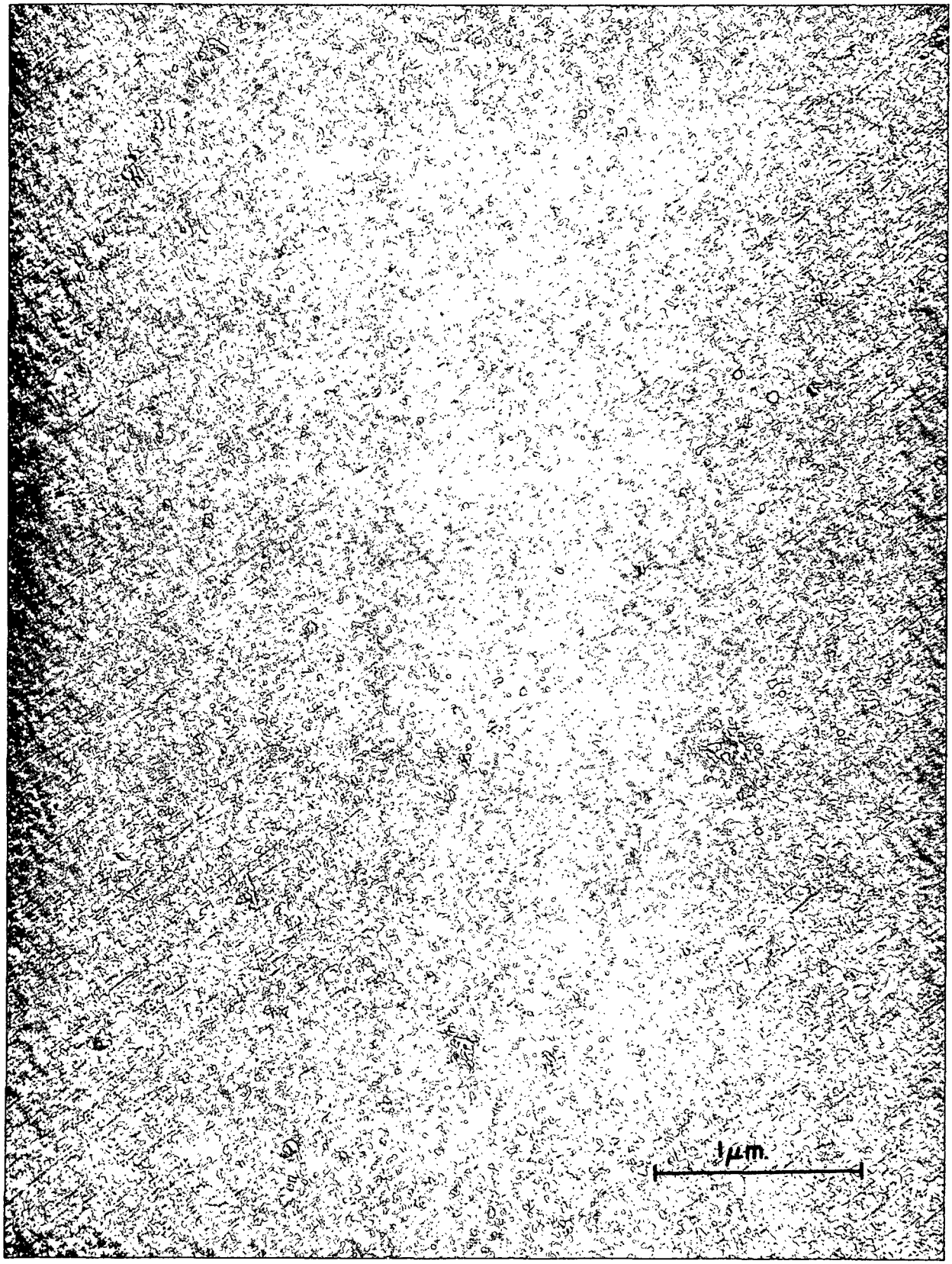


Figure 15. Replica of Cellophane Soaked in Water, Air-Dried Against Lucite: (Lucite Side)

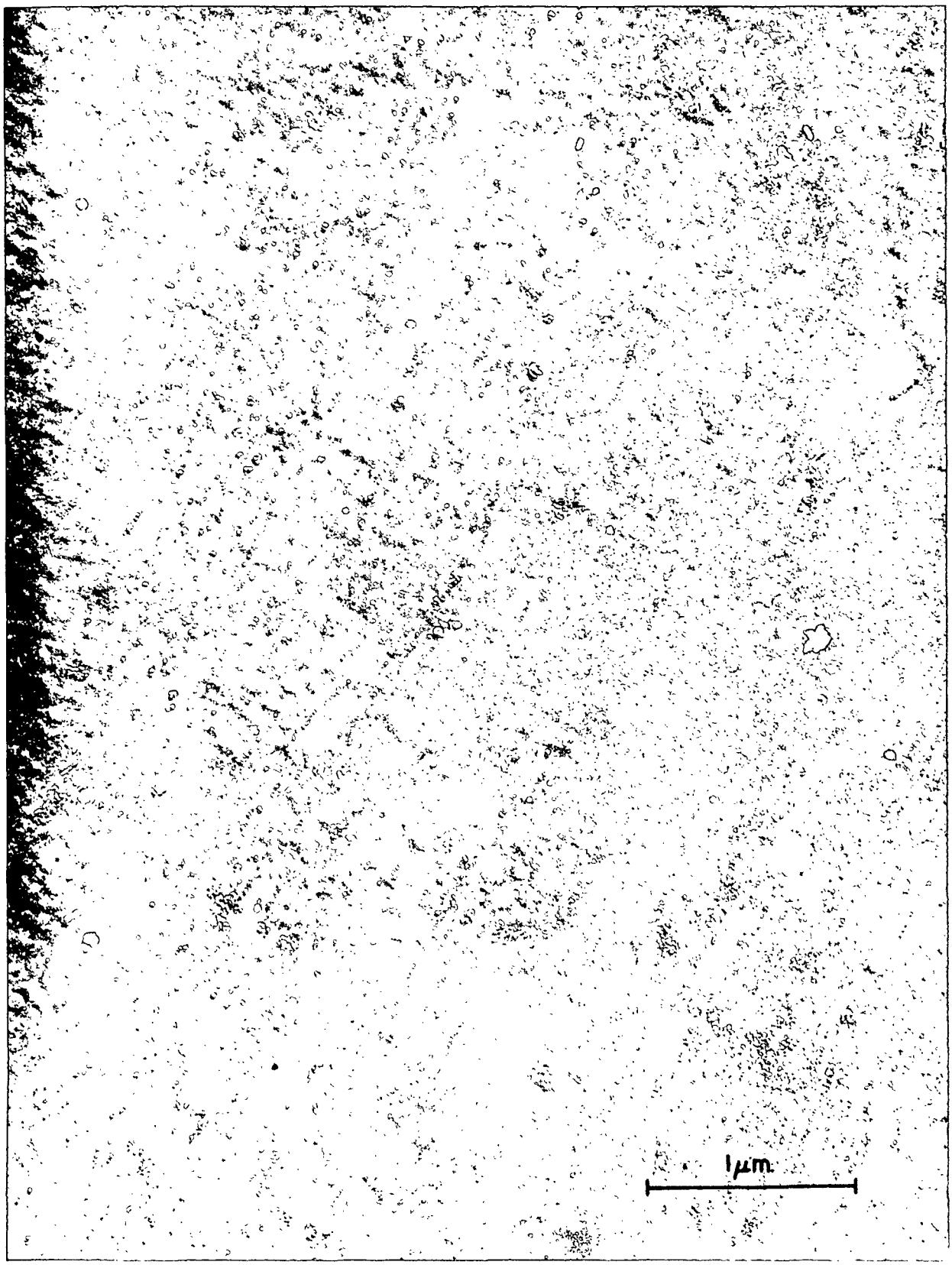


Figure 16. Replica of Presoaked Cellophane, 5 Minutes Corona: (Lucite Side)


Figure 17. Replica of Presoaked Cellophane, 5 Minutes Corona: (Air Side)

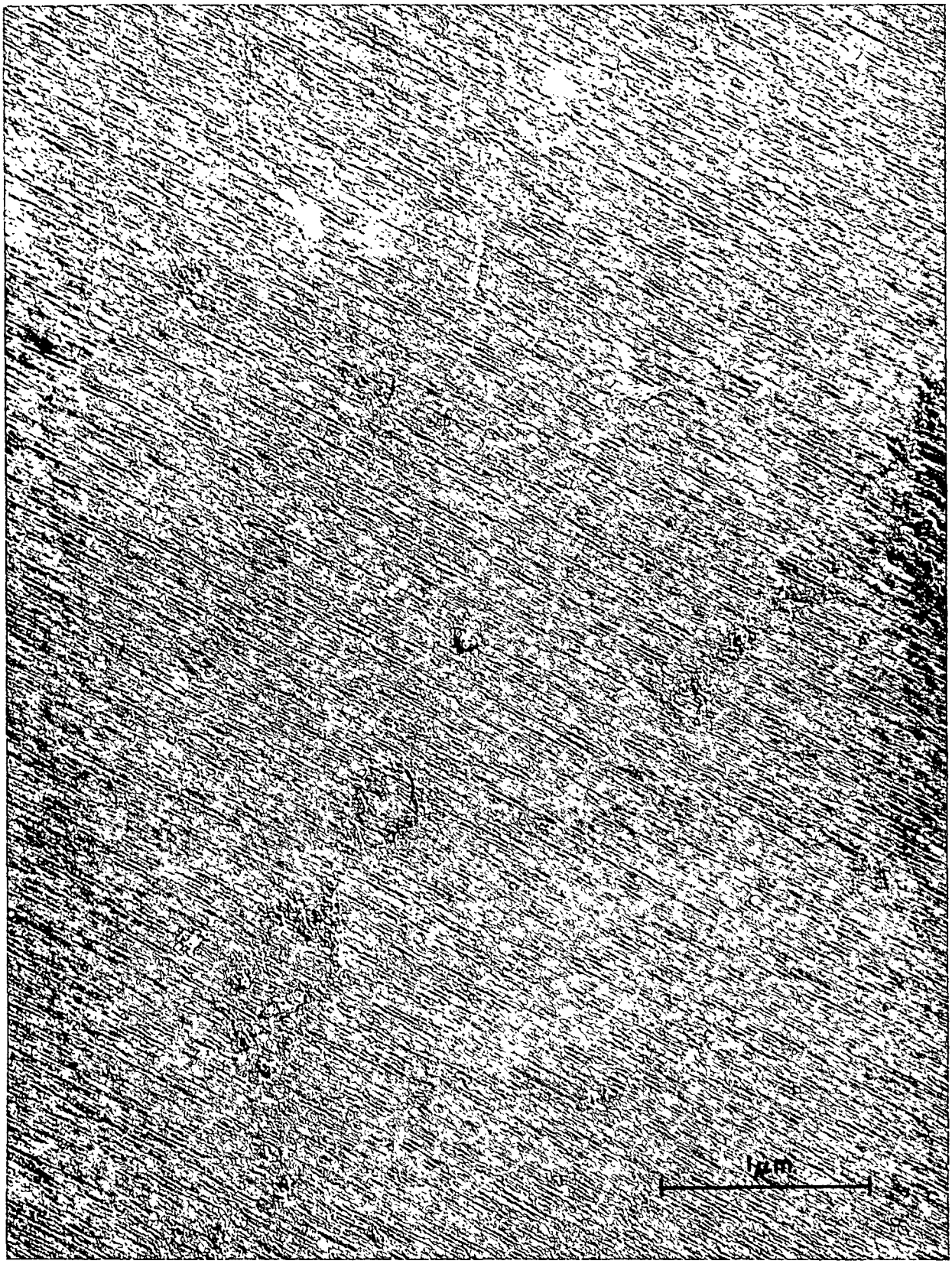


Figure 18. Replica of Previously-Bonded Surface, No Corona: (Lucite Side)

peeling. Little evidence is seen for the occurrence of failure outside of the interface. Apparently, the strength of the surface region is not the limiting factor here.

This should be compared to Fig. 19 and 20, which represent the surfaces of corona-treated material which had been similarly bonded with subsequent delamination. Here there is clear evidence of failure beneath the interface. Apparently, the bond between the treated surfaces is often locally stronger than the adjacent bulk material.

## CHEMICAL EFFECTS

### MULTIPLE INTERNAL REFLECTION SPECTROSCOPY

The differential MIR spectra indicated stronger infrared absorption in the vicinity of 1720 $cm.^{-1}$ for samples which had been corona treated for five minutes, as compared to an untreated sample. These differences are attributed to an increase in the carboxyl content of the surface.

### METHYLENE BLUE ADSORPTION

A carboxyl content of 4.85 meq./100 g. (ovendry basis) was obtained for both the corona-treated and untreated samples, from the measurements of methylene blue adsorption. No measurable effects of the corona treatment could be detected by this technique.

These results indicate that any oxidation which occurs is confined within a very thin surface layer, so that the modified material makes up a very small part of the total bulk material. (A measurable difference in carboxyl content by these procedures is about 0.05 meq./100 g.)

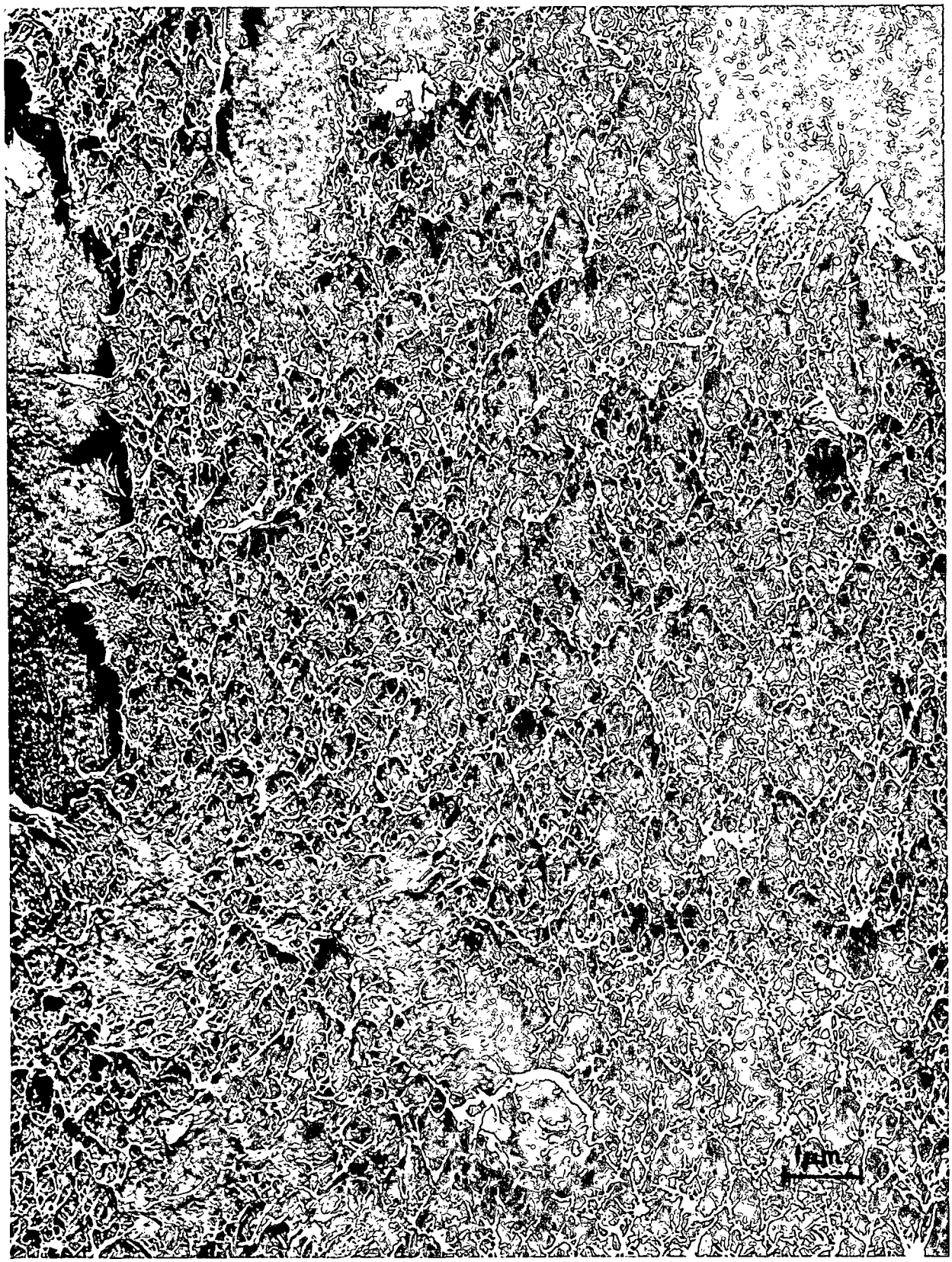


Figure 19. Replica of Previously-Bonded Surface, 5 Minutes Corona: (Air Side)

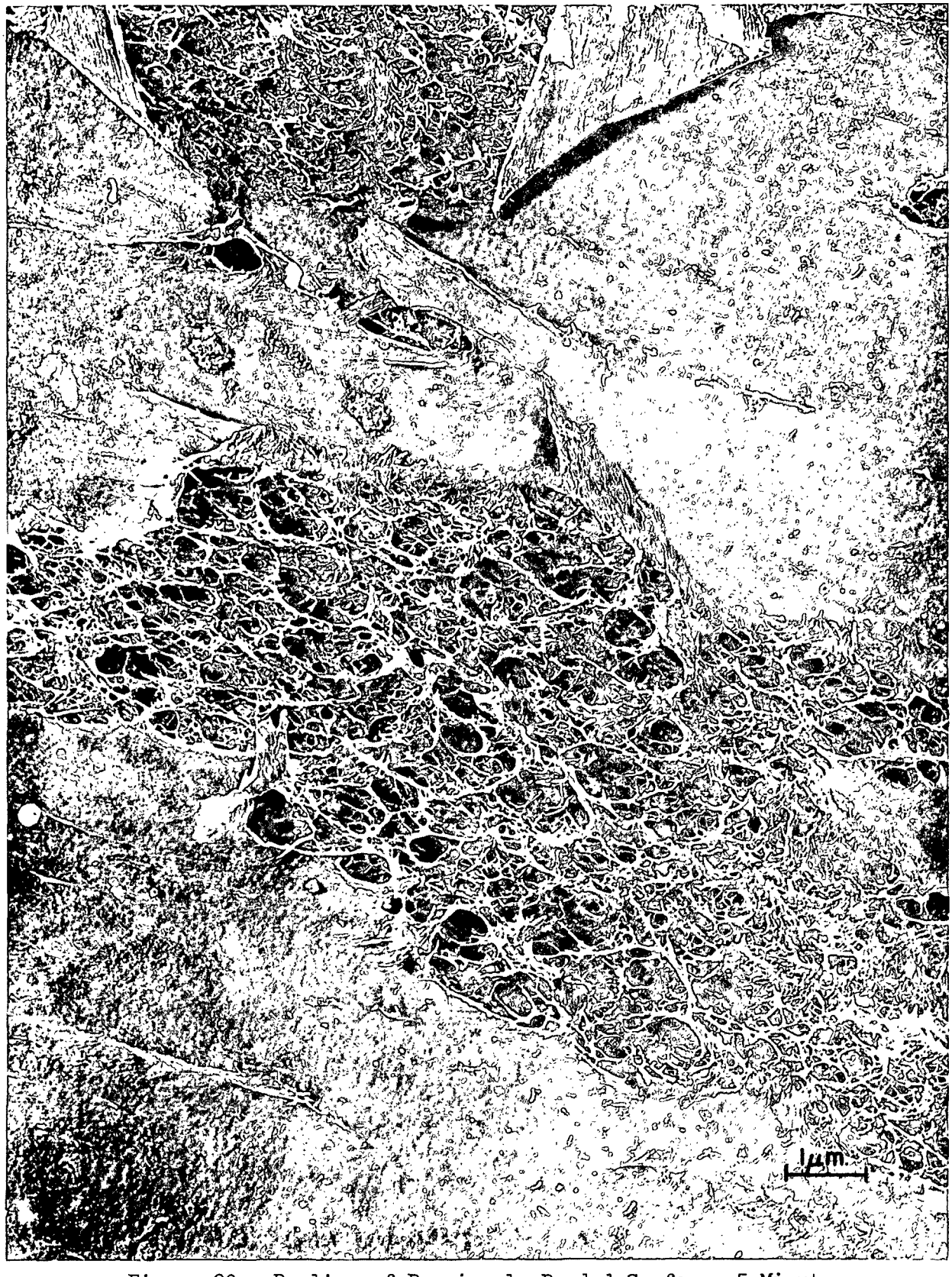


Figure 20. Replica of Previously-Bonded Surface, 5 Minutes Corona: (Lucite Side)

## SUMMARY OF CONCLUSIONS

The treatment of a cellulosic material in a corona discharge results in a very significant increase in the solid surface free energy. This change in surface free energy is primarily due to an increase in the polarity of the surface. These changes are accompanied by a small decrease in the magnitude of dispersion-type forces. These observations appear to be applicable also to the corona treatment of other materials. Similar conclusions can be drawn from data in the literature, describing the corona treatment of polyethylene and Saran films.

The increase in the polarity of the surfaces could, in itself, provide for stronger bonding to occur by virtue of an increased interaction of polar forces across the interface. These results indicate that this increase in polarity also gives rise to increased interaction with polar liquids such as water. The resulting increase in the swelling of the substrate may be an important part of the mechanism whereby the strength of water-induced bonds is increased.

Oxidation is a primary chemical effect of the corona treatment of cellulose. The observation of the rapid increase in bonding strength at very short treatment times, along with the results of the methylene blue adsorption studies, indicate that these modifications are confined within very thin surface layers. The oxidation produces a surface which is more hydrophilic and more conformable after exposure to water vapor than is the untreated material.

During the initial stages of corona treatment, the observed increases in strength are attributed to a strengthening of the interfacial bond rather than to a strengthening of the surface region itself. Electron micrographs of ruptured surfaces indicate that at higher degrees of treatment, the interfacial bond becomes stronger than the adjacent bulk material.

Contact-angle data have been used to separately evaluate the polar and nonpolar components to the surface free energy of a cellulosic material. The application of this method to polar substances has previously received only limited attention in the literature. This work has provided a theoretical justification of the method, for situations where induction-type forces can be neglected, and where the sizes of the molecules involved are similar.

## SUGGESTIONS FOR FUTURE RESEARCH

The application of corona discharge to adhesion situations within the paper industry warrants further consideration. Several possible industrial applications have been suggested by Goring (5,32,103), and include improvement of interply adhesion of paper and board, strengthening of particle board, and improvement of fiber-to-fiber bonding by pretreatment of individual fibers prior to sheet formation. Another possible application is in the manufacture of nonwoven fabrics. The latter suggestion seems particularly interesting in view of the reported (104) use of corona discharge to improve the shrink resistance of wool and mohair fabrics.

An area of more fundamental interest is the quantitative characterization of the swelling process, with particular emphasis on the interaction of polar materials. This subject has been reviewed by Gardon (101), and by Burrell and Immergut (105), and it is clear that although much qualitatively useful information has been gained from application of the present theory, it cannot be quantitatively applied to most systems involving polar substances. Many of the available relationships which define swelling were empirically derived from swelling data in nonpolar systems. Data which are now available in the literature on the swelling of polar materials should be useful in extending this theory. The recent publications of Robertson (106) and Craver (107) on the interaction of cellulose with a variety of liquids would be useful here. The latter article describes a very interesting analytical technique, involving the measurement of sonic velocities, for evaluating solid-liquid interaction, and this should prove to be particularly relevant to such an effort.

An extension of the present research might include measurements of bonded area by gas adsorption techniques. Such measurements, made on bonded laminates with and without corona treatment, should help to clarify whether the observed increases in adhesion are primarily due to an increase in the intrinsic bond strength or to better molecular contact.

Another investigation might involve a study of the bonding of corona-treated surfaces which have been subsequently abraded to various depths. This could be accompanied by a study of the chemical effects at various depths below the surface. These measurements could be effected by MIR techniques using various reflection crystals and angles of light-incidence, as described by Carlsson and Wiles (19).

## NOMENCLATURE

$A$ = a constant in Equations (31) and (32), defined by $V_o/RT$, cc./cal.

$a$ = square root of liquid capillary constant, cm.

$A_{ij}$ = attractive constant in Lennard-Jones potential function for interaction of phases $i$ and $j$, ergs cm.$^6$

$A_{ij}^d$ = dispersion-force contribution to $A_{ij}$, ergs cm.$^6$

$A_{ij}^i$ = induction-force contribution to $A_{ij}$, ergs cm.$^6$

$A_{ij}^o$ = orientation-force contribution to $A_{ij}$, ergs cm.$^6$

$B$ = a constant in Equations (31) and (32), dimensionless

$B_s$ = a parameter used in calibration of the Chapman smoothness tester, dimensionless

$C_a$, $C_b$ = Chapman smoothness photocell readings, dimensionless

$D$ = a parameter defined by $2\sqrt{\gamma_\ell^d/\gamma_\ell}$, cm./erg$^{0.5}$

$d_i$ = fractional contribution of dispersion forces to the surface energy of substance $i$, dimensionless

$\Delta F_i^c$ = free energy of cohesion of substance $i$, ergs/cm.$^2$

$\Delta F_{ij}^a$ = free energy of adhesion between phases $i$ and $j$, ergs/cm.$^2$

$F$ = Chapman smoothness value, %

$f$ = correction factor for the ring method, dimensionless

$g$ = acceleration due to gravity, 980 cm./sec.$^2$

$H$ = a parameter defined by $2\sqrt{\gamma_\ell^p/\gamma_\ell}$, cm./erg$^{0.5}$

$I_i$ = ionization energy of substance $i$, ergs

$k$ = Boltzmann constant, $1.380 \times 10^{-16}$ ergs/(°K)

$M$, $N$ = instrument constants for Chapman smoothness tester, dimensionless

$p_i$ = fractional polarity of substance $i$, dimensionless

$Q$ = degree of swelling, dimensionless

$\underline{R}$ = Wenzel's surface-roughness factor, dimensionless

= radius of ring used in determination of liquid surface tension, cm.

= gas constant, 1.987 cal. $mole^{-1}$ $(°K)^{-1}$

$\underline{r}$ = intermolecular distance, Angstroms

= radius of wire used in the measurement of liquid surface tension by the ring method, cm.

$\underline{T}$ = absolute temperature, °K

$\underline{V}$ = volume of liquid pulled above equilibrium surface by the duNouy ring, cc.

$\underline{V_m}$ = molar volume of a polymer repeating unit, cc./mole

$\underline{V_o}$ = molar volume of solvent, cc./mole

$\underline{W_A}$ = work of adhesion, ergs/$cm.^2$

$\underline{W_c}$ = work of cohesion, ergs/$cm.^2$

$\underline{Z}$ = vertical distance coordinate, cm.

$\underline{\alpha_i}$ = polarizability of substance $\underline{i}$, cc.

$\beta$ = a parameter defined by $0.5(\gamma_1 + \gamma_2 - \gamma_{12})/\sqrt{\gamma_1^d}$, $ergs^{0.5}/cm.$

$\gamma$ = surface free energy, ergs/$cm.^2$

$\underline{\gamma_c}$ = Zisman's critical surface tension of wetting, dynes/cm.

$\underline{\gamma_\ell}$ = liquid surface free energy, ergs/$cm.^2$

$\underline{\gamma_m}$ = uncorrected, measured value of liquid surface tension, dynes/cm.

$\underline{\gamma_s}$ = solid surface free energy, ergs/$cm.^2$

$\gamma_{12}$ = interfacial free energy between phases 1 and 2, ergs/$cm.^2$

$\underline{\gamma_{s\ell}}$ = solid-liquid interfacial free energy, ergs/$cm.^2$

$\underline{\gamma_{sv}}$ = solid-vapor interfacial free energy, ergs/$cm.^2$

$\underline{\gamma_i^d}$ = dispersion-force component to the surface free energy of substance $\underline{i}$, ergs/$cm.^2$

$\underline{\gamma_i^p}$ = polar component to the surface free energy of substance $\underline{i}$, ergs/$cm.^2$

$\delta$ = solubility parameter, $(cal./cc.)^{0.5}$

$\delta_o$ = solubility parameter of solvent, $(\text{cal./cc.})^{0.5}$

$\theta$ = contact angle, degrees

$\kappa$ = a parameter defined by $\sqrt{\gamma_{\underline{l}}^{p}/\gamma_{\underline{l}}^{d}}$, dimensionless

$\mu_{\underline{i}}$ = dipole moment of substance i, Debyes

$\pi_{\underline{e}}$ = equilibrium film pressure of adsorbed vapor, ergs/cm.$^2$

$\rho$ = density, g./cc.

$\phi_{12}$ = Girifalco-Good interaction parameter for substances 1 and 2, dimensionless

$\phi_{\underline{A}}$ = component of $\phi$ dependent upon attractive force constants in potential energy function; independent of intermolecular distance terms, dimensionless

$\phi_{\underline{r}}$ = component of $\phi$ dependent upon terms involving intermolecular distance; independent of attractive constants, dimensionless

$\Omega$ = nonplar component of solubility parameter $(\text{cal./cc.})^{0.5}$

$\omega$ = polar component of solubility parameter, $(\text{cal./cc.})^{0.5}$

## ACKNOWLEDGMENTS

The author is indebted to a great many people for their contributions to this thesis. Special appreciation is expressed to the members of his Faculty Advisory Committee, which was chaired by Mr. J. W. Swanson and included Dr. R. M. Leekley and Dr. J. P. Brezinski, for their time and guidance. The many helpful discussions with and suggestions from other members of the Institute staff and faculty as well as fellow students are also acknowledged. The encouragement and counsel of Dean J. M. Parker and Dr. R. H. Atalla are worthy of particular note.

Other members of the Institute staff who gave unselfishly of their time and talents include Mr. Bruce Andrews, Mr. John Bachhuber, Mr. Marvin Filz, Jr., Mr. Lowell Sell, Miss Olga Smith, and Mr. Paul Van Rossum.

The financial support of The Institute of Paper Chemistry and its member companies is also gratefully acknowledged.

Finally, sincere thanks are extended to my wife, Gail, for her patience, encouragement, and understanding throughout the course of this work and for typing the original manuscript.

## LITERATURE CITED


1. Allen, A. J. G., J. Polymer Sci. 38, no. 134:297-306(Aug., 1969).

2. Leeds, S., Tappi 44, no. 4:244-50(April, 1961).

3. Schonhorn, H., and Hansen, R. H., J. Appl. Polymer Sci. 11, no. 8:1461-74 (Aug., 1967).

4. Neimo, L., Paperi Puu 49, no. 8:509-16(Aug., 1967).

5. Goring, D. A. I., and Suranyi, G., Pulp Paper Mag. Can. 70, no. 10:103-10 (Oct. 17, 1969).

6. Desai, R. L., Pulp Paper Mag. Can. 71, no. 14:51-2(July 17, 1970).

7. Gould, R. F., editor. Advances in Chemistry Series no. 66: Irradiation of polymers. Washington, D.C., American Chemical Society, 1967. 275 p.

8. Huntsberger, J. R. The nature of adhesion. Paper delivered at Adhesion Course II-Polymer Conference Series. University of Utah, May 11-16, 1970.

9. Society of Chemical Industry. Adhesion and adhesives — fundamentals and practice. New York, Wiley, 1954. 229 p.

10. Bikerman, J. J. The science of adhesive joints. New York, Academic Press, 1961. 248 p.

11. Bikerman, J. J. Adhesion and bonding — theory of adhesive joints. In Mark's Encyclopedia of polymer science and technology. Vol. 1. p. 477-82. New York, Interscience, 1964.

12. Ross, S., Symposium Chairman. Chemistry and physics of interfaces. Washington, D.C., American Chemical Society, 1965. 177 p. (Reprinted from Ind. Eng. Chem: Sept., 1964-Sept., 1965.)

13. Zisman, W. A. Adhesion and bonding — effect of chemical constitution. In Mark's Encyclopedia of polymer science and technology. Vol. 1. p. 445-77. New York, Intersceince, 1964.

14. Fowkes, F. M., Symposium Chairman. Advances in Chemistry Series no. 43: Contact angle, wettability, and adhesion. Washington, D.C., American Chemical Society, 1964. 389 p.

15. Maxfield, F. A., and Benedict, R. R. Theory of gaseous conduction and electronics. p. 287. New York, McGraw-Hill, 1941. 483 p.

16. Coffman, J. A., and Browne, W. R., Sci. Am. 212, no. 6:90-8(June, 1965).

17. Shahin, M. M., J. Chem. Phys. 45, no. 7:2600-5(Oct. 1, 1966).

18. Shahin, M. M., Applied Optics Supplement on Electrophotography, no. 3:106-10(1969).

19. Carlsson, D. J., and Wiles, D. M., Can. J. Chem. 48, no. 15:2397-2406 (Aug. 1, 1970).

20. Eidman, R. A. L. Surface activation of polymer films by electrical discharge. Doctor's Dissertation. St. Louis, Mo., Washington Univ., 1963. 123 p.; Diss. Abstr. 24:1955.

21. Lohkamp, D. T. Surface reactions on polyethylene film due to corona-discharge treatment. Doctor's Dissertation. St. Louis, Mo., Washington Univ., 1964. 165 p.; Diss. Abstr. 26:1537.

22. Porter, J. C. Surface activation of polyethylene by electrical discharge. Doctor's Dissertation. St. Louis, Mo., Washington Univ., 1960. 144 p.; Diss. Abstr. 21:2224.

23. Lohkamp, D. T., et al. Surface activation of polyethylene films in electrical discharge. Paper presented at Symposium on Surface Phenomena-Engineering Aspects. American Institute of Chemical Engineers, 57th Annual Meeting, Minneapolis, Sept. 26-29, 1965.

24. Anderson, J. R. Determination of the wetting characteristics of starches and other polymers as measured by contact angles. Doctor's Dissertation. Urbana, Ill., Univ. of Illinois, 1958. 115 p.; Diss. Abstr. 19:965.

25. Rossman, K., J. Polymer Sci. 19, no. 91:141-4(Jan., 1956).

26. Greene, R. E., Tappi 48, no. 9:80-84A(Sept., 1965).

27. Hofling, E., and Breu, H., Adhaesion 10, no. 6:252-5(June, 1966).

28. Kayan, W. S., U.S. pat. 2,859,481(Nov. 11, 1958).

29. Nelson, I. L., U.S. pat. 3,200,313(Feb. 21, 1962).

30. Wechsberg, H. E., and Webber, J. B., Mod. Plastics 36, no. 11:101-9, 160-1 (July, 1959).

31. Wilson, H. L., and von der Heide, J. C., Mod. Plastics 38, no. 9:199-206, 344(May, 1961).

32. Goring, D. A. I., Pulp Paper Mag. Can. 68, no. 8:T372-6(Aug., 1967).

33. Goring, D. A. I. Personal communication, 1969.

34. Swanson, J. W., and Becher, J. J., Tappi 49, no. 5:198-202(May, 1966).

35. Glossman, N., Tappi 50, no. 5:224-6(May, 1967).

36. Rauhut, H. W. Surface pretreatment of polyethylene for optimum structural adhesive joints. American Chemical Society Reprint 28, no. 1:545-59 (1968).

37. Zisman, W. A., Ind. Eng. Chem. 55, no. 10:19-38(Oct., 1963).

38. Hildebrand, J. H., and Scott, R. L. The solubility of nonelectrolytes. 3rd ed. New York, Reinhold, 1950. 488 p.

39. Jurecic, A., Tappi 49, no. 7:306-10(July, 1966).

40. Chem. Eng. 72, no. 21:114(Oct. 11, 1965).

41. Tabor, D., Reference (9), p. 27.

42. Voyutskii, S. S., and Vakula, V. L., J. Appl. Polymer Sci. 7, no. 2:475-92(March-April, 1963).

43. Voyutskii, S. S., Deryagin, B. V., and Raeskii, V. G., Dokl. Akad. Nauk. SSSR. 161, no. 2:377-9(1955); ABIPC 36:A8633.

44. Voyutskii, S. S., and Vakula, V. L., Vysokomol. Soed. 2, no. 1:51-60 (1960). (Russian; English summary.)

45. Vasenin, R. M., Vysokomol. Soed. 3, no. 5:679-85(May, 1961); ABIPC 32:A3777.

46. Bueche, F., J. Chem. Phys. 20, no. 12:1959-64(Dec., 1952).

47. Deryagin, B. V., Research 8:70-4(1955); Transl. from Vestn. Akad. Nauk SSSR 7:30(1954).

48. Karasev, V. V., Krotova, N. A., and Deryagin, B. V., Doklady Akad. Nauk SSSR 89:109-12(March 1, 1953).

49. Voyutskii, S. S., Adhesives Age 5, no. 4:30-6(April, 1962).

50. Skinner, S. M., Savage, R. L., and Rutzler, R. E., Jr., J. Appl. Phys. 24, no. 4:438-50(April, 1953).

51. Skinner, S. M., Gaynor, J., and Sohl, G. W., Mod. Plastics 33, no. 6:127-36, 246(Feb., 1956).

52. Czyzak, S. J., Reference (9), p. 16-20.

53. Young, T., Phil. Trans. Roy. Soc. (London) 16:65(1805); Reference (14), p. 2.

54. Johnson, R. E., Jr., J. Phys. Chem. 63, no. 10:1655-8(Oct., 1959).

55. Lester, G. R., J. Colloid Sci. 16, no. 4:315-26(Aug., 1961).

56. Bangham, D. H., and Razouk, R. I., Trans. Faraday Soc. 33:145-72(1937).

57. Bangham, D. H., Trans. Faraday Soc. 33:805-11(1937).

58. Fowkes, F. M. In Marchessault and Skaar's Surfaces and coatings related to paper and wood. Chapter 5. Syracuse, N.Y., Syracuse University Press, 1967. 507 p.

58A. Dupre, A., Theorie mecanique de la chaleur., p. 368-9. Paris, 1869.

59. Barbarisi, M. J., Nature 215, no. 5099:383-4(July 22, 1967).

60. Wenzel, R. N., Ind. Eng. Chem. 28, no. 8:988-94(Aug., 1936).

61. Cassie, A. B. D., and Baxter, S., Trans. Faraday Soc. 40:546-51(1946).

62. Cassie, A. B. D., Discussions Faraday Soc. 3:11-16(1948).

63. Shuttleworth, R., and Failey, G. L. R., Discussions Faraday Soc. 3:16-22 (1948).

64. Yarnold, G. D., Proc. Phys. Soc. (London) 58:120-5(1946).

65. Yarnold, G. D., and Mason, B. J., Proc. Phys. Soc. (London) 62B:121-8 (1949).

66. Johnson, R. E., Jr., and Dettre, R. H., Reference (14), p. 112.

67. Dettre, R. H., and Johnson, R. E., Jr., Reference (14), p. 136.

68. Johnson, R. E., Jr., and Dettre, R. H., J. Phys. Chem. 68, no. 7:1744-50 (July, 1964).

69. Dettre, R. H., and Johnson, R. E., Jr., J. Phys. Chem. 69, no. 5:1507-15 (May, 1965).

70. Sharpe, L. H., and Schonhorn, H., Reference (14), p. 189.

71. Girifalco, L. A., and Good, R. J., Phys. Chem. 61, no. 7:904-9(July, 1957).

72. Chan, R. K. S., J. Colloid Interface Sci. 32, no. 3:492-504(March, 1970).

73. Dann, J. R., J. Colloid Interface Sci. 32, no. 2:302-31(Feb., 1970).

74. Fowkes, F. M., Ind. Eng. Chem. 56, no. 12:40-52(Dec., 1964).

75. Owens, D. K., and Wendt, R. D., J. Appl. Polymer Sci. 13, no. 8:1741-7 (Aug., 1969).

76. Bartell, F. E., and Ray, B. R., J. Am. Chem. Soc. 74, no. 3:778-83 (Feb. 5, 1952).

77. Ray, B. R., and Bartell, F. E., J. Phys. Chem. 57, no. 1:49-56(Jan., 1953).

78. Ray, B. R., Anderson, J. R., and Scholz, J. J., J. Phys. Chem. 62, no. 10:1220-30(Oct., 1958).

79. Sandell, M. A. Wetting of wood polysaccharides. M.S. Thesis. Syracuse, N.Y., State University College of Forestry, 1967. 166 p.

80. Luner, P., and Sandell, M. A., J. Polymer Sci., Part C, no. 28:115-42 (1969).

81. Good, R. J., Reference (14), p. 74.

82. Good, R. J., J. Phys. Chem. 61, no. 6:810-13(June, 1957).

83. Good, R. J., and Elbing, E., Ind. Eng. Chem. 62, no. 3:54-78(March, 1970).

84. Fowkes, F. M., Reference (14), p. 99.

85. Fowkes, F. M., J. Phys. Chem. 67, no. 12:2538-41(Dec., 1963).

86. Fowkes, F. M., J. Colloid Interface Sci. 28, no. 3/4:493-505(Nov.-Dec., 1968).

87. Wu, S., J. Phys. Chem. 74, no. 3:632-8(Feb. 5, 1970).

88. Adamson, A. W. Physical chemistry of surfaces. Chapter 5. New York, Interscience, 1960. 630 p.

89. Bauer, N., and Lewin, S. Z. In Weissberger's Techniques of organic chemistry. Vol. 1. Part 1. p. 136. Interscience, New York, 1959.

90. Janes, R. L. A study of adhesion in the cellulose-starch-cellulose system. Doctor's Dissertation. Appleton, Wis., The Institute of Paper Chemistry, 1968.

91. Wink, W. A., and Van Eperen, R. H., Tappi 50, no. 8:393-400(Aug., 1967).

92. Harkins, W. D., and Jordan, H. F., J. Am. Chem. Soc. 52, no. 5:1751-72 (May, 1930).

93. Freud, B. B., and Freud, H. Z., J. Am. Chem. Soc. 52, no. 5:1772-82 (May, 1930).

94. Sears, G. R., Van den Akker, J. A., Aprison, M. H., Beckman, N. J., and Denzer, C. W., Tappi 38, no. 2:96-105(Feb., 1955).

95. Hicks, C. R. Fundamental concepts in the design of experiments. p. 268. New York, Holt Rinehart and Winston, 1964.

96. Weast, R. C., Chief Editor. Handbook of chemistry and physics. 46th edition. Cleveland, The Chemical Rubber Co., 1965.

97. National Research Council. International critical tables of numerical data. Vol. 4. p. 436. New York, McGraw-Hill, 1928.

98. Borgin, K., Norsk Skogind. 13, no. 11:429-42(Nov., 1959); 14, no. 11:485-95(Nov., 1960).

99. Persinger, H., and Rivas, W., Unpublished work, 1970.

100. Lee, L. H., J. Appl. Polymer Sci. 12, no. 4:719-30(April, 1968).

101. Gardon, J. L. In Encyclopedia of polymer science and technology. Vol. 3. p. 833-62. New York, Interscience, 1965.

102. Thode, E. F., and Guide, R. G., Tappi 42, no. 1:35-9(Jan., 1959).

103. Goring, D. A. I., Can. pat. 830,468(Dec. 23, 1969).

104. Thorsen, W. J., and Landwehr, R. C., Textile Res. J. 40, no. 8:688-95(Aug., 1970).

105. Burrell, H., and Immergut, B. Solubility parameter values. In Brandrup and Immergut's Polymer handbook. p. 341-68. New York, Interscience, 1966.

106. Robertson, A. A., Tappi 53, no. 7:1331-9(July, 1970).

107. Craver, J. K., J. Appl. Polymer Sci. 14, no. 7:1755-65(July, 1970).

# APPENDIX I

## CORONA-TREATING EQUIPMENT

A photograph of the corona-treating equipment is given in Fig. 21. The major components are: (1) high-voltage power supply; (2) treatment chamber; (3) web-drive control; (4) sample web; (5) gas-scrubbing flasks; (6) web-tension control; (7) gas-flow rotameter; (8) needle valve for regulating gas flow; (9) web-drive motor.

The web drive consists of a variable-speed electric motor, connected to a rubber drive roll by a chain drive. The speed calibration data are presented in Fig. 22, for drive sprockets having the ratio of 1/1. An additional set of sprockets, in the ratio of 2.4/1.0, was available and could be used in either order to further increase the range of available web speeds.

A schematic diagram of the power supply may be found in Fig. 23. The main power switch is keyed, to minimize the chances of accidental activation of the high-voltage circuit. A safety switch opens the primary circuit when the door of the chassis is opened. The voltage-measuring circuit was calibrated in the range of 0 to 5,000 volts with a suitable AC voltmeter. These data are presented in Fig. 24.

The electrode configuration is sketched in Fig. 25.

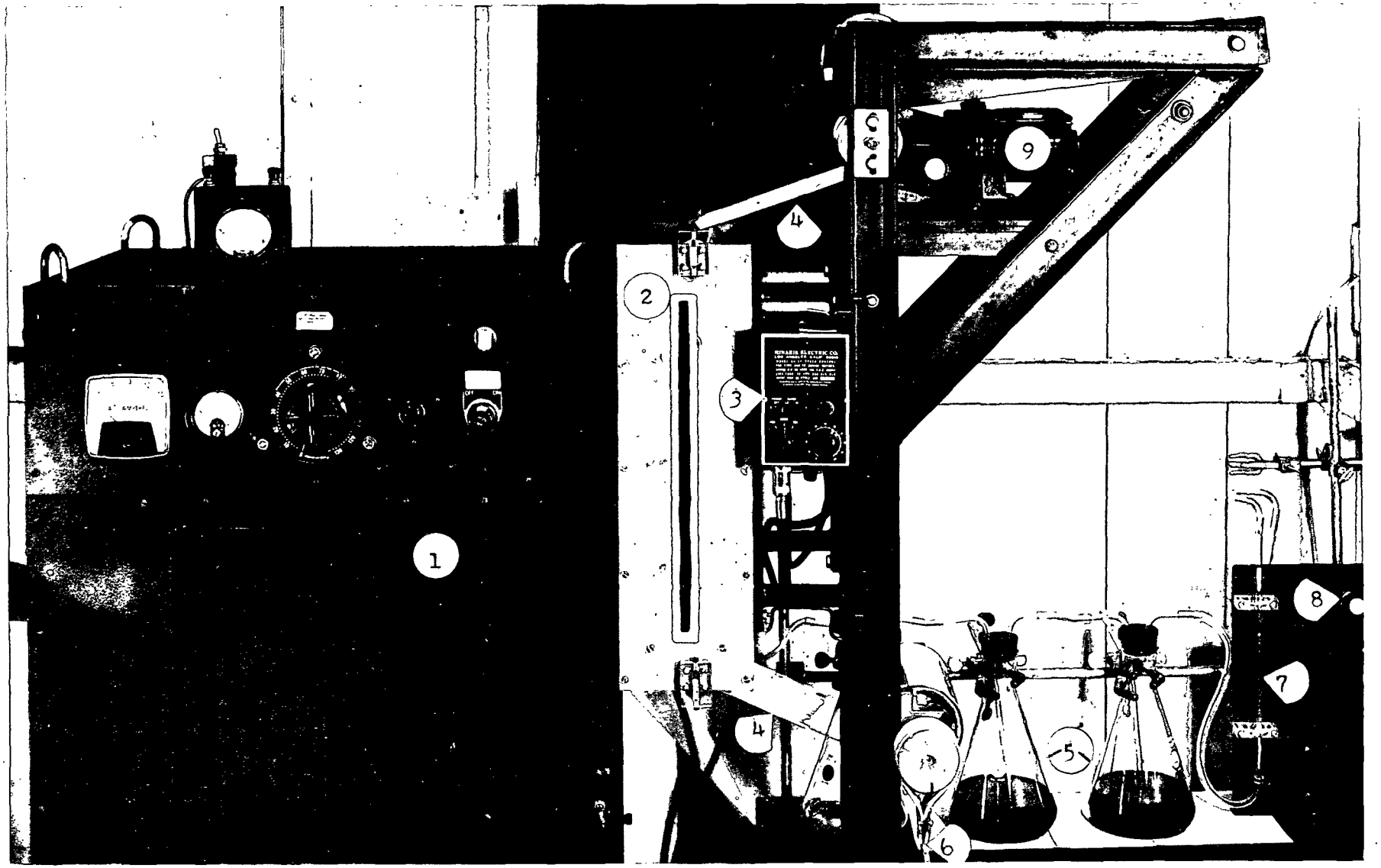


Figure 21. Corona-Treating Equipment: (1) High-Voltage Power Supply; (2) Treatment Chamber; (3) Web-Drive Control; (4) Sample Web; (5) Gas-Scrubbing Flasks; (6) Web-Tension Control; (7) Gas-Flow Rotameter; (8) Needle Valve; (9) Web-Drive Motor

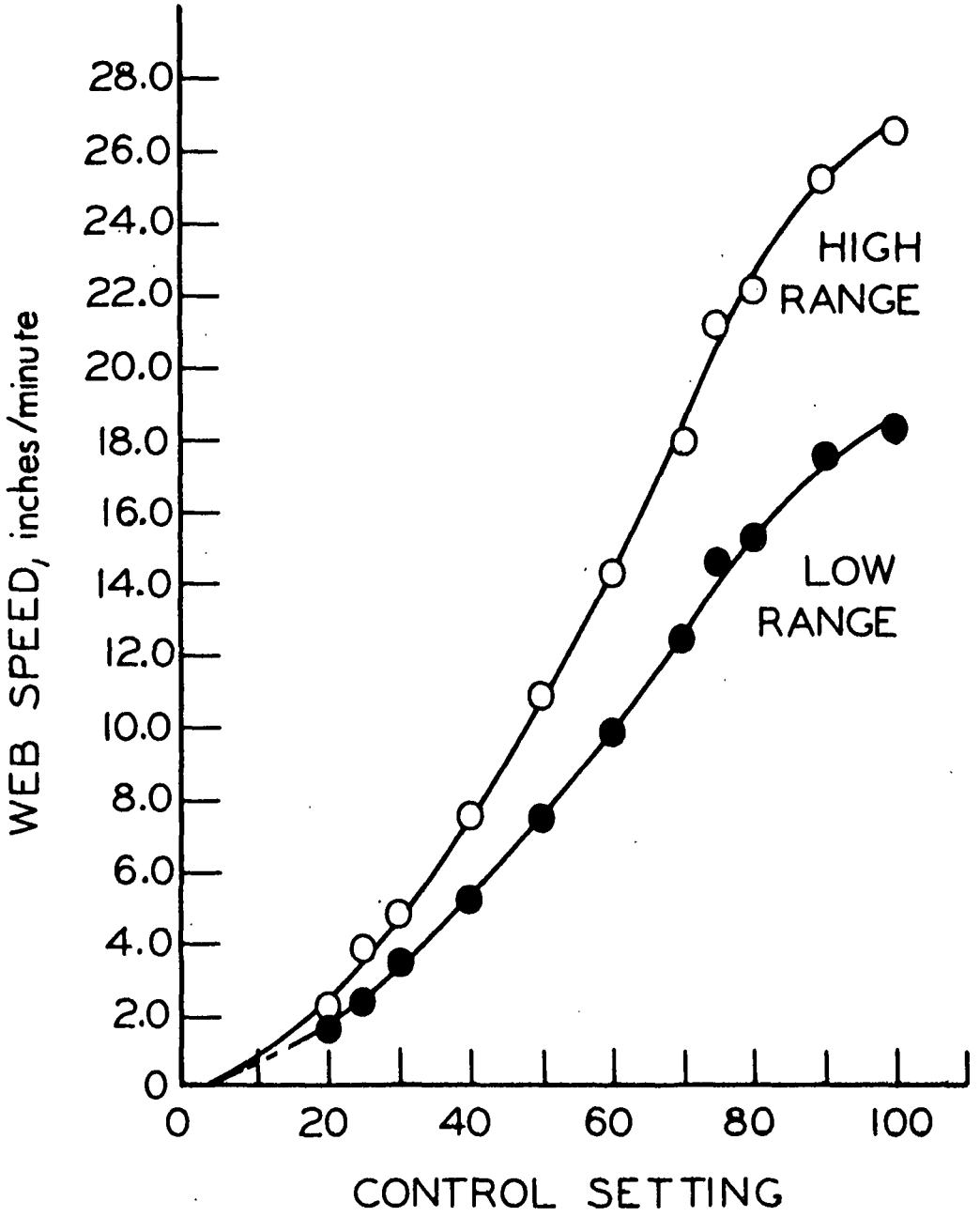


Figure 22. Calibration Data for Web Drive with 1/1 Sprockets in Place

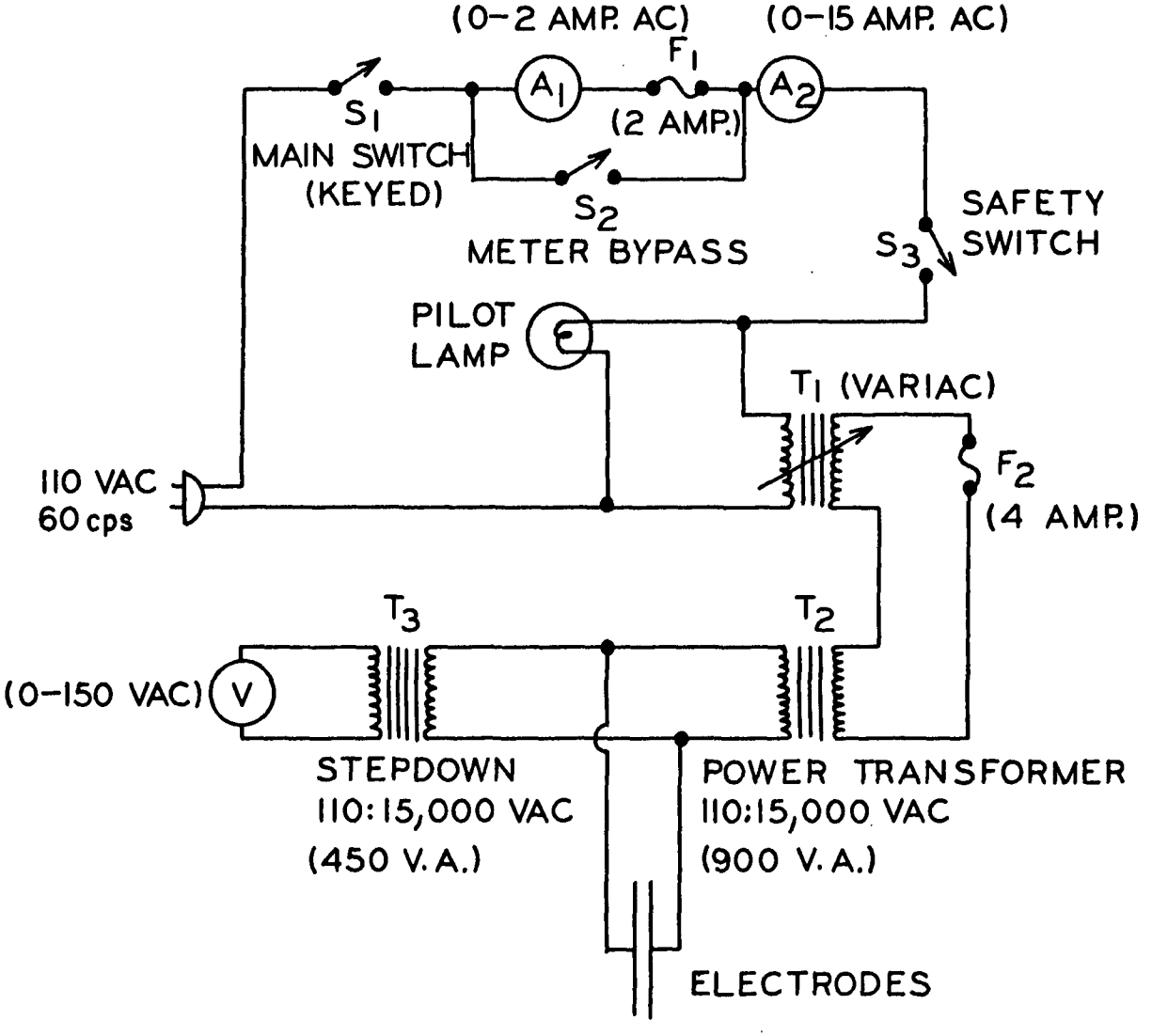


Figure 23. Power Supply

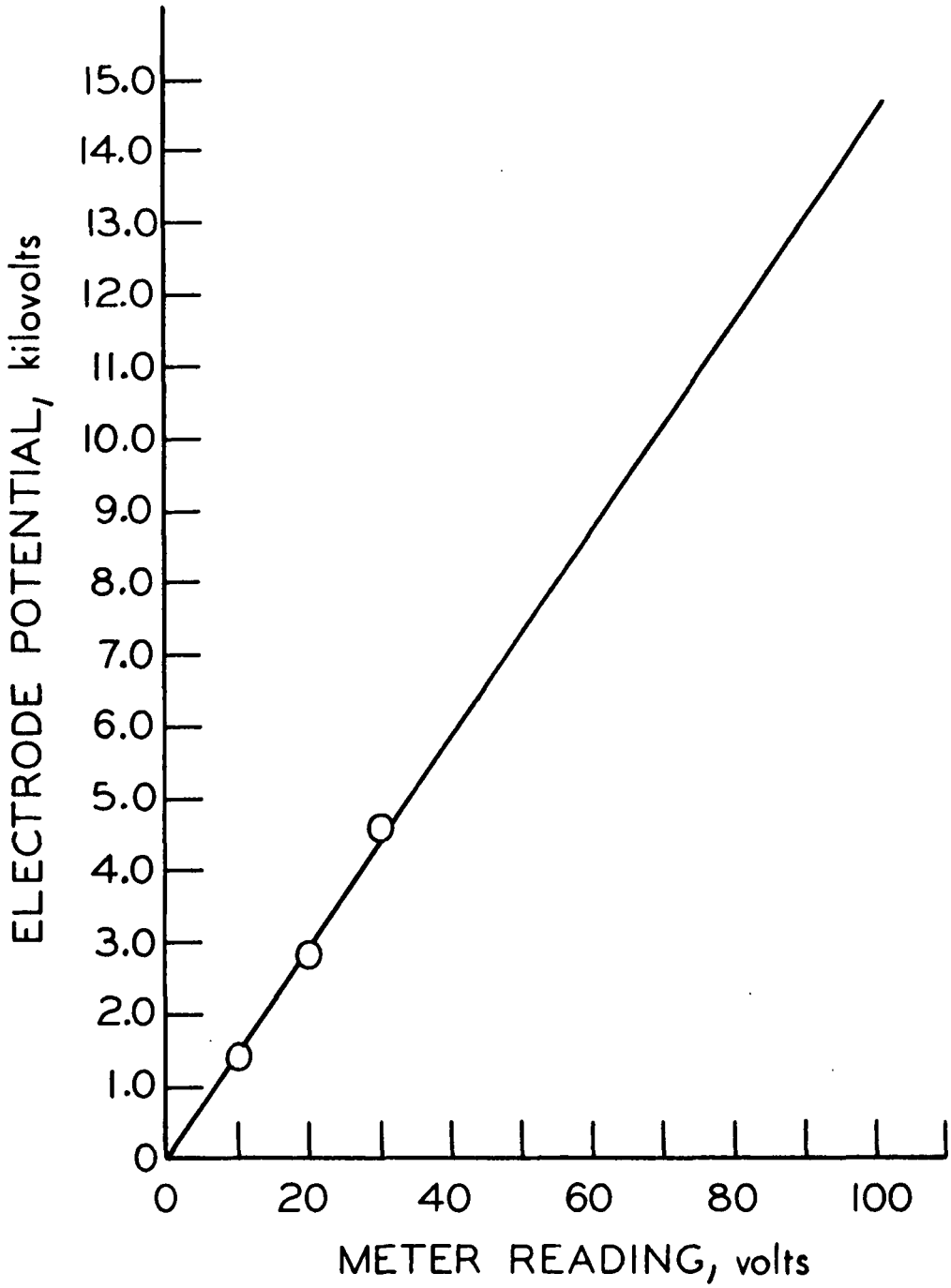


Figure 24. Calibration Curve for Voltage-Measuring Circuit

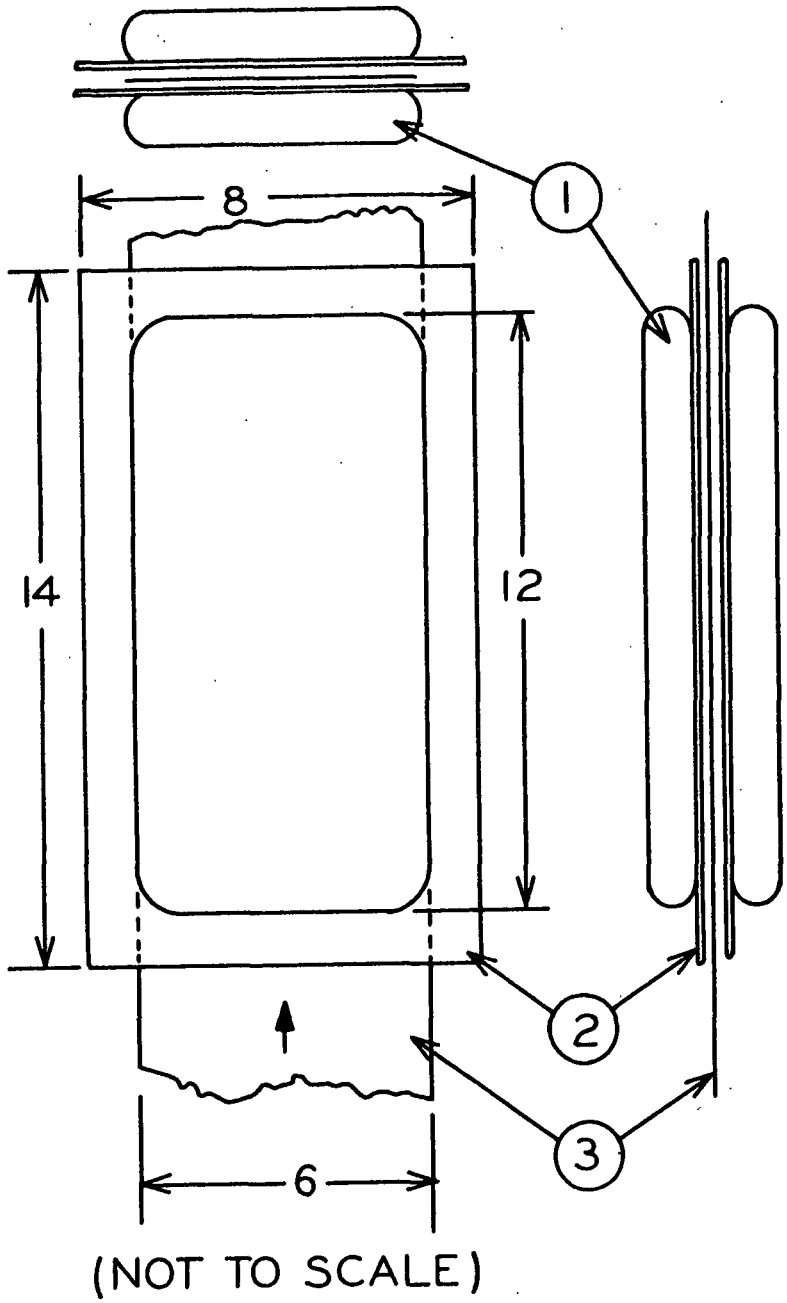


Figure 25. Electrode Configuration: (1) 1-Inch Thick, Polished Aluminum Electrodes; (2) 0.030-Inch Thick, Natural Mica Dielectric; (3) Sample Web. Total Air-Gap is 0.25 Inch

# APPENDIX II

## PURIFICATION OF CONTACTING LIQUIDS

Water was triply-distilled as previously described on page 30. The remaining contacting liquids were obtained as reagent-grade products from Sargent Welch Scientific Co., and were subsequently purified by vacuum distillation. A Nester/Faust spinning-band distillation column was used, and the conditions are given below:

Methylene Iodide (EK 167)

57.0°C. at 8.5 mm. Hg.

1,1,2,2-Tetrabromoethane (EK 240)

103.0°C. at 8.5 mm. Hg.

After distillation, the liquids were stored in tightly stoppered glass bottles, covered with aluminum foil to exclude light.

## APPENDIX III

## CORRECTION FACTORS FOR THE RING METHOD

The measurements of liquid surface tension by the ring method must be corrected for the effects of meniscus shape. A set of correction factors were experimentally determined by Harkins and Jordan (95), and tabulated as functions of the parameters $R/r$ and $R^3/V$, where $R$ is the radius of the ring, $r$ the radius of the wire from which the ring is constructed, and $V$ is the volume of the liquid held above the equilibrium liquid-surface at detachment.

It was found that for the ring sizes on hand ($R \approx 1.0$ cm.), methylene iodide and tetrabromoethane gave values of $R^3/V$ which were greater than 3.50, and beyond the range of the published data.

A theoretical treatment of the effects of meniscus shape has been given by Freud and Freud (96) in terms of the dimensionless variables $\overline{R} = R/a$ and $\overline{V} = V/a^3$, where $a^2$ is the capillary constant of the liquid as defined by Equation (33).

$$a^2 = 2\gamma/(\rho g) \quad , \tag{33}$$

where $\gamma$ is the liquid surface tension, $\rho$ the liquid density, and $g$ the acceleration due to gravity. The rigorous application of this theory requires the use of some rather involved graphical methods in order to determine the appropriate correction factor, $f$.

The method used in this study involved conversion of the data of Harkins and Jordan (95) to the dimensionless form suggested by Freud and Freud (96).

These data could then be extrapolated to cover the range of interest. The method is outlined below.

The correction factor, $\underline{f}$, is equal to the ratio of the true surface tension, $\gamma$, to the uncorrected, measured value, $\gamma_{\underline{m}}$, which is represented by Equation (34):

$$\gamma_m = V\rho g/(2\pi R) \quad . \tag{34}$$

Combination of Equations (33) and (34) yields expressions for the dimensionless variables $\overline{\underline{R}}$, and $\overline{\underline{V}}$, in terms of the quantities tabulated by Harkins and Jordan:

$$\overline{R} = \sqrt{2\pi(R^3/V)/f} \quad , \tag{35}$$

$$\overline{V} = \sqrt{(R^3/V) \cdot (2\pi/f)^3} \quad . \tag{36}$$

For chosen values of $\underline{R}/\underline{r}$, corresponding to the rings available, Equations (34) and (36) were used to calculate values of $\overline{\underline{R}}$ and $\overline{\underline{V}}$ from the published data. Polynomial regression analysis was then used to establish the relationship between $\overline{\underline{R}}$ and $\overline{\underline{V}}$. The best fit was obtained by a second-degree equation in the following form for $\underline{R}/\underline{r} = 54.0$:

$$\overline{V} = -1.473 + 6.885\ (\overline{R}) + 0.1528\ (\overline{R})^2 \quad . \tag{37}$$

Now for a chosen value of $\overline{\underline{R}}$, the corresponding value of $\overline{\underline{V}}$ could be determined from Equation (37). The values of $\underline{f}$ and $\underline{R}^3/\underline{V}$ could then be calculated from Equations (38) and (39):

$$R^3/V = \overline{R}^3/\overline{V} \quad , \tag{38}$$

$$f = 2\pi\overline{R}/\overline{V} \quad . \tag{39}$$

The results of these calculations, covering the desired range of values, are given in Table XI, and represent the correction factors used in this study.

TABLE XI

CALCULATED CORRECTION FACTORS FOR THE RING METHOD
($R/r = 54$)

| $R^3/V$ | $f$ |
|---|---|
| 3.40 | 0.854 |
| 3.50 | 0.852 |
| 3.60 | 0.851 |
| 3.70 | 0.849 |
| 3.80 | 0.847 |
| 3.90 | 0.845 |
| 4.00 | 0.843 |
| 4.10 | 0.842 |
| 4.20 | 0.840 |
| 4.30 | 0.838 |
| 4.40 | 0.837 |
| 4.50 | 0.835 |
| 4.60 | 0.834 |
| 4.70 | 0.832 |

The surface tension data and the appropriate correction factors for the liquids used in this study are listed below:

| Water | $CH_2I_2$ | TBE |
|---|---|---|
| $\gamma_m = 77.38$ | $\gamma_m = 60.23$ | $\gamma_m = 58.45$ ergs/cm.$^2$ |
| $R^3/V = 0.942$ | $R^3/V = 3.919$ | $R^3/V = 3.606$ |
| $R/r = 53.0$ | $R/r = 54.0$ | $R/r = 53.0$ |
| $f = 0.940$ | $f = 0.845$ | $f = 0.849$ |
| $\gamma = 72.74$ | $\gamma = 50.89$ | $\gamma = 49.67$ ergs/cm.$^2$ |

APPENDIX IV

CONSTRUCTION OF CONTACT-ANGLE CHAMBER

The contact-angle chamber was constructed from a Lucite tube, and contained two transparent glass windows to permit undistorted viewing of the liquid drops. The details of the design are given in the following drawing.

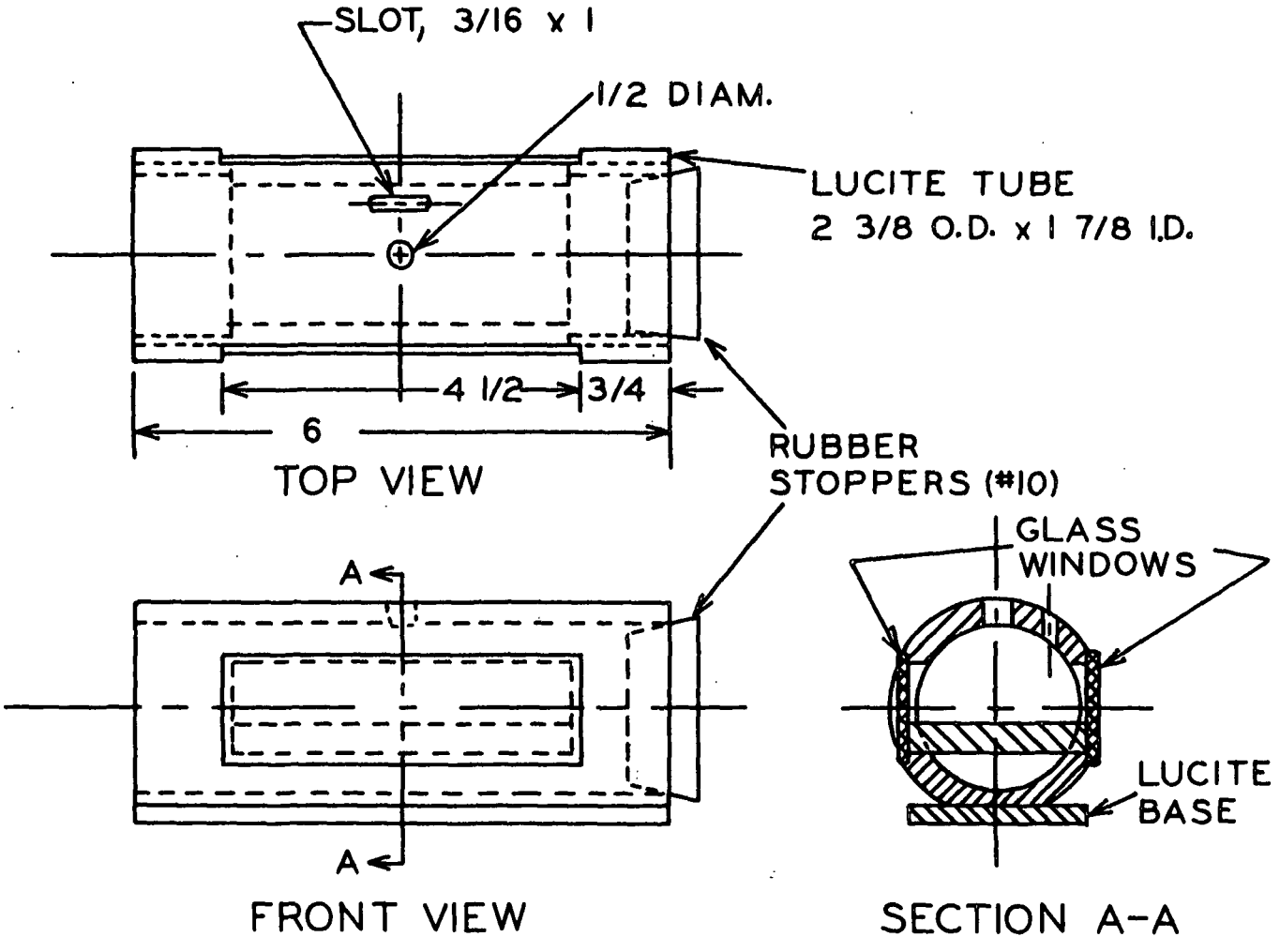


Figure 26. Contact-Angle Chamber

# APPENDIX V

## CALIBRATION OF THE CHAPMAN SMOOTHNESS TESTER

The general calibration procedures for the Chapman smoothness tester have been sufficiently described by Sears, et al. (97). It is only necessary to describe here the application of these procedures to the presently used instrument, which was equipped with a modified readout circuit.

It was shown (97) that the fractional smoothness value, F, is given by an equation of the form,

$$F = M/(N + C_b/C_a) \ .$$

In this equation, M and N are instrument constants, and $C_a$, $C_b$ are readings of Photocells A and B, respectively. In the calibration procedure, readings were first taken with the opal-glass standard in close proximity to, but not in contact with, the upper prism of the instrument. Under these conditions, F is equal to zero and the photocell readings were denoted as $C'_a$ and $C'_b$, respectively. Complete optical contact was then obtained between the standard block and the instrument prism by means of a film of clear mineral oil. The quantity, F, then becomes unity, and the photocell readings were labelled $C''_a$ and $C''_b$. Substitution of these quantities into the above equation yields the following expressions for the instrument constants, M and N:

$$M = C'_b/C''_a \ ,$$

$$N = (C'_b - C''_b)/C''_a \ .$$

Having determined the values of the constants $\underline{M}$ and $\underline{N}$, a calibration curve could then be constructed to give $\underline{F}$ as a function of the ratio $\underline{C_b}/\underline{C_a}$. To simplify this procedure, the electronic circuit was adjusted for each reading so that $\underline{C_b}$ was equal to a constant, $\underline{B_s}$, having a value such that $\underline{C_a}$ represented a full-scale galvanometer reading when $\underline{F}$ was equal to unity.

For the particular opal-glass block which was used as a standard in this work, the following constant values were determined:

$\underline{M} = 1.557$

$\underline{N} = 0.685$

$\underline{B_s} = 0.865$

From these values, the calibration curve shown in Fig. 27 was constructed.

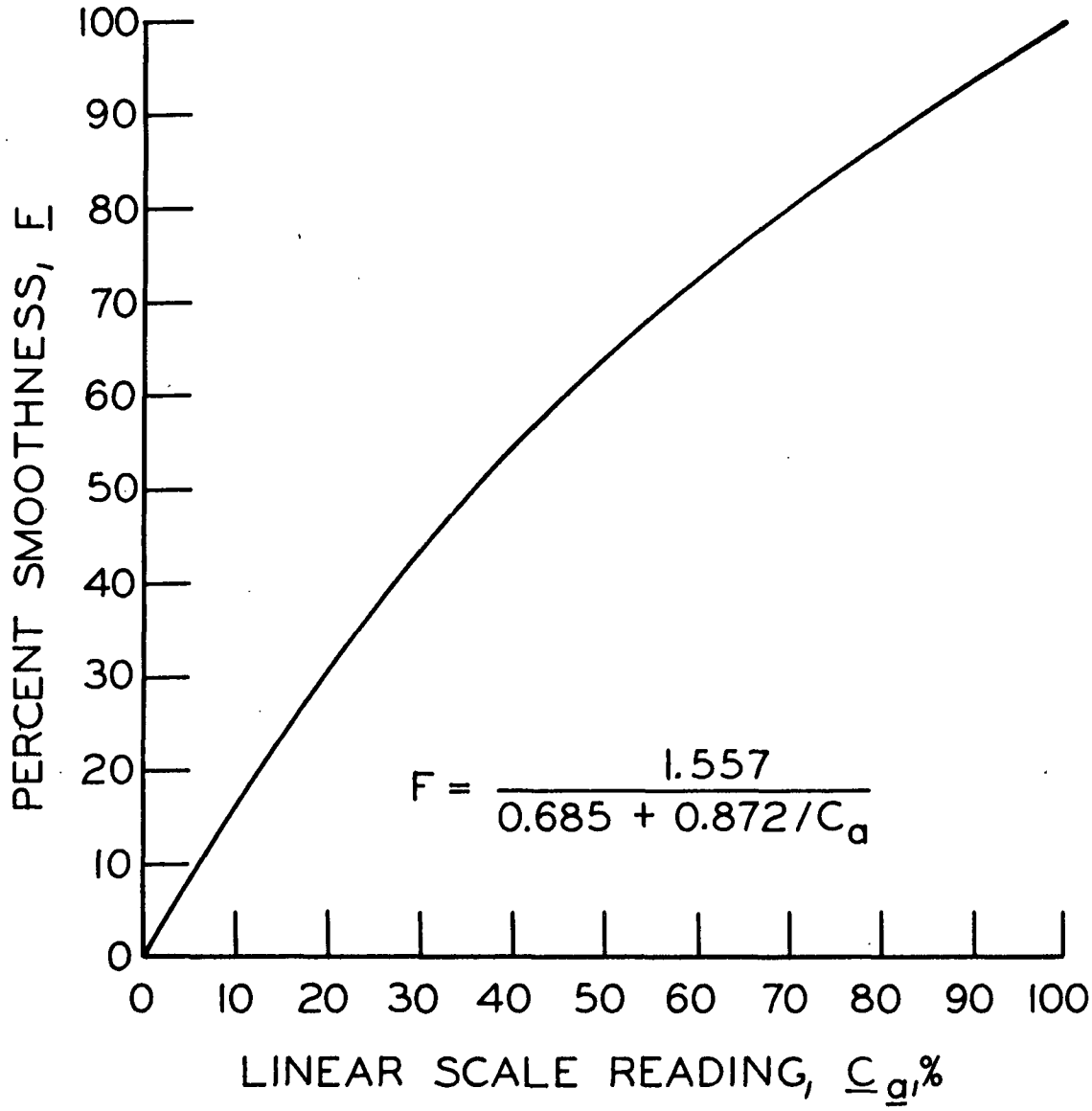


Figure 27. Chapman Smoothness Calibration Curve

# APPENDIX VI

## BOND STRENGTH DATA

### TABLE XII

BOND STRENGTH DATA
(BREAKING LOADS IN LBS.)

UNTREATED
515. 580. 575. 620. 590.
N= 5 MEAN= 576.0 VARIANCE= 1467.5
STD. DEV.= 38.31 STD. ERROR OF MEAN=17.1

0.2 MINUTES CORONA TREATMENT
1230. 1355. 1310. 1295. 1265. 1250. 1285. 1205.
1275. 1330.
N=10 MEAN=1280.0 VARIANCE= 2061.1
STD. DEV.= 45.40 STD. ERROR OF MEAN=14.4

0.5 MINUTES CORONA TREATMENT
1645. 1395. 1675. 1605. 1550. 1420. 1440. 1565.
1490. 1620. 1505. 1720. 1520. 1520. 1320. 1580.
1455. 1475. 1365. 1535.
N=20 MEAN=1520.0 VARIANCE=10897.4
STD. DEV.=104.39 STD. ERROR OF MEAN=23.3

1.0 MINUTES CORONA TREATMENT
1855. 1700. 1590. 1665. 1680. 1735. 1610. 1625.
1715. 1565. 1820. 1455. 1750. 1905. 1670. 1540.
1505. 1645. 1775. 1795.
N=20 MEAN=1680.0 VARIANCE=13910.5
STD. DEV.=117.94 STD. ERROR OF MEAN=26.4

3.0 MINUTES CORONA TREATMENT
2000. 2020. 2065. 1710. 2040. 1880. 2120. 2090.
1800. 1980. 1860. 2210. 1940. 1950. 2155. 1900.
1765. 1960. 1920. 1835.
N=20 MEAN=1960.0 VARIANCE=17363.2
STD. DEV.=131.77 STD. ERROR OF MEAN=29.5

5.0 MINUTES CORONA TREATMENT
2130. 1900. 2390. 1900. 2445. 1775. 1915. 2230.
1710. 2130. 2505. 1485. 2160. 2045. 2155. 2055.
1800. 2000. 2050. 2100. 1885. 1950. 2305. 2040.
2215.
N=25 MEAN=2051.0 VARIANCE=54906.3
STD. DEV.=234.32 STD. ERROR OF MEAN=46.9

# APPENDIX VII

## CONTACT ANGLE DATA

### TABLE XIII
### CONTACT ANGLES ON AIR-SIDES (DEGREES)

#### NO CORONA TREATMENT

WATER, 50 PERCENT R.H.

| | | | | | | | | | | | |
|---|---|---|---|---|---|---|---|---|---|---|---|
| 36. | 37. | 37. | 38. | 37. | 39. | 39. | 40. | 36. | 37. | 38. | 36. |
| 35. | 34. | 38. | 38. | 36. | 37. | 38. | 37. | 40. | 41. | 35. | 37. |
| 28. | 28. | 29. | 27. | 40. | 33. | 36. | 40. | 35. | 38. | 40. | 41. |
| 39. | 45. | 31. | 40. | 44. | 41. | 38. | 34. | 42. | 43. | 41. | 36. |

N=48 MEAN=37.2 VARIANCE=15.39
STD. DEV.=3.92 STD. ERROR OF MEAN=0.57

METHYLENE IODIDE, 50 PERCENT R.H.

| | | | | | | | | | | | |
|---|---|---|---|---|---|---|---|---|---|---|---|
| 42. | 41. | 41. | 41. | 39. | 40. | 37. | 40. | 40. | 40. | 41. | 41. |
| 43. | 40. | 39. | 39. | 41. | 40. | 39. | 41. | 40. | 36. | 33. | 43. |
| 43. | 43. | 37. | 41. | 42. | 39. | 40. | 40. | 38. | 40. | 42. | 42. |
| 39. | 39. | 43. | 40. | | | | | | | | |

N=40 MEAN=40.1 VARIANCE= 4.16
STD. DEV.=2.04 STD. ERROR OF MEAN=0.32

TETRABROMOETHANE, 50 PERCENT R.H.

| | | | | | | | | | | | |
|---|---|---|---|---|---|---|---|---|---|---|---|
| 27. | 27. | 28. | 29. | 28. | 28. | 26. | 27. | 26. | 30. | 31. | 30. |
| 30. | 30. | 29. | 28. | 27. | 27. | 28. | 28. | | | | |

N=20 MEAN=28.2 VARIANCE= 2.06
STD. DEV.=1.44 STD. ERROR OF MEAN=0.32

WATER, 2 PERCENT R.H.

| | | | | | | | | | | | |
|---|---|---|---|---|---|---|---|---|---|---|---|
| 45. | 46. | 44. | 43. | 42. | 42. | 44. | 45. | 45. | 43. | 46. | 46. |
| 48. | 47. | 45. | 45. | 45. | 44. | 44. | 43. | | | | |

N=20 MEAN=44.6 VARIANCE= 2.46
STD. DEV.=1.57 STD. ERROR OF MEAN=0.35

METHYLENE IODIDE, 2 PERCENT R.H.

| | | | | | | | | | | | |
|---|---|---|---|---|---|---|---|---|---|---|---|
| 35. | 36. | 38. | 37. | 37. | 36. | 35. | 36. | 37. | 38. | 33. | 34. |
| 36. | 38. | 37. | 37. | 38. | 37. | 37. | 36. | | | | |

N=20 MEAN=36.4 VARIANCE= 1.83
STD. DEV.=1.35 STD. ERROR OF MEAN=0.30

TETRABROMOETHANE, 2 PERCENT R.H.

| | | | | | | | | | | | |
|---|---|---|---|---|---|---|---|---|---|---|---|
| 26. | 25. | 26. | 28. | 23. | 22. | 24. | 24. | 25. | 27. | 25. | 27. |
| 26. | 27. | 26. | | | | | | | | | |

N=15 MEAN=25.4 VARIANCE= 2.69
STD. DEV.=1.64 STD. ERROR OF MEAN=0.42

TABLE XIII (Continued)
CONTACT ANGLES ON AIR-SIDES

0.5 MINUTES CORONA TREATMENT

WATER, 50 PERCENT R.H.

32. 33. 33. 34. 31. 35. 32. 33. 34. 31. 33. 32.
30. 29. 30. 28. 30. 32. 31. 31.
N=20 MEAN=31.7 VARIANCE= 3.17
STD. DEV.=1.78 STD. ERROR OF MEAN=0.40

METHYLENE IODIDE, 50 PERCENT R.H.

39. 38. 40. 41. 41. 40. 42. 42. 40. 40. 40. 41.
38. 39. 38. 40. 41. 40. 39. 41.
N=20 MEAN=40.0 VARIANCE= 1.47
STD. DEV.=1.21 STD. ERROR OF MEAN=0.27

TETRABROMOETHANE, 50 PERCENT R.H.

27. 26. 26. 26. 28. 27. 28. 29. 25. 24. 24. 23.
27. 28. 27. 26. 27. 26. 28. 26.
N=20 MEAN=26.4 VARIANCE= 2.36
STD. DEV.=1.54 STD. ERROR OF MEAN=0.34

WATER, 2 PERCENT R.H.

39. 39. 38. 37. 40. 41. 38. 38. 37. 36. 37. 35.
40. 39. 39. 38. 37. 37. 38. 38.
N=20 MEAN=38.0 VARIANCE= 2.05
STD. DEV.=1.43 STD. ERROR OF MEAN=0.32

METHYLENE IODIDE, 2 PERCENT R.H.

38. 37. 37. 35. 36. 34. 33. 35. 36. 36. 39. 38.
37. 37. 36. 35. 35. 34. 36. 36.
N=20 MEAN=36.0 VARIANCE= 2.21
STD. DEV.=1.49 STD. ERROR OF MEAN=0.33

TETRABROMOETHANE, 2 PERCENT R.H.

24. 23. 23. 24. 25. 25. 25. 27. 21. 23. 24. 24.
23. 22. 24.
N=15 MEAN=23.8 VARIANCE= 2.03
STD. DEV.=1.42 STD. ERROR OF MEAN=0.37

TABLE XIII (Continued)
CONTACT ANGLES ON AIR-SIDES

1.0 MINUTES CORONA TREATMENT

WATER, 50 PERCENT R.H.

30. 29. 30. 30. 31. 29. 32. 29. 29. 30. 31. 29.
28. 30. 28. 27. 28. 30. 28. 28.
N=20 MEAN=29.3 VARIANCE= 1.59
STD. DEV.=1.26 STD. ERROR OF MEAN=0.28

METHYLENE IODIDE, 50 PERCENT R.H.

41. 41. 39. 38. 40. 40. 41. 42. 43. 40. 37. 38.
40. 39. 41. 40. 41. 40. 41. 40.
N=20 MEAN=40.1 VARIANCE= 1.99
STD. DEV.=1.41 STD. ERROR OF MEAN=0.32

TETRABROMOETHANE, 50 PERCENT R.H.

28. 27. 26. 26. 25. 24. 28. 27. 26. 26. 25. 27.
27. 26. 24. 28. 25. 26. 26. 25.
N=20 MEAN=26.1 VARIANCE= 1.46
STD. DEV.=1.21 STD. ERROR OF MEAN=0.27

WATER, 2 PERCENT R.H.

34. 35. 34. 34. 37. 37. 33. 38. 36. 36. 35. 34.
37. 32. 35. 33. 36. 37. 35. 36.
N=20 MEAN=35.2 VARIANCE= 2.59
STD. DEV.=1.61 STD. ERROR OF MEAN=0.36

METHYLENE IODIDE, 2 PERCENT R.H.

36. 35. 35. 34. 38. 37. 33. 35. 36. 36. 37. 38.
36. 35. 38. 35. 37. 37. 38. 36.
N=20 MEAN=36.1 VARIANCE= 1.99
STD. DEV.=1.41 STD. ERROR OF MEAN=0.32

TETRABROMOETHANE, 2 PERCENT R.H.

23. 23. 23. 24. 25. 21. 22. 26. 25. 24. 24. 24.
22. 22. 24.
N=15 MEAN=23.5 VARIANCE= 1.84
STD. DEV.=1.36 STD. ERROR OF MEAN=0.35

TABLE XIII (Continued)
CONTACT ANGLES ON AIR-SIDES

3.0 MINUTES CORONA TREATMENT

WATER, 50 PERCENT R.H.

26. 27. 25. 27. 28. 25. 26. 26. 27. 28. 25. 24.
26. 25. 27. 28. 27. 26. 27. 26.
N=20 MEAN=26.3 VARIANCE= 1.27
STD. DEV.=1.13 STD. ERROR OF MEAN=0.25

METHYLENE IODIDE, 50 PERCENT R.H.

39. 39. 40. 42. 41. 40. 42. 42. 42. 44. 42. 41.
40. 38. 39. 41. 42. 43. 43. 42.
N=20 MEAN=41.1 VARIANCE= 2.52
STD. DEV.=1.59 STD. ERROR OF MEAN=0.35

TETRABROMOETHANE, 50 PERCENT R.H.

26. 27. 26. 28. 28. 27. 27. 26. 28. 30. 30. 28.
25. 26. 26. 27. 26. 25. 27. 27.
N=20 MEAN=27.0 VARIANCE= 1.89
STD. DEV.=1.38 STD. ERROR OF MEAN=0.31

WATER, 2 PERCENT R.H.

31. 32. 32. 32. 30. 31. 34. 35. 34. 31. 31. 32.
33. 32. 33. 30. 30. 29. 30. 30.
N=20 MEAN=31.6 VARIANCE= 2.57
STD. DEV.=1.60 STD. ERROR OF MEAN=0.36

METHYLENE IODIDE, 2 PERCENT R.H.

36. 36. 38. 37. 39. 35. 40. 39. 37. 36. 36. 35.
36. 34. 37. 37. 38. 38. 39. 37.
N=20 MEAN=37.0 VARIANCE= 2.42
STD. DEV.=1.56 STD. ERROR OF MEAN=0.35

TETRABROMOETHANE, 2 PERCENT R.H.

27. 25. 24. 25. 23. 21. 22. 24. 24. 23. 25. 24.
25. 26. 26.
N=15 MEAN=24.3 VARIANCE= 2.50
STD. DEV.=1.58 STD. ERROR OF MEAN=0.41

TABLE XIII (Continued)
CONTACT ANGLES ON AIR-SIDES

5.0 MINUTES CORONA TREATMENT

WATER, 50 PERCENT R.H.

| | | | | | | | | | | | |
|---|---|---|---|---|---|---|---|---|---|---|---|
| 25. | 24. | 25. | 26. | 26. | 28. | 27. | 25. | 23. | 24. | 22. | 26. |
| 24. | 25. | 26. | 23. | 23. | 24. | 25. | 24. | 28. | 15. | 28. | 14. |
| 23. | 27. | 30. | 27. | 19. | 30. | 34. | 28. | 27. | 28. | 13. | 22. |
| 31. | 22. | 21. | 27. | 28. | 19. | 27. | 27. | 35. | 23. | 14. | |

N=47 MEAN=24.7 VARIANCE=21.20
STD. DEV.=4.60 STD. ERROR OF MEAN=0.67

METHYLENE IODIDE, 50 PERCENT R.H.

| | | | | | | | | | | | |
|---|---|---|---|---|---|---|---|---|---|---|---|
| 41. | 42. | 44. | 43. | 39. | 40. | 42. | 44. | 43. | 42. | 40. | 45. |
| 39. | 40. | 42. | 42. | 43. | 43. | 41. | 40. | 42. | 45. | 46. | 45. |
| 45. | 40. | 45. | 42. | 45. | 42. | 42. | 42. | 40. | 44. | 39. | 43. |
| 40. | 40. | 42. | 40. | 40. | 39. | 38. | 38. | | | | |

N=44 MEAN=41.8 VARIANCE= 4.54
STD. DEV.=2.13 STD. ERROR OF MEAN=0.32

TETRABROMOETHANE, 50 PERCENT R.H.

| | | | | | | | | | | | |
|---|---|---|---|---|---|---|---|---|---|---|---|
| 26. | 26. | 27. | 30. | 29. | 27. | 27. | 26. | 28. | 28. | 30. | 30. |
| 29. | 27. | 28. | 27. | 29. | 30. | 30. | 28. | | | | |

N=20 MEAN=28.1 VARIANCE= 2.09
STD. DEV.=1.45 STD. ERROR OF MEAN=0.32

WATER, 2 PERCENT R.H.

| | | | | | | | | | | | |
|---|---|---|---|---|---|---|---|---|---|---|---|
| 29. | 29. | 30. | 31. | 31. | 30. | 33. | 28. | 26. | 30. | 29. | 28. |
| 29. | 30. | 28. | 30. | 30. | 31. | 30. | 30. | | | | |

N=20 MEAN=29.6 VARIANCE= 2.15
STD. DEV.=1.47 STD. ERROR OF MEAN=0.33

METHYLENE IODIDE, 2 PERCENT R.H.

| | | | | | | | | | | | |
|---|---|---|---|---|---|---|---|---|---|---|---|
| 39. | 38. | 40. | 37. | 38. | 35. | 36. | 35. | 37. | 37. | 39. | 38. |
| 38. | 39. | 36. | 35. | 39. | 40. | 38. | 38. | | | | |

N=20 MEAN=37.6 VARIANCE= 2.46
STD. DEV.=1.57 STD. ERROR OF MEAN=0.35

TETRABROMOETHANE, 2 PERCENT R.H.

| | | | | | | | | | | | |
|---|---|---|---|---|---|---|---|---|---|---|---|
| 22. | 24. | 24. | 26. | 28. | 25. | 25. | 26. | 26. | 27. | 24. | 23. |
| 26. | 27. | 26. | | | | | | | | | |

N=15 MEAN=25.3 VARIANCE= 2.64
STD. DEV.=1.62 STD. ERROR OF MEAN=0.42

TABLE XIV
CONTACT ANGLES ON LUCITE SIDES
(DEGREES)

NO CORONA TREATMENT

WATER, 50 PERCENT R.H.

| | | | | | | | | | | | |
|---|---|---|---|---|---|---|---|---|---|---|---|
| 61. | 63. | 61. | 60. | 64. | 59. | 58. | 60. | 61. | 62. | 64. | 61. |
| 60. | 59. | 62. | 61. | 62. | 60. | 61. | 62. | 62. | 49. | 69. | 72. |
| 57. | 68. | 50. | 58. | 63. | 56. | 63. | 63. | 58. | 62. | 65. | 61. |
| 58. | 67. | 53. | 65. | 62. | 63. | 60. | 60. | | | | |

N=44 MEAN=61.0 VARIANCE=17.84
STD. DEV.=4.22 STD. ERROR OF MEAN=0.64

METHYLENE IODIDE, 50 PERCENT R.H.

| | | | | | | | | | | | |
|---|---|---|---|---|---|---|---|---|---|---|---|
| 40. | 42. | 39. | 38. | 41. | 41. | 42. | 41. | 41. | 44. | 45. | 42. |
| 43. | 44. | 42. | 42. | 41. | 42. | 40. | 41. | 26. | 44. | 43. | 43. |
| 41. | 39. | 43. | 35. | 42. | 47. | 42. | 46. | 44. | 46. | 46. | 38. |
| 41. | 43. | | | | | | | | | | |

N=38 MEAN=41.6 VARIANCE=12.63
STD. DEV.=3.55 STD. ERROR OF MEAN=0.58

TETRABROMOETHANE, 50 PERCENT R.H.

| | | | | | | | | | | | |
|---|---|---|---|---|---|---|---|---|---|---|---|
| 36. | 37. | 36. | 36. | 34. | 38. | 35. | 35. | 36. | 37. | 34. | 35. |
| 36. | 36. | 37. | 36. | 37. | 35. | 35. | 35. | | | | |

N=20 MEAN=35.8 VARIANCE= 1.12
STD. DEV.=1.06 STD. ERROR OF MEAN=0.24

WATER, 2 PERCENT R.H.

| | | | | | | | | | | | |
|---|---|---|---|---|---|---|---|---|---|---|---|
| 72. | 73. | 74. | 71. | 75. | 74. | 72. | 72. | 73. | 71. | 72. | 72. |
| 73. | 74. | 75. | 71. | 76. | 75. | 76. | 73. | | | | |

N=20 MEAN=73.2 VARIANCE= 2.59
STD. DEV.=1.61 STD. ERROR OF MEAN=0.36

METHYLENE IODIDE, 2 PERCENT R.H.

| | | | | | | | | | | | |
|---|---|---|---|---|---|---|---|---|---|---|---|
| 35. | 38. | 38. | 39. | 40. | 34. | 36. | 36. | 37. | 38. | 37. | 38. |
| 38. | 36. | 37. | 36. | 38. | 39. | 40. | 38. | | | | |

N=20 MEAN=37.4 VARIANCE= 2.46
STD. DEV.=1.57 STD. ERROR OF MEAN=0.35

TETRABROMOETHANE, 2 PERCENT R.H.

| | | | | | | | | | | | |
|---|---|---|---|---|---|---|---|---|---|---|---|
| 30. | 33. | 32. | 34. | 30. | 34. | 33. | 35. | 29. | 31. | 31. | 33. |
| 32. | 34. | 32. | | | | | | | | | |

N=15 MEAN=32.2 VARIANCE= 3.03
STD. DEV.=1.74 STD. ERROR OF MEAN=0.45

TABLE XIV (Continued)
CONTACT ANGLES ON LUCITE SIDES

0.5 MINUTES CORONA TREATMENT

WATER, 50 PERCENT R.H.

51. 50. 52. 51. 52. 51. 51. 52. 52. 53. 52. 49.
48. 51. 50. 52. 52. 51. 50. 52.
N=20 MEAN=51.1 VARIANCE= 1.46
STD. DEV.=1.21 STD. ERROR OF MEAN=0.27

METHYLENE IODIDE, 50 PERCENT R.H.

42. 41. 41. 41. 39. 38. 40. 41. 40. 40. 42. 42.
39. 44. 40. 40. 39. 38. 38. 39.
N=20 MEAN=40.2 VARIANCE= 2.48
STD. DEV.=1.58 STD. ERROR OF MEAN=0.35

TETRABROMOETHANE, 50 PERCENT R.H.

30. 31. 30. 30. 32. 31. 33. 29. 28. 32. 33. 32.
32. 33. 31. 31. 34. 33. 32. 33.
N=20 MEAN=31.5 VARIANCE= 2.37
STD. DEV.=1.54 STD. ERROR OF MEAN=0.34

WATER, 2 PERCENT R.H.

58. 60. 62. 61. 61. 63. 64. 60. 59. 62. 60. 61.
59. 64. 61. 61. 62. 63. 63. 62.
N=20 MEAN=61.3 VARIANCE= 2.75
STD. DEV.=1.66 STD. ERROR OF MEAN=0.37

METHYLENE IODIDE, 2 PERCENT R.H.

38. 37. 38. 36. 35. 35. 36. 36. 33. 34. 38. 37.
35. 37. 37. 34. 37. 38. 36. 37.
N=20 MEAN=36.2 VARIANCE= 2.17
STD. DEV.=1.47 STD. ERROR OF MEAN=0.33

TETRABROMOETHANE, 2 PERCENT R.H.

30. 31. 29. 29. 26. 28. 25. 26. 28. 27. 29. 28.
30. 29. 29.
N=15 MEAN=28.3 VARIANCE= 2.78
STD. DEV.=1.67 STD. ERROR OF MEAN=0.43

TABLE XIV (Continued)
CONTACT ANGLES ON LUCITE SIDES

1.0 MINUTES CORONA TREATMENT

WATER, 50 PERCENT R.H.

48. 48. 47. 50. 51. 49. 50. 48. 47. 49. 46. 46.
47. 50. 48. 47. 46. 47. 46. 48.
N=20 MEAN=47.9 VARIANCE= 2.31
STD. DEV.=1.52 STD. ERROR OF MEAN=0.34

METHYLENE IODIDE, 50 PERCENT R.H.

38. 38. 39. 38. 40. 42. 43. 41. 40. 39. 39. 39.
40. 41. 42. 40. 41. 39. 41. 40.
N=20 MEAN=40.0 VARIANCE= 2.00
STD. DEV.=1.41 STD. ERROR OF MEAN=0.32

TETRABROMOETHANE, 50 PERCENT R.H.

29. 29. 31. 30. 30. 28. 27. 31. 33. 28. 30. 31.
30. 32. 33. 29. 30. 32. 33. 30.
N=20 MEAN=30.3 VARIANCE= 2.96
STD. DEV.=1.72 STD. ERROR OF MEAN=0.38

WATER, 2 PERCENT R.H.

59. 58. 58. 56. 55. 56. 57. 57. 58. 56. 55. 60.
59. 57. 58. 56. 58. 59. 58. 57.
N=20 MEAN=57.3 VARIANCE= 1.92
STD. DEV.=1.39 STD. ERROR OF MEAN=0.31

METHYLENE IODIDE, 2 PERCENT R.H.

37. 37. 36. 35. 38. 39. 33. 34. 35. 36. 36. 37.
35. 34. 35. 36. 38. 36. 36. 37.
N=20 MEAN=36.0 VARIANCE= 2.21
STD. DEV.=1.49 STD. ERROR OF MEAN=0.33

TETRABROMOETHANE, 2 PERCENT R.H.

27. 27. 28. 24. 26. 30. 29. 27. 27. 28. 26. 29.
27. 28. 26.
N=15 MEAN=27.3 VARIANCE= 2.21
STD. DEV.=1.49 STD. ERROR OF MEAN=0.38

TABLE XIV (Continued)
CONTACT ANGLES ON LUCITE SIDES

3.0 MINUTES CORONA TREATMENT

WATER, 50 PERCENT R.H.

44. 43. 42. 44. 46. 45. 44. 46. 47. 44. 43. 42.
45. 46. 43. 41. 46. 44. 44. 43.
N=20 MEAN=44.1 VARIANCE= 2.52
STD. DEV.=1.59 STD. ERROR OF MEAN=0.35

METHYLENE IODIDE, 50 PERCENT R.H.

40. 40. 41. 40. 39. 40. 43. 40. 41. 38. 37. 39.
40. 41. 40. 40. 42. 43. 42. 42.
N=20 MEAN=40.4 VARIANCE= 2.36
STD. DEV.=1.54 STD. ERROR OF MEAN=0.34

TETRABROMOETHANE, 50 PERCENT R.H.

32. 30. 31. 33. 29. 28. 30. 27. 29. 29. 30. 31.
30. 29. 31. 30. 31. 32. 29. 29.
N=20 MEAN=30.0 VARIANCE= 2.11
STD. DEV.=1.45 STD. ERROR OF MEAN=0.32

WATER, 2 PERCENT R.H.

53. 52. 53. 53. 50. 51. 54. 55. 53. 53. 54. 56.
51. 50. 51. 52. 55. 54. 54. 54.
N=20 MEAN=52.9 VARIANCE= 2.83
STD. DEV.=1.68 STD. ERROR OF MEAN=0.38

METHYLENE IODIDE, 2 PERCENT R.H.

36. 36. 37. 34. 37. 35. 37. 38. 36. 39. 36. 33.
35. 36. 36. 37. 38. 37. 37. 38.
N=20 MEAN=36.4 VARIANCE= 2.04
STD. DEV.=1.43 STD. ERROR OF MEAN=0.32

TETRABROMOETHANE, 2 PERCENT R.H.

24. 25. 27. 27. 29. 30. 28. 28. 27. 26. 25. 28.
27. 26. 28.
N=15 MEAN=27.0 VARIANCE= 2.57
STD. DEV.=1.60 STD. ERROR OF MEAN=0.41

TABLE XIV (Continued)
CONTACT ANGLES ON LUCITE SIDES

5.0 MINUTES CORONA TREATMENT

WATER, 50 PERCENT R.H.

41. 40. 42. 43. 42. 42. 42. 42. 43. 44. 40. 39.
40. 40. 41. 42. 43. 42. 43. 42. 40. 40. 42. 48.
36. 51. 46. 47. 45. 35. 35. 30. 22. 40. 38. 43.
54. 46. 44. 43. 35. 42. 35. 42. 51. 39. 42. 51.
43.

N=49 MEAN=41.6 VARIANCE=27.83
STD. DEV.=5.28 STD. ERROR OF MEAN=0.75

METHYLENE IODIDE, 50 PERCENT R.H.

41. 40. 42. 41. 43. 42. 39. 40. 38. 39. 41. 41.
42. 40. 39. 41. 42. 42. 41. 41. 42. 41. 40. 40.
44. 39. 41. 41. 44. 41. 39. 41. 43. 39. 42. 40.
42. 39. 39. 41. 39.

N=41 MEAN=40.8 VARIANCE= 2.08
STD. DEV.=1.44 STD. ERROR OF MEAN=0.22

TETRABROMOETHANE, 50 PERCENT R.H.

29. 28. 30. 29. 33. 32. 27. 28. 29. 30. 30. 30.
31. 32. 31. 29. 31. 30. 30. 31.

N=20 MEAN=30.0 VARIANCE= 2.21
STD. DEV.=1.49 STD. ERROR OF MEAN=0.33

WATER, 2 PERCENT R.H.

48. 47. 49. 50. 53. 52. 51. 50. 50. 49. 48. 50.
51. 52. 50. 49. 50. 49. 50. 50.

N=20 MEAN=49.9 VARIANCE= 2.09
STD. DEV.=1.45 STD. ERROR OF MEAN=0.32

METHYLENE IODIDE, 2 PERCENT R.H.

38. 36. 37. 37. 39. 38. 33. 34. 36. 35. 37. 37.
35. 38. 39. 38. 37. 36. 37. 37.

N=20 MEAN=36.7 VARIANCE= 2.43
STD. DEV.=1.56 STD. ERROR OF MEAN=0.35

TETRABROMOETHANE, 2 PERCENT R.H.

30. 27. 26. 28. 29. 24. 26. 26. 27. 27. 25. 29.
28. 27. 26.

N=15 MEAN=27.0 VARIANCE= 2.57
STD. DEV.=1.60 STD. ERROR OF MEAN=0.41

# APPENDIX VIII

## CALCULATION OF SURFACE FREE-ENERGY COMPONENTS

### ESTIMATION OF $\gamma_{\underline{\ell}}^d$ FROM INTERFACIAL TENSION

Equation (21) was used to determine the components of liquid surface tension from the published values of interfacial tension with water. The procedure is outlined below. (The subscript 1 refers to water, and 2 refers to the other liquid.)

Rearrangement of Equation (21) yields

$$\gamma_2^d = \beta - \kappa\sqrt{\gamma_2^p} ,$$

where

$$\beta = 0.5(\gamma_1 + \gamma_2 - \gamma_{12})/\sqrt{\gamma_1^d} ,$$

and

$$\kappa = \sqrt{\gamma_1^p/\gamma_1^d} .$$

This equation is combined with the expression, $\gamma_{\underline{2}}^d + \gamma_{\underline{2}}^p = \gamma_2$, to give $(\kappa^2 + 1)\gamma_{\underline{2}}^p - 2\beta\kappa(\sqrt{\gamma_{\underline{2}}^p}) + (\beta^2 - \gamma_2) = 0$. This equation is quadratic with respect to $\sqrt{\gamma_{\underline{2}}^p}$, and may be explicitly solved as follows:

$$\gamma_2^p = \left[\frac{\beta\kappa \pm \sqrt{(\beta\kappa)^2 - (\kappa^2 + 1)(\beta^2 - \gamma_2)}}{(\kappa^2 + 1)}\right]^2$$

### ESTIMATION OF $\gamma_{\underline{s}}^d$ FROM CONTACT-ANGLE DATA

Equation (26) was applied to contact-angle data for each surface and two different liquids to yield two simultaneous equations. Definition of the following quantities simplifies the solution somewhat. We define,

for liquid 1:

$$D_1 = 2\sqrt{\gamma_\ell^d}/\gamma_\ell \ ,$$

$$H_1 = 2\sqrt{\gamma_\ell^p}/\gamma_\ell \ ,$$

and for liquid 2:

$$D_2 = 2\sqrt{\gamma_\ell^d}/\gamma_\ell \ ,$$

$$H_2 = 2\sqrt{\gamma_\ell^p}/\gamma_\ell \ .$$

Substitution of these quantities into Equation (26) yields the following two equations:

$$\cos \theta_1 = -1 + D_1\sqrt{\gamma_s^d} + H_1\sqrt{\gamma_s^p} \ ,$$

$$\cos \theta_2 = -1 + D_2\sqrt{\gamma_s^d} + H_2\sqrt{\gamma_s^p} \ .$$

The solution to these equations may be written in the form:

$$\sqrt{\gamma_s^d} = (H_2 - H_1 + H_2 \cos \theta_1 - H_1 \cos \theta_2)/(D_1H_2 - D_2H_1) \ ,$$

$$\sqrt{\gamma_s^p} = (1 + \cos \theta_2 - D_2\sqrt{\gamma_s^d})/H_2 \ ,$$

and

$$\gamma_s = \gamma_s^d + \gamma_s^p \ .$$

# APPENDIX IX

## CALCULATED COMPONENTS OF SOLID SURFACE FREE ENERGY

### TABLE XV

CALCULATED COMPONENTS OF SOLID SURFACE FREE ENERGY[a] FOR PRESOAKED, CORONA-TREATED CELLOPHANE "AIR-SIDE"

| Relative Humidity, % | Treatment Time, min. | Water-$CH_2I_2$[b] | | | Water-TBE[b] | | |
|---|---|---|---|---|---|---|---|
| | | $\gamma_s^d$ | $\gamma_s^p$ | $\gamma_s$ | $\gamma_s^d$ | $\gamma_s^p$ | $\gamma_s$ |
| 50 | Untreated | 34.2 | 28.4 | 62.6 | 32.6 | 29.4 | 62.0 |
| | 0.5 | 33.9 | 31.6 | 65.6 | 32.6 | 32.5 | 65.1 |
| | 1.0 | 33.8 | 33.0 | 66.8 | 32.4 | 33.9 | 66.3 |
| | 3.0 | 33.2 | 34.8 | 68.0 | 31.8 | 35.8 | 67.5 |
| | 5.0 | 32.7 | 35.8 | 68.6 | 31.2 | 36.9 | 68.1 |
| Dry $N_2$ | Untreated | 36.5 | 22.8 | 59.3 | 34.7 | 23.7 | 58.5 |
| | 0.5 | 36.2 | 26.8 | 63.0 | 34.3 | 27.9 | 62.2 |
| | 1.0 | 36.0 | 28.5 | 64.5 | 34.0 | 29.7 | 63.7 |
| | 3.0 | 35.4 | 30.8 | 66.2 | 33.3 | 32.1 | 65.4 |
| | 5.0 | 35.0 | 32.0 | 67.1 | 32.7 | 33.5 | 66.2 |

[a] Calculated from Equation (26); units are ergs/cm.$^2$

[b] Contact-liquid pair.

TABLE XVI

CALCULATED COMPONENTS OF SOLID SURFACE FREE ENERGY[a] FOR PRESOAKED, CORONA-TREATED CELLOPHANE "LUCITE-SIDE"

| Relative Humidity, % | Treatment Time, min. | Water-$CH_2I_2$[b] | | | Water-TBE[b] | | |
|---|---|---|---|---|---|---|---|
| | | $\gamma_s^d$ | $\gamma_s^p$ | $\gamma_s$ | $\gamma_s^d$ | $\gamma_s^p$ | $\gamma_s$ |
| 50 | Untreated | 35.2 | 13.6 | 48.8 | 33.3 | 14.4 | 47.7 |
| | 0.5 | 35.1 | 19.6 | 54.7 | 33.4 | 20.4 | 53.8 |
| | 1.0 | 34.9 | 21.6 | 56.6 | 33.4 | 22.4 | 55.8 |
| | 3.0 | 34.5 | 24.2 | 58.7 | 32.9 | 25.1 | 58.0 |
| | 5.0 | 34.1 | 25.9 | 60.0 | 32.5 | 26.9 | 59.3 |
| Dry $N_2$ | Untreated | 38.4 | 6.3 | 44.8 | 37.6 | 6.6 | 44.2 |
| | 0.5 | 37.9 | 12.4 | 50.3 | 36.7 | 12.8 | 49.6 |
| | 1.0 | 37.6 | 14.7 | 52.3 | 36.3 | 15.2 | 51.6 |
| | 3.0 | 37.1 | 17.6 | 54.6 | 35.6 | 18.3 | 53.8 |
| | 5.0 | 36.7 | 19.5 | 56.2 | 35.0 | 20.3 | 55.4 |

[a] Calculated from Equation (26); units are ergs/cm.$^2$

[b] Contact-liquid pair.